DOCTOR OF PHILOSOPHY

Study of SCR using Cu-Zeolite catalysts on a light-duty diesel engine under steady state and transient conditions

Gall, Miroslaw

Award date:
2015

Awarding institution:
Coventry University

Study of SCR using Cu-Zeolite catalysts on a light-duty diesel engine under steady state and transient conditions

By

Miroslaw Gall

April 2015

Study of SCR using Cu-Zeolite catalysts on a light-duty diesel engine under steady state and transient conditions

By

Miroslaw Gall

April 2015

A thesis submitted in partial fulfilment of the University's requirements for the Degree of Doctor of Philosophy

Table of Contents

Abstract……..v

Acknowledgements……..vii

Publications……viii

Summary of abbreviations and symbols……..ix

List of tables……....xii

List of figures……..xiii

List of appendices……...…..xviii

Chapter 1: Introduction

1.0 The impact of pollution……1

1.1 The context of legislation……..1

1.2 The impact of evolving regulations……..2

1.3 Diesel CI engine emissions overview ……....3

1.3.1 HC, CO and PM emissions……4

1.3.2 NOx formation and engine-based reduction techniques ……...…5

1.3.3 Diesel engine emissions summary ……....6

1.3.4 Role of DOC and DPF in diesel engine after-treatment system ……...7

1.4 Diesel engine emissions after-treatment……...…7

1.4.1 NOx after-treatment overview ……..7

1.4.2 Lean NOx traps ……..8

1.4.3 Selective Catalytic Reduction (SCR) ……..10

1.4.4 SCR reductant……..11

1.4.5 SCR potential limitations .……..12

1.4.6 Comparison of SCR with LNT……...…….....12

1.5 Overall aim of SCR studies ……12

1.6 Outline of the thesis ……....13

Chapter 2: Literature review of SCR

2.0 Selective catalytic reduction (SCR) overview ……...…… 14

2.1 SCR catalyst types and application ……..……...14

2.1.1 Vanadium based catalyst ……..14

2.1.2 Zeolite based catalyst ……...15

2.2 Importance of SCR copper zeolite testing and modelling ……..17

2.2.1 SCR copper zeolite testing under steady and transient conditions……...18

2.2.1.1 Steady state testing ……...18

2.2.1.2 Engine transient testing ……..19
2.2.2 Effect of flow and 3D geometry on SCR performance ……..20
2.3 Rationale for this thesis; novelty of the current studies ……..…21
2.4 Objectives of the project ……..22
Chapter 3: Experimental methodology
3.0 Overview……...24
3.1 Engine and test cell……...24
3.2 SCR Exhaust System Setup……..25
3.3 Ammonia gas injection…….27
3.4 Urea in water solution (Adblue) injection system setup……...28
3.5 Engine emissions gas analysers……29
3.5.1 Horiba EXSA 1500 analyser……..29
3.5.2 Horiba 6000FT FTIR Analyser……..…30
3.5.3 Cambustion CLD500 Fast NOx Analyser…….…31
3.6 Test procedures plus engine testing conditions……31
3.6.1 Cleaning the DPF…….……..31
3.6.2 Emission gas analysers; set up and calibration procedure……...……..31
3.6.3 Engine warm up procedure……32
3.6.4 Engine steady state testing…….32
3.6.5 Engine transient testing……..33
4. Chapter 4: Experimental results and discussion
4.0 The overview of experimental configuration……....36
4.1 Experiment with 5% ammonia gas dosing. ……...……...37
4.1.1 Steady state SCR performance for NO_2:NOx=0……....37
4.1.2 The effect of NO_2:NOx ratio on NOx conversion during a low temperature test…..39
4.1.3 The effect of NO_2:NOx ratio on NO and NO_2 selectivity……..40
4.1.4 Ammonia slip…….42
4.1.5 N_2O formation……44
4.1.6 SCR measurement with 180° expansion diffuser……..46
4.1.7 Summary of steady state SCR studies with ammonia gas dosing……..…52
4.1.8 Overview of transient engine tests…….52
4.1.8.1 Transient engine tests: Short transient……53
4.1.8.2 Transient engine tests: Long transient……59
4.1.8.3 Summary of results from transient engine testing……..65
4.2 Urea dosing..…….66
4.2.1 The effect of the injection position on droplet size…….…..66
4.2.2 Steady state engine testing…….67

4.2.3 Urea hydrolysis and NO conversion during steady state experiment……72
4.2.4 Urea spray under transient engine conditions test……76
4.2.5 Summary of results from the SCR studies with urea injection……..…80
5. Chapter 5: Conclusions
5.0 Overview of work undertaken……..……81
5.1 Strengths of the project ……81
5.1.1 Testing programme……...….81
5.1.2 Novelty of the results……82
5.1.2.1 Testing under steady state conditions……82
5.1.2.2 Testing under transient engine conditions……..…82
5.1.2.3 Urea dosing experiments……..……83
5.1.2.4 The effect of 3D diffuser geometry on SCR performance……..83
5.2 Limitations and recommendations for future work…….……..…84
6. Reference..……..85
Appendix

Abstract

The recognition of the negative impact of NOx resulted in increasingly tighter automotive emission regulations. Companies are under pressure to develop methods, which can meet the legislative demands. After treatment solutions, and especially Selective Catalytic Reduction, became the focus of research and have shown so far promising results. However, more in depth understanding of the SCR process under different conditions is needed.

This thesis describes an investigation of the SCR performance using gas and urea injections under steady state and transient conditions undertaken on a light duty diesel engine using a 1D exhaust system designed for uniform flow across the catalyst.

Under steady state conditions, the SCR performance was examined for low and high temperature conditions. Ammonia was supplied either as 5% ammonia gas or in form of urea injection. The engine was operating at 1500 rpm and 6 and 8 bar BMEP to provide an exhaust gas temperature of 210 °C and 265 °C respectively. Also, the effect of SCR brick length on the NOx conversion was investigated using SCR catalysts of length 30, 45 and 75 mm. To measure the influence of NO_2:NOx ratio on the SCR performance, different sizes of standard DOC were used. NH_3:NOx dosage levels included; α~0.5 - deficient ammonia, α~1.0 - stoichiometric ammonia, α~1.25 - excess ammonia. Gas emissions were measured before and after the SCR catalysts with a Horiba FTIR analyser during steady state and long transient tests. It was found that conditions such as temperature and NO_2:NOx had the biggest impact on the SCR performance. During the steady state engine conditions, at α~1.0 ammonia dosing and NO_2:NOx ratio of 0, only 17% of NO was converted in the first 30 mm of the SCR brick length. The conversion was improved at high temperature (263 °C) to 31%.

A fast response CLD analyser was used during short transient testing to sample emissions with a high resolution. The short transient test with standard 0.5 and 1 DOC, and fixed ammonia dosing, showed that NOx conversion was reduced during the ramp event due to deficient ammonia and a drop in the supplied NO_2:NOx ratio.

During urea injection experiments, urea was injected either through an oblique pipe arrangement with a mixer device placed downstream or directly into a mixing can. In this case the mixer device was replaced with a straight pipe. A 75mm SCR was fitted and to ensure that supplied NO_2:NOx ratio was zero, a palladium only DOC was used post a DPF. It was found that a large proportion of urea decomposition and hydrolysis was occurring on the surface of the SCR catalyst. Comparing NOx performance between urea injection and ammonia gas dosing experiment, more NO was converted for a given NH_3:NOx ratio when ammonia was supplied in the form of gas. That was true for low and high temperature tests.

For most studies, a long 10 degree diffuser was used in front of the SCR to provide uniform gas distribution across the catalyst. In addition SCR performance was investigated with a 180 degree sudden expansion diffuser in order to measure the influence of temperature and velocity profiles. During this study, a 45 mm SCR catalyst was used to provide a moderate amount of NO conversion and ammonia slip. The results showed that the flow and temperature distribution upstream of the SCR catalyst will have an effect on the NOx conversion, and that gas velocity has bigger impact on NOx conversion than gas temperature.

Acknowledgements

I would like to extend my appreciation to a number of people without whom this PhD project would not be possible. Firstly, I would like to thank my supervisors Prof Steve Benjamin and Dr Carol Roberts for their continuous support, kindness and guidance in my work. They provided me with a unique opportunity to develop my knowledge and skills for which I am very grateful. Secondly, I would like to thank Robert Gartside who provided substantial support in managing and undertaking engine testing and dealing with any arising challenges.

I would also like to thank my partner for her ongoing support and encouragement.

Publications

As part of this PhD, the following articles have been published (Attached in the Appendix 3):

- Benjamin, S.F. Gall, M. Roberts, C.A. (2014) 'Conversion of nitric oxide in an engine exhaust by selective catalytic reduction with a urea spray under steady-state and transient engine-load conditions' IMechE 2014, Vol. 228(7) 758–770

- Benjamin, S. F., M. Gall, and C. A. Roberts. (2012). Tuning the Standard SCR Reaction Kinetics to Model NO Conversion in a Diesel Engine Exhaust SCR Catalyst System Under Steady State Conditions in 1D and 3D Geometries Using Ammonia Gas as the Reductant. No. 2012-01-1636. SAE Technical Paper

- Benjamin, S.F. Gall, M. Roberts, C.A. (2012). Modelling of NOx conversion in 1d diesel engine exhaust SCR catalyst system under transient conditions using ammonia gas as the reductant. SAE 2012-01-1743

- Benjamin, S.F., M. Gall, M.P Sturgess and C.A. Roberts (2011) Experiments on a light duty SCR test exhaust system using ammonia gas to provide data for validation of a CFD model. Internal Combustions Engines: Improving performance, Fuel economy and emissions (pp. 219-234). Cambridge. Woodhead Publishing

Summary of abbreviations and symbols

Symbol	Description
α	(alpha) NH_3:NOx Ratio
Δ	Consumed Value
λ	Actual AFR to Stoichiometric Ratio
ACEA	European Automobile Manufacturers Association
AdBlue	Registered Trademark for AUS32
AFR	Air Fuel Ratio
$AI_2(SO_4)_3$	Aluminium Sulphate
AI_2O_3	Aluminium Oxide
ANR	Ammonia to NOx ratio
AUS32	Aqueous Urea Solution 32.5%
BMEP	Brake Mean Effective Pressure
CA	Crank Angle
CFD	Computational Fluid Dynamics
CI	Compression Ignition
CLD	Chemiluminescence Detector
CO	Carbon Monoxide
CO_2	Carbon Dioxide
CR	Compression Ratio
Cu	Copper
DOC	Diesel Oxidation Catalyst
DPF	Diesel Particulate Filter
ECU	Engine Control Unit

EGR	Exhaust Gas Recirculation
EMS	Engine Management System
EPA	Environmental Protection Agency, United States
FTIR	Fourier Transform Infrared Spectroscopy
GDI	Gasoline Direct Injection
GHG	Green House Gases
H_2O	Water
HBF	Horiba Backflush Filter
HC	Hydrocarbon
HD-FTP	Heavy-Duty Federal Test Procedure
HLDT	Heavy Light-Duty Truck
kW	Kilowatt (Power)
LDD	Light Duty Diesel
LDT	Light Duty Truck
LDV	Light Duty Vehicle
LEV	Low Emission Vehicle
LEV II	Low Emission Vehicle II
LPG	Liquid Petroleum Gas
MAF	Intake Mass Air Flow (kg/h)
N_2	Nitrogen Gas
NEDC	New European Driving Cycle
NH_2	Amine
NH_3	Ammonia
NOx	Nitrogen Oxides

NRTC	Non-Road Transient Cycle
O_2	Oxygen Gas
O_3	Ozone
OEHHA	The Office of Environmental Health Hazard Assessment
OEM	Original Equipment Manufacturer
PM	Particulate Matter
ppm	Parts Per Million
Pt	Platinum
Pd	Palladium
ρ	Density (kg/m3)
RPM	Revolutions per Minute (1/min)
SAE	Society of Automotive Engineers
SCR	Selective Catalysts Reduction
SCRF	Combined SCR Catalyst and Particulate Filter
SI	Spark-ignition
SO_2	Sulphur Dioxide
SO_3	Sulphur Trioxide
SULEV	Super Ultra Low Emission Vehicle
TDC	Top Dead Centre
tNH_3	Theoretical Ammonia Released from Injected Urea
V_2O_5	Vanadium Oxide
VGT	Variable Geometry Turbocharger
VPU	Vacuum Pump Unit
ZSM-5	Zeolite Sieve of Molecular Porosity

List of tables

Number	Description	Page Number
1.2	Summary of the effect of Euro5 and combined effect of Euro 5 and 6 (reproduced from European Commission)	2
3.1	Ford Puma 5FM engine specification.	25
3.5.2	Performance of Horiba 6000FT FTIR analyser (Horiba, 2015)	30
3.5.3	Specification of Cambustion CLD500 Fast NOx Analyser (Cambustion, 2014).	31
3.6.4	Conditions for steady state engine testing.	32
4.0	Summary of experiments	36
4.2.2	Inlet conditions for the urea injection steady-state tests at low and high temperature.	68
4.2.3	Consumed NO and measured NH_3 slip at the end of each urea dosing periods (α~0.5, 0.75 and 1) during steady state tests at low and high temperatures.	72

List of figures

Number	Description	Page
1.3a	Common rail system diagram. Injection pressure of 1800 bar (taken from Denso, 2014).	4
1.3b	Typical heat release rate curve during four major phases of combustion process of a CI engine (reproduced from Mohan et al, 2013).	4
1.3.2a	Dependency of EGR rate and AFR on DI diesel engine's NOx and PM (Johnson et al., 2010).	5
1.3.2b	Pilot injection timing effect on emission and noise during low load engine operation (Hotta et al, 2005)	6
1.3.3	Summary of diesel engine evolution from Euro 3 to Euro 6 (reproduced from Bression et al., 2008)	7
1.4.2a	Lean NOx trap working principle under lean (normal engine operating conditions) and rich (high fuel purge engine conditions) conditions. (Reproduced from Bosteels et al., 2002)	9
1.4.2b	1.4.2b LNT performance dependency on platinum loading (Johnson, 2009).	9
1.4.3	Common SCR system configuration with AdBlue injection used in LDV application (available from Emitec).	10
2.1.1	NOx conversion of conventional and improved vanadium SCR catalyst (Heck et al., 2009).	14
2.1.2a	NOx conversion profiles for Fe and vanadium based zeolite catalyst at range of temperatures. Supplied NO_2:NOx ratio was 0.5 and SV=126000 h^{-1} (Grossale et al., 2008)	15
2.1.2b	NOx conversion profiles for Cu and Fe based zeolite. NO_2:NOx ratio was 0 and 0.5. SV 40,000 h^{-1} (Kamasamudram et al., 2010).	16
2.1.2c	2.1.2c NOx conversion against ammonia storage at 250ºC for Cu and Fe based zeolite at NO_2NOx ratio 0.5. SV 40,000 h^{-1} (Kamasamudram et al., 2010).	16
2.1.2d	The comparison of NOx conversion profile of different Cu zeolites (Sultana et al., 2011)	17
2.2.1.1a	Cu zeolite model (solid lines) comparison with measured steady state data (points) for NO_2:NOx:0.7 (Watling et al., 2011)	18

2.2.2a	Effect of uniformity index on NOx conversion and NH_3 slip. Data obtained using CFD tool (Johansson, 2008).	21
3.1a	Ford Puma 2.2 litres 5FM diesel engine mounted into engine dynamometer. View A: Location of air filter box, Mass Flow Meter (MAF), exhaust inlet. View B: Control Unit (ECU), Exhaust Gas Recirculation (EGR) and Intercooler.	24
3.1b	Froude Hofmann AC 150 dynamometer and transducers box.	25
3.2a	Schematic diagram of the experimental test exhaust connected to the 2.2 litre Diesel engine, showing the expansion box and the angled side branch pipe downstream of the converging nozzle, which were the alternative points for the introduction of urea spray	26
3.3a	Gas flow meter with needle valve used to control dosed NH_3 gas.	27
3.3b	Gas injection nozzle	28
3.4a	Urea injection system layout	28
3.4b	Calibration curves of urea injector	30
3.6.4a	Example of steady state test procedure with NH3 gas injection.	33
3.6.5a	Engine load change during short transient experiment for 5, 10 and 20 s engine ramp.	34
3.6.5b	Engine load change during long transient experiment.	35
4.1.1	NO and NH_3 conversion profiles for deficient, stoichiometric, and excess ammonia. For low (T=210^{o}C) and high (T=265^{o}C) SCR temperature and zero NO_2:NOx ratio.	38
4.1.2a	NO_2:NOx ratio effect on NOx and NH_3 conversion profiles for deficient ammonia at low SCR temperature (T = 210 ^{o}C).	39
4.1.2b	NO_2:NOx ratio effect on NOx and NH_3 conversion profiles for stoichiometric, and excess ammonia at low SCR temperature (T = 210^{o}C).	40

4.1.3	NO_2:NOx ratio effect on NO and NO_2 consumed profiles for deficient, stoichiometric, and excess ammonia at low SCR temperature (T = 210 ^oC).	42
4.1.4a	Ammonia slip against inlet NH_3:NOx ratio (α) for range of SCR catalyst length and NO_2:NOx ratio. Low temperature case 210 ^oC.	43
4.1.4b	Relationship between ammonia slip and NOx conversion for range of SCR catalyst length and NO_2:NOx ratio. Low temperature case 210 ^oC.	44
4.1.5a	Impact of NO_2:NOx ratio on low temperature N_2O formation.	45
4.1.6a	3D 180 ° expansion diffuser measurement. NO and NH3 concentration profiles 20 mm upstream of 45 mm SCR brick in the expansion can; α~0.5 - deficient ammonia, α~1.0 - stoichiometric ammonia, α~1.25 - excess ammonia.	46
4.1.6b	Normalised velocity measured 30mm downstream of catalyst using hot wire anemometry (HWA) at mass flow of 16 g/s. Horizontal and vertical traverses are indicated by x_1 (-60 to 0mm), x_2 (0 to 60mm) and y_1 (-60 to 0mm), y_2 (0 to 60mm) (Benjamin et al. 2012).	47
4.1.6c	Temperature profiles 20 mm upstream (top plot) and 30 mm downstream (bottom plot) of 45 mm SCR brick. X-axis and y-axis represent horizontal and vertical traverse.	48
4.1.6d	NO concentration profile 30 mm downstream of the 45 mm SCR brick for deficient ammonia (α~0.5), stoichiometric ammonia (α~1.0) and excess ammonia (α~1.25). X-axis and y-axis represent horizontal and vertical traverse.	49
4.1.6e	NH_3 concentration profiles 30 mm downstream of 45 mm SCR brick for deficient ammonia (α~0.5), stoichiometric ammonia (α~1.0) and excess ammonia (α~1.25). X-axis and y-axis represent horizontal and vertical traverse.	50
4.1.6f	NO conversion profiles of 45 mm SCR brick for deficient ammonia (α~0.5), stoichiometric ammonia (α~1.0) and excess ammonia (α~1.25). X-axis and y-axis represent horizontal and vertical traverse.	51
4.1.8.1a	SCR inlet temperatures during the engine transient tests with standard 0.5 (left graph) and 1 (right graph) DOC.	53

4.1.8.1b	Inlet NO_2:NOx ratios during the engine transient tests with standard 0.5 (left graph) and 1 DOC (right graph).	54
4.1.8.1c	Calculated input ammonia during the engine transient tests with standard 0.5 DOC (left graph) and 1 DOC (right graph).	55
4.1.8.1d	NO and NO_2 concentration during the engine transient tests with standard 0.5 DOC (left graphs) and 1 DOC (right graphs).	56
4.1.8.1e	Comparison of consumed NO_2:NOx ratio to supplied NO_2:NOx ratio during the engine transient tests with standard 0.5 DOC (left graph) and 1 DOC (right graph).	58
4.1.8.2a	Temperature trace at 45 mm SCR inlet during the long engine transient test with Pd DOC (left graph) and standard 0.5 DOC (right graph).	59
4.1.8.2b	NO and NH_3 concentration during the long engine transient test with Pd only DOC and 45 mm SCR.	60
4.1.8.2c	Comparison of NOx and NH_3 conversion profile during the long engine transient test with Pd only DOC and 45 mm SCR.	61
4.1.8.2d	SCR inlet temperature effect on NO consumed during the long engine transient test with Pd only DOC and 45 mm SCR..	62
4.1.8.2e	NOx and NH_3 concentration during the long engine transient test with standard 0.5 DOC and 45 mm SCR.	63
4.1.8.2f	Comparison of consumed NO_2:NOx ratio to supplied NO_2:NOx ratio and NH_3 conversion during the long engine transient test with standard 0.5 DOC and 45 mm SCR.	64
4.1.8.2g	SCR inlet temperature effect on NOx consumed during the long engine transient test with standard 0.5 DOC and 45 mm SCR.	65
4.2.1a	Droplet size distribution downstream of the urea mixer when water was sprayed into pipe through the oblique side branch. Air flow temperature of 180 ^oC.	67
4.2.1b	Droplet size distribution measurements at the nozzle exit when the spray was sprayed into the top of the expansion can at air flow temperature of 180 ^oC.	67
4.2.2a	Proportion of the measured NH_3 to the calculated potential NH_3 25 mm before SCR catalyst.	69

4.2.2b	NO, NH_3 and N_2O concentration measured after the SCR during spray into pipe. Low temperature experiment.	70
4.2.2c	NO, NH_3 and N_2O concentration measured after the SCR during spray into to the can test. Low temperature experiment	70
4.2.2d	NO, NH_3 and N_2O concentration measured after the SCR during spray into the pipe. High temperature experiment	71
4.2.2e	NO, NH_3 and N_2O concentration measured after the SCR during spray into the can test. High temperature experiment.	71
4.2.3a	Calculated ammonia deficit during urea injection at low and high temperature for both dosing configurations.	73
4.2.3b	Steady state NO conversion against NH_3:NOx ratio for 0.8 litre SCR. Comparison of NH_3 gas injection and urea injection at low and high temperature	75
4.2.4a	FTIR measurements and gas temperature profile during the transient experiment measured upstream of the SCR catalyst	77
4.2.4b	FTIR measurements and gas temperature profile during the transient experiment measured downstream of the SCR catalyst.	78
4.2.4c	Analysis of data from transient test showing deficit of ammonia that possibly passed through the SCR catalyst as undetected substance.	79
4.2.4d	NO conversion and changing NH_3:NOx during transient experiment	80

List of appendices

1. Gas emission analysers

2. Urea dosing

3. Publications

Chapter 1: Introduction

1.0 The impact of pollution

The increase of use of motor vehicles has been recognised as having a range of negative effects on the environment, including noise, accidents, congestion, increased energy consumption, as well as air pollution (Faiz et al., 1996). In fact, Heck and Farrauto (2009) identified reducing air pollution as one of the key priorities of the future. Previously, the main focus was on the pollution caused by the hydrocarbons, carbon monoxide and carbon dioxide. In recent years, the impact of NOx on health problems has been increasingly recognised (EPA, 2008), with diesel engines contributing to this type of pollution (Faiz et al., 1996). Diesel engines are a popular alternative to gasoline engines, mainly due to their fuel efficiency and durability (Katare et al., 2007; Konieczny et al., 2008). However, their impact of NOx on the environment is a serious concern.

1.1 The context of legislation

The recognition of the negative impact of air pollution on the environment has been mirrored in the number as well as the scope of the regulations (Maus et al., 2007). In Europe, the regulations related to emissions were initially formalised in 1993 (Euro 1), when the European Commission focused on the amount of pollutants generated by diesel engine. Over the last few decades, the decrease of the allowed NOx emissions from passenger cars was phased in Europe: while in 2000 it was 0.50 g/km, in 2014 it was reduced to 0.08 g/km (DieselNet, 2013). The most recent regulations (Euro 6) are to be implemented in September 2014 for approval and January 2015 for sale and registration of cars. They involve a substantial reduction even in comparison to Euro 5 regulations: NOx reduction from 0.18 to 0.08 g/km. The estimated health benefit as a result of Euro 6 regulations in comparison to Euro 5 are 60-90% (European Commission, 2006). The combined emissions of hydrocarbons and nitrogen oxides were also reduced from 0.56 g/km to 0.17 g/km. Since the introduction of Euro 3, the new testing procedure is also used, which saw the removal of the warm up period (vehicle preconditioning procedure). The most recent regulations (Euro 5/6) focused also not only on the mass- based limits but also on particle number emission limits (European Commission, 2013). In addition to that, the recent regulations also impose a number of requirements on the vehicle manufacturers including fitting cars with appropriate devices for controlling pollution and ensuring their longevity.

In the United States, the Environmental Protection Agency (EPA) sets standards related to the allowed amount of pollutants. Equally, the California Air Resources Board is also influential in a number of states. Nitrogen oxides are recognised by the EPA as one of the six principal pollutants (EPA, 2008). The current legislation employed in the US is Federal Tier 2. However, the updated strict rules have not been implemented across all countries, with China only following regulations

similar to Euro 4, with the implementation date of China 5 (equivalent to Euro 5) set for January 2018 (Transport Policy, 2014).

1.2 The impact of evolving regulations

The increase in regulations has put more pressure on companies to develop technologies to meet new legislative demands. Because of the differences between gasoline and diesel engines when using oxygen, it is not possible to use the same technology to reduce engine emissions and new solutions are needed (Heck et al., 2009). After treatment technologies can be the solution for reducing NOx emissions. The difficulties in developing new technologies are reflected in the higher allowance of NOx for diesel engines in comparison to gasoline engines: 0.15g/km and 0.06 g/km respectively (DieselNet, 2013). Table 1.2 presents the effect of Euro 5 and combined effects of Euro 5 and 6 in relation to the reduction of exhaust emissions for gasoline and diesel engines (European Commission, 2006).

Table 1.2 Summary of the effect of Euro5 and combined effect of Euro 5 and 6 (reproduced from European Commission, 2006).

1.3. Diesel CI engine emissions overview

Current diesel CI engines are very efficient and therefore fuel consumption and emitted CO_2 levels are lower in comparison to spark ignition (SI) engines with similar power outputs. In last decade, the constant increase in sale of diesel engine powered vehicles, made them the major source of urban air pollution. The main pollutants emitted by diesel engine are carbon monoxide (CO), unburned hydrocarbons (HC) and NOx, which is composed of nitric oxide (NO) and nitrogen dioxide (NO_2). In comparison to SI engines (but not with gasoline direct injection GDI), current diesel engines emit a high number of particulate emissions, also known as particulate matter (PM) or smoke.

The ignition and combustion process of CI engine is different to conventional SI engine. In the diesel CI engine, the fuel is injected into high temperature and high pressure air (above fuel ignition point) towards the end of the compression cycle. In order to atomise fuel to micro size droplets, the injection happens at a very high pressure. During this short period of time, the fuel evaporates while mixing with air to ignite and start the combustion process. Fuel distribution in a chamber is non-uniform and the combustion is rapid. Literature shows that the fuel distribution (local air fuel ratio- AFR) and combustion temperature have a strong impact on pollutant formation (Heywood, 1988).

The common rail (CR) fuel injection system (developed by Bosch) is a sophisticated commercial DI fuel injection system used in current diesel engines. The CR systems can provide fuel injection at very high pressures, while controlling fuel quantity, rate of injection and injection timing (start and end of injection in relation to crank angle (CA)). Furthermore, the injection can be split into multiple injections, which provides more control over the combustion process (Stumpp et al., 1996).

A schematic of a typical common rail system is shown in figure 1.3a. A high pressure fuel pump driven by the engine supplies fuel into the solenoid injectors via a common rail. High pressure injection can be achieved independently from the engine speed. The individual injectors are controlled by the engine ECU (Denso, 2014).

Figure 1.3b represents the heat release during the major phases of the combustion process for a typical CI diesel engine. Ignition delay, premixed burning, mixing controlled combustion and late burning are the four main combustion phases. Control of the injection timing described above has a crucial effect on ignition delay and consequently on the whole combustion process (Mohan et al., 2013)

Figure 1.3a Common rail system diagram. Injection pressure of 1800 bar (taken from Denso, 2014)

Figure 1.3b Typical heat release rate curve during four major phases of combustion process of a CI engine (reproduced from Mohan et al, 2013).

1.3.1 HC, CO and PM emissions

CO and partially oxidised or unburned HC emissions are the products of diesel incomplete combustion, caused mainly by local over-rich fuel mixture and low flame temperature. Thus, HCs are usually formed during the premixed combustion phase as a result of very rich conditions. Low oxygen conditions also facilitate the increase in PM formation. Studies show that higher injection pressure improves fuel atomization; this improves mixing and the vaporisation process.

Subsequently, the combustion temperature is higher and HC, CO and PM emissions are reduced. The ignition delay has an undesirable impact on HC formation and fuel consumption (Mohan et al., 2013). To reduce the ignition delay, the fuel pilot injection (small fuel dose just before the main dose) has to be introduced before the main injection. It was shown that this has a positive effect on HC and CO emissions reduction, especially during low load and low engine speed operation (Babu et al., 2007). Additionally, at the low engine load, post injection is used to reduce HC and PM emissions (Hotta et al., 2005).

1.3.2 NOx formation and engine-based reduction techniques

During the combustion process, HC, CO and smoke are produced in the richer fuel mixture regions, while NOx is produced in the leaner fuel mixture region by the oxidation of nitrogen. The leaner fuel region corresponds to higher flame temperatures and higher rate of heat release (Heywood, 1988).

Exhaust gas recirculation (EGR) is one of the most effective and commonly used methods for reduction of combustion temperature and subsequently NOx formation. The EGR system recirculates exhaust gas back to the combustion chamber to displace some air. This reduces oxygen concentration (effective AFR), which effectively reduces flame temperature. Figure 1.3.2a specifies how EGR has a significant effect on the NOx emission and also demonstrates that there is a trade-off between NOx and PM formation in diesel exhaust (Johnson, Mollenhauer, & Tschöke, 2010). Furthermore, reduction in NOx formation can be achieved by retarded fuel injection; however this method might have a negative impact on fuel consumption. Therefore, a fine balance is required between EGR rate and fuel injection timings (Mohan et al., 2013).

Figure 1.3.2a Dependency of EGR rate and AFR on DI diesel engine's NOx and PM (Johnson et al., 2010).

The study done by Hotta et al (2005) on the effects of multiple injection on emission formation has shown that the timing of main fuel injection and pilot injection has a significant effect on NOx and PM formation. Figure 1.3.2b shows how NOx can be reduced without the increase in PM by using early pilot injection. Additionally, during higher EGR rates, the fuel consumption, HC and PM formation can be reduced by using after-injection without a significant impact on NOx (Hotta et al., 2005)

Figure 1.3.2b Pilot injection timing effect on emission and noise during low load engine operation (Hotta et al., 2005).

1.3.3 Diesel engine emissions summary

Figure 1.3.3 demonstrates tightening NOx and PM limits since Euro 3 and describes engine based techniques used for emission reduction. Even latest EGR and fuel injection technology together with state of the art engine design are not sufficient to reduce NOx emissions down to required legislation levels of Euro 5/6. In order to pass the required limits, car manufactures are using aftertreatment system as part of an exhaust to reduce tailpipe NOx and PM emissions.

For Euro 4 and 5 PM standards, particulate filters have been introduced as part of the aftertreatment, and currently they are an efficient technology in PM filtration. However, the most challenging pollutant for Euro 6 and onwards is NOx. Therefore, car manufactures have undertaken further work to improve aftertreatment technology.

Figure 1.3.3 Summary of diesel engine evolution from Euro 3 to Euro 6 (reproduced from Bression et al., 2008)

1.3.4 Role of DOC and DPF in diesel engine after-treatment system

DOC and DPF are the essential parts of the diesel after-treatment systems (Kodama et al., 2010). The aim of the DPF is to collect particulates (Zhang et al., 2005). In order to maintain efficient engine performance, these particulates need to be removed during the process of oxidation (Konstandopoulos et al., 2000). There are a number of factors, which need to be considered when choosing a DPF, with filter media (e.g. ceramic vs. metallic) and geometric configurations (e.g. honeycomb design) often recognised as the main ones (Konstandopoulos et al., 2000). DOC is used to remove hydrocarbons (HC) and carbon monoxide (CO). These reactions will depend on a number of factors including the characteristics of the metal, as well as, the conditions of the operating catalysts (Russell et al., 2011). The location of the DOC can also have an impact on the catalyst's temperature, which in turn affects the process of oxidation (Russell et al., 2011).

1.4 Diesel engine emissions after-treatment

1.4.1 NOx after-treatment overview

Current diesel engines are forced to operate at a high air/fuel ratio (AFR) to improve fuel efficiency and reduce CO_2 emissions, which are part of "Green House Gases" (GHG). NOx reduction under excess oxygen (O_2) conditions is impossible with a conventional three-way catalyst (TWC) without the fuel consumption penalty.

To date, the two most common technologies used for diesel engine NOx after-treatment are (Heck et al., 2009; Kodama et al., 2010):

- Lean NOx trap (LNT)
- Selective catalytic reduction (SCR)

1.4.2 Lean NOx traps

Lean NOx trap (LNT) is the NOx reduction technology alternative to SCR, especially where application of a urea dosing system might be challenging. LNT has been used successfully in light and heavy duty applications. The main function of LNT is to store NOx under lean engine conditions and then release NOx under rich engine conditions (rich purge), with subsequent reduction to nitrogen (N_2) (Johnson, 2009).

The main steps of LNT operation are described below (Wang et al., 1999):

Step I
NO is oxidized to NO_2 over Pt under lean engine conditions.

$$NO + \frac{1}{2}O_2 \rightarrow NO_2 \qquad \text{Eq.1.4.2a}$$

Step II
NO_2 is stored on the surface of barium oxide as barium nitrate.

$$BaO_3 + 2NO_2 \rightarrow Ba(NO_3)_2 \qquad \text{Eq.1.4.2b}$$

Step III
Stored NO_2 is released from the LNT during rich engine operation. During this period there is excess of CO, HC and H_2 in the exhaust stream that is used as a reductant for NOx conversion over a Pt/Rh catalyst.

$$Ba(NO_3)_2 \rightarrow BaO + 2NO_2 \qquad \text{Eq.1.4.2c}$$

$$2NO_2 + 2CO/HC \rightarrow N_2 + 2CO_2 \qquad \text{Eq.1.4.2d}$$

$$BaO + CO_2 \rightarrow BaO_3 \qquad \text{Eq.1.4.2e}$$

The illustrated version of LNT working principle is presented in figure 1.4.2a.

Figure 1.4.2a Lean NOx trap working principle under lean (normal engine operating conditions) and rich (high fuel purge engine conditions) conditions. (Reproduced from Bosteels et al., 2002)

LNT NOx conversion performance depends on LNT storage capacity and NOx reduction efficiency over Pt/Rh during the purging phase. A study conducted by Alimin et al. (2009) has shown that at temperatures of 250°C, LNT storage efficiency was only 30%. The NOx storage improves to 80-90% at temperatures of 400°C, but the trap requires frequent rich purges to sustain a high efficiency (Alimin et al., 2009). LNT also depends on Pt loading, particularly at temperatures between 200-250°C. Above 300°C, the Pt loading can be lowered from 100 to 75 g/ft^3 without any impact on the NOx performance, as presented in figure 1.4.2b (Johnson, 2009).

Figure 1.4.2b LNT performance dependency on platinum loading. (Johnson, 2009)

One of the main disadvantages of LNT application is fuel penalty during rich purges which also increases tailpipe CO_2. Another problem is the sulphur intolerance of LNT. The sulphur present in the fuel is absorbed by LNT and has a poisoning effect on alkaline earth metals. During the sulphur exposure, the storage operation function of LNT deteriorates with time, which depends on the sulphur

content. In order to restore the NOx storage capacity, the trap has to be regenerated under excess oxygen conditions and very high temperatures (Bosteels et al., 2002). This increases fuel penalty, which is another disadvantage of the LNT system.

1.4.3 Selective Catalytic Reduction (SCR)

Selective catalytic reduction (SCR) is an established technology for NOx reduction that has been investigated for more than two decades (Birkhold et al., 2006). Moreover, for heavy duty vehicles (HDV) and light duty vehicle (LDV) this technology proved to be the most promising method for NOx after treatment, especially in comparison to, sometimes costly, LNT (Kodama et al., 2010). In recent years, the SCR technology started to be used more frequently in the automotive sector (Johnson, 2009). A reducing agent (urea) is introduced into the exhaust to react with the NOx.

Figure 1.4.3 represents the configuration of a commonly used SCR system with AdBlue (aqueous urea) injection unit designed by Emitec for LDVs. Typically, the light duty after-treatment system contains four major components; diesel oxidation catalyst (DOC), diesel particulate filter (DPF), AdBlue injector and selective catalytic reduction catalyst (SCR). The layout of the SCR system may vary and it will depend on the application; however, the principle and role of each component will be similar.

Figure 1.4.3 Common SCR system configuration with AdBlue injection used in LDV application (avaiable from Emitec).

The SCR reaction is the reduction of nitrogen oxides (NOx) with ammonia from the urea (reductant) by chemical reaction on a catalyst. Because ammonia is not present in an exhaust gas, it has to be supplied to an exhaust system in the form of gas or from urea in a water solution (commercially

known as AdBlue). As the storage of ammonia gas would be hazardous in the vehicle, the commercially used ammonia is supplied in the form of urea that is injected as a water solution. Then, the injected urea is decomposed and hydrolysed in the exhaust to ammonia. This ammonia is absorbed by the SCR catalyst to react with NOx.

When ammonia and NOx are present, there are three main reactions that will occur in the SCR catalyst (Heck et al., 2009). Depending on the NOx content, different reaction will take place.

Standard SCR reaction: $4NH_3 + 4NO + O_2 \rightarrow 4N_2 + 6H_2O$ Eq. 1.4.3a

Fast SCR reaction: $2NH_3 + NO + NO_2 \rightarrow 2N_2 + 3H_2O$ Eq. 1.4.3b

Slow SCR reaction: $4NH_3 + 3NO_2 \rightarrow 3\frac{1}{2}N_2 + 6H_2O$ Eq. 1.4.3c

Apart from these three main reactions, there are also side reactions that may occur on the catalyst which are less desirable (Sjovall et al., 2009). For example, ammonium nitrate (NH_4NO_3) can be formed at low temperatures described by equation 1.4.3d, and then decomposed at higher temperatures to NOx. Also, N_2O formation can occur.

$4NH_3 + 4NO_2 \rightarrow 2N_2 + 2H_2O + 2NH_4NO_3$ Eq. 1.4.3d

Another undesirable reaction is oxidation of ammonia. At high temperatures ammonia can oxidise (Eq. 1.4.3e) and become unavailable for the SCR reaction with NOx. This can reduce performance of the SCR catalyst. In order to compensate for the loss of ammonia, more urea will have to be injected.

$4NH_3 + 3O_2 \rightarrow 2N_2 + 6H_2O$ Eq. 1.4.3e

1.4.4 SCR reductant

Ammonia is a commonly used agent to react with NOx on the catalysts. Due to well-known difficulties with safety and storage (Koebel et al., 2000; Yi, 2007), the urea-water solution is a preferred choice over gaseous ammonia (Yi, 2007). It is usually injected into the exhaust gas stream as a spray and goes through a number of reactions (Koebel et al., 2000). Firstly, it undergoes atomisation as the interaction between liquid jet and gas phase occurs. The atomisation of the liquid jet is an important process as it impacts not only the drop size distribution but also the distance travelled by droplets. The atomisation also depends on a number of factors including exhaust gas flow, injection parameters and the liquid wall impingement (Yi, 2007). Atomisation leads to evaporation of water from the droplets, which results in the following reaction (Koebel et al., 2000):

$NH_2\text{-}CO\text{-}NH_2$ (aqueous) $\rightarrow NH_2\text{-}CO\text{-}NH_2$(solid)$+xH_2O$(gas) Eq. 1.4.4a

Under heat, urea will decompose at temperatures above 137°C to ammonia and isocyanic acid. The next stage involves the hydrolysis of isocyanic acid to ammonia on the surface of the SCR catalyst. All three processes: atomisation, evaporation and hydrolysis may occur on the surface of the catalyst when the position of the injector is closely located to the front of the catalyst (Koebel et al., 2000).

1.4.5 SCR potential limitations

It is important to also acknowledge potential limitations of the SCR systems. Narayanaswamy and He (2008) pointed out that the SCR technology used in light duty diesels is complex, mainly due to the use of urea reductant required for the SCR reactions. The complexity of on-board urea injection system is demonstrated in figure 1.5.4. This has an impact on the overall costs of the SCR system, even though urea itself is cheap.

Current SCR systems are also equipped with a urea mixer in order to reduce the possibility of urea deposition along the system and on the catalyst substrate. They are rigorously designed to improve evaporation and atomization of the urea droplets and to ensure uniformity of droplet distribution (Zheng et al., 2009). Finally, it is essential to highlight that during certain operating conditions there is a possibility of ammonia slip into the atmosphere.

1.4.6 Comparison of SCR with LNT

NOx removal performance of a small LNT catalyst might be sufficient for smaller engine (less than 2.0 litres) applications. Therefore, LNT system with lower precious metals loading might be a preferable as a cheaper alternative to the SCR with its complex urea dosing system (Johnson, 2009).

While LNT has its advantages, as described above, the use of SCR technology has particular benefits. These include: more effective NOx conversion across a wide range of engine operating temperatures, no fuel penalty due to lack of rich purges and lower catalyst costs due to lack of precious metals. Moreover, SCR catalysts are exposed to lower temperatures and as a result have greater durability (Narayanaswamy et al., 2008). Consequently, the SCR system has become the system of choice for passenger car manufacturers and are the subject of the study in this thesis.

1.5 Overall aim of SCR studies

The overall long term aim of the SCR study described in this thesis is to improve SCR performance through the development and subsequent optimization of an SCR model. This project complements this aim by studying and investigating SCR behaviour and performing real engine tests. This study thus focused on providing reliable data for SCR modelling.

1.6 Outline of the thesis

In order to achieve the aim stated above, this thesis describes the work carried out in detail in the following chapters.

- Chapter 2 will provide an overview of the literature related to the recent developments in relation to the SCR and sets four specific objectives for this work.
- Chapter 3 describes the methodology of the project.
- Chapter 4 describes and discusses the experimental results.
- Chapter 5 provides a summary of the key findings, their significance and suggestions for future research.

Chapter 2: Literature review of SCR

2.0 Selective catalytic reduction (SCR) overview

In the context of the challenges outlined earlier, close monitoring of NOx became the priority. It was and is important to develop new technologies, which can help to reduce harmful pollutants (Parks et al., 2000).

2.1 SCR catalyst types and application

Depending on the operating temperature, there are three types of material presently used for the SCR catalysts. These are platinum, vanadium and zeolite. Platinum catalysts are the catalysts designed to work at very low temperatures (175 - 250^{o}C), while vanadium is used for medium temperatures (300 – 450^{o}C), and zeolite is used for high temperatures (350 – 650^{o}C) (Heck et al., 2009). Because of a very narrow operating temperature window of the platinum based catalyst, their application is very limited and therefore, the focus of this review will be on vanadium and zeolite based catalysts.

2.1.1 Vanadium based catalyst

Due to limitations with platinum based catalysts, other materials such as vanadium V_2O_5, that operates best between 260 ^{o}C and 450 ^{o}C, have been studied extensively. However, while the operating temperature window is wider for V_2O_5 catalyst, the NOx conversion is limited. A modified V_2O_2/TiO_2 catalyst has shown improved selectivity to N_2 and a better durability. It also has a wider temperature window, see figure 2.1.1. This type of catalyst has been used widely in heavy duty applications. However, there are some safety contraindications for the use of vanadium (Costigan et al., 2001).

Figure 2.1.1 NOx conversion of conventional and improved vanadium SCR catalyst (Heck et al., 2009).

2.1.2 Zeolite based catalyst

Low and high temperature types of zeolite catalyst were developed to further improve the stability of the vanadium based SCR catalyst. The low temperature zeolite operate best at temperatures between 150 – 450^{o}C, while the high temperature zeolite are designed to best operate between 350 – 600^{o}C.

The main components of mordenite zeolite are SiO_2 and Al_2O_3 with a ratio of 10:1 used for high temperature zeolite catalysts that can operate up to 600^{o}C without the ammonia oxidation to NOx. This gives mordenite zeolite a substantial advantage over platinum and vanadium SCR, i.e. it is free from expensive precious metals. However, at 600^{o}C temperature it can be permanently deactivated by the process called de-alumination (Heck et al., 2009).

For the light duty vehicle applications, new types of zeolite were developed to operate at low temperatures. By using either copper (Cu)-based zeolite or iron (Fe)-based zeolite, the activity can be improved for temperatures of 200 – 400^{o}C. Castagnola et al. showed that Cu-based zeolite offered better selectivity at lower temperatures compared to Fe-based zeolite (Castagnola et al., 2011). However, Cu-based zeolite SCR after exposure to sulphur (S) showed deactivation at low temperatures.

Grossale et al. compared the performance of the Fe zeolite SCR with vanadium based zeolite and the outcome is presented in figure 2.1.2a (Grossale et al., 2008). In the presence of NO_2:NOx ratio of 0.5, the Fe zeolite catalyst shows a higher activity at low temperatures (225 - 325^{o}C), then with increasing temperature the difference is reduced. However, above 450^{o}C, the selectivity to N_2 of vanadium catalyst is reduced by the increased rate of ammonia oxidation.

Figure 2.1.2a NOx conversion profiles for Fe and vanadium based zeolite catalyst at range of temperatures. Supplied NO_2:NOx ratio was 0.5 and SV=126000 h^{-1} (Grossale et al., 2008).

Kamasamudram et al. (2010) also studied the performance of Cu and Fe based zeolite catalysts over a temperature range of 200 – 600°C and using different NO_2:NOx ratios- this can be seen in figure 2.1.2b. It was demonstrated that the NOx conversion of Cu-based zeolite was superior to the Fe-based zeolite at temperatures of 200 – 300°C when the NO_2:NOx ratio was zero (Kamasamudram et al., 2010). Fe-based zeolite showed better performance at very high temperatures. When NO_2:NOx ratio was increased to 0.5, the low temperature NOx conversion was identical, and again, Fe-based zeolite performed slightly better at 500 – 600°C. Figure 2.1.2c compares the transient response at 250 °C between Cu and Fe based zeolite at NO_2:NOx ratio of 0.5. It was also observed that Fe-based zeolite had lower storage capacity and faster transient response curve. This means that peak performance could be reached quicker with less ammonia supplied, which might be beneficial under some circumstances. However, controlling the ammonia storage level in order to maintain a desirable NOx performance will be more difficult. Also, because of the sensitivity of Fe-based zeolite to supplied NO_2:NOx ratio, the calibration of SCR system could prove problematic and costly for it to reach its full potential.

Figure 2.1.2b NOx conversion profiles for Cu and Fe based zeolite. NO_2:NOx ratio was 0 and 0.5. SV 40,000 h^{-1}. (Kamasamudram et al., 2010)

Figure 2.1.2c NOx conversion against ammonia storage at 250°C for Cu and Fe based zeolite at NO_2:NOx ratio 0.5. SV=40,000 h^{-1}. (Kamasamudram et al., 2010)

Sultana et al. (2011) reported that zeolite structure, acidity and copper content are major parameters that influence performance of Cu-zeolite based catalyst. Measurement of ammonia desorption profiles showed that Cu/MOR and Cu/ERI had much weaker acid site strength compared to Cu/ZSM-5 or Cu/FER. It was expected that a stronger acid site would show a higher activity. However, below 300 °C, the highest NOx conversion was observed for Cu/ZSM-5 and Cu/ERI. Figure 2.1.2d shows NOx conversion profiles of four studied Cu zeolites. It was concluded that apart from acid strength of the zeolite, the NOx conversion was also influenced by a number of isolated Cu2+ species.

Figure 2.1.2d The comparison of NOx conversion profile of different Cu zeolites (Sultana et al., 2011)

To summarise, the advantages of using copper zeolite catalysts include wide ranging temperatures, in particular high NOx conversion in the region of 180 to 500°C and higher ammonia storage of Cu-zeolite SCR, which gives a more stable NOx performance over transient cycle and a very good durability.

2.2 Importance of SCR copper zeolite testing and modelling

As SCR modelling becomes part development, and part optimization tool of the future aftertreatment systems, there is a need to conduct studies exploring the behaviour of the SCR catalysts under various conditions. SCR NOx reduction systems have been initially used in heavy duty vehicles and majority of evidence comes from studies based on vanadium SCR catalysts (Benjamin et al., 2011)However, in light duty diesels, due to its wide-ranging operating temperature, zeolite catalyst, and particularly Copper zeolite, has started to become widely used for NOx reduction. Consequently, there is a need for more studies to explore the behaviour and characteristics of copper zeolite SCR.

Testing under steady test conditions is usually a starting point for building an SCR model in order to optimise a number of parameters. These include the rate constants for the main SCR reactions (equation 1.4.3a-c), including ammonia and NO oxidation. Moreover, the kinetics of ammonia

adsorption and desorption are also an important part of that. Narayanaswamy and He (2008) highlighted that it is important to understand SCR catalyst behaviour under various conditions that it will be exposed to during engine operations.

2.2.1 SCR copper zeolite testing under steady and transient conditions

2.2.1.1 Steady state testing

Steady state testing is a very important benchmarking tool during the SCR catalyst development process. It allows a comparison of different SCR catalyst technologies at chosen conditions and helps in understanding the mechanisms and reactions. The idea behind the steady state testing is to measure catalyst performance under pre-defined conditions such as temperature, flow rate, or gas mixture. Tested catalyst has to be exposed to these conditions for a time period long enough to allow attainment of stable NOx or ammonia slip concentration.

Results from recent studies in steady state conditions showed that models are better at predicting for high temperatures than for lower temperatures. During the SCR kinetic modelling development, Watling evaluated SCR behaviour under high NO_2:NOx, range of temperatures from 150 to 500°C and NH_3:NOx=1. Catalyst tests were performed with three NOx concentrations. However, only a small effect on conversion was observed by increasing NOx from 100 to 200ppm, as shown in figure 2.2.1a. Overall, model showed a very good prediction at temperatures above 250°C; however, conversion was over predicted at 150 and 200°C by 40% (Watling et al., 2011). Future SCR applications in LDD will require operating at low temperatures (200°C and below). Therefore, it is important that kinetics can describe SCR behaviour also in these conditions.

0

Figure 2.2.1.1a Cu zeolite model (solid lines) comparison with measured steady state data (points) for NO_2:NOx=0.7 (Watling et al., 2011).

Narayanaswamy and He, (2008) also tested copper zeolite catalysts using a gas reactor under four NO_2:NOx ratios (0, 0.5, 0.25 and 0.75). Both catalysts have been tested under a range of temperatures of 150-550°C. Apart from conditions described above, two space velocities of 25k and 50k h^{-1} were chosen to test the copper zeolite catalysts. Correlation of the model with experimental data showed quite good agreement for NO_2:NOx 1 and 0.25 for most of the simulated temperatures. However, for NO_2:NOx 0.5 and especially 0.75, the model was under predicting NOx conversion at low and high temperatures. Consequently, previous work conducted at Coventry University by Sturgess focused on low temperature operation (just above 210°C) and space velocity effect on SCR (Benjamin et al., 2011; Sturgess, 2012). Importantly, instead of a gas reactor, a real engine exhaust was used for testing. Modification to the existing kinetics lead to a good agreement between data and experiment for inlet NO_2:NOx ratio close to 0.5. However, similarly to Watling et al (2011) it was also concluded that the model was over predicting NOx conversion at NO_2:NOx above 0.6.

Although, the gas reactor testing is the simplification of real engine conditions, it substantially reduces testing time and cost. Moreover, the specific gas mixture or flowrate can be easily adjusted from test to test. However, reactor testing requires the use of ammonia gas instead of urea injection (no urea decomposition and hydrolysis). In addition, it is also important to highlight that real engine exhaust produces soot and hydrocarbon so the exhaust composition is more complex.

2.2.1.2 Engine transient testing

Vehicle after-treatment systems need to pass a number of tests in relation to the NOx tailpipe emission under pre-defined driving cycles. In order to understand the performance of the SCR catalysts, it is crucial to undertake testing under transient conditions, as they resemble to a great extent the behaviour of SCR under real-world driving conditions. However, the behaviour of the SCR catalysts under these real-world driving conditions is very complex; therefore the simplification of these conditions is necessary in order to understand the SCR process. As a result, a number of studies have focused on conducting transient testing.

Wurzenberger and Wanker developed a very simple transient test with ammonia concentration ramp from 0-840 ppm while supplied NO was constant at 750ppm (Wurzenberger et al., 2005). The temperature and the flow of the system were also kept constant (280°C, SV=140k h^{-1}). This test was particularly beneficial to examine the kinetics for the adsorption and desorption of ammonia, which takes place on the catalyst. Narayanaswamy and He (2008) have recently conducted a more complex transient testing on a reactor on a Cu- and Fe- zeolite using step-transient conditions of NH_3:NOx ratio and its effect on the NOx conversion efficiency. During the period of 240s, the NH_3:NOx ratio initially equalled 1 and then it was changed every 30s of the test between the excess (2:1) and deficient (1:1.7) ratio. The gas stream feed also contained 8% O_2, 5% H_2O and 5% CO_2. The sequence was repeated three times and the reactor temperature was controlled at 225°C or 450°C.

The results from NOx performance were used for an SCR model validation, which showed a good correlation during the steady state period. However, the NOx conversion was slightly over predicted by the model during transient intervals. While they have demonstrated a good correlation between model and data obtained, it is important to note that data used for the model validation was gathered using gas reactor.

Chatterjee et al. have undertaken tests on two types of catalysts (vanadium- and zeolite-based); however, they were tested only under steady state conditions (Chatterjee et al., 2007). They used SCR model built for vanadium and zeolite based catalysts in order to predict the real engine transient cycles and compare the behaviour of the two catalysts. However, the model was used to make predictions but was not based on transient experimental data.

Watling et al (2011) have developed a model for a copper zeolite catalyst, based on some steady state and transient testing using gas reactor. The main aim of their study was to build a model, which could predict NOx performance over the legislation-based requirements for transient cycles. The model showed good NOx predictions over the NEDC cycle; however, for the HD-FTP and the NRTC it had the tendency to under predict. This was especially the case with the increased NO_2 to NOx ratio. The model also showed a good NOx conversion prediction when increasing the supplied NH_3. During majority of the tested cycles, ammonia slip was overpredicted, which the authors attributed to the sensitivity of the ammonia measurement or to the incomplete hydrolysis of urea to NH_3, as the model assumed that 100% of urea was hydrolysed.

2.2.2 Effect of flow and 3D geometry on SCR performance

Constantly tightening legislation in relation to NOx emissions for passenger cars, has meant that the SCR system needs to deliver a maximum performance. Therefore, it is important that the application of the SCR catalyst is most efficient. Flow distribution and reactant uniformity are crucial in achieving high NOx conversion efficiencies from the SCR system. However, this is not easy to achieve with constrains related to packaging, geometry of pipe bend and short distances between urea injector and SCR catalyst leading to mixing difficulties. Therefore, it is important to investigate the performance of exhaust gas flow through after-treatment system. The uniformity index and velocity ratio are tools commonly used by car manufactures to describe flow properties during exhaust design process. It was found that SCR system characterised by a lower uniformity index showed reduced NOx conversion and higher NH_3 slip which is illustrated in figure 2.2.2a (Johansson et al., 2008).

Figure 2.2.2a Effect of uniformity index on NOx conversion and NH_3 slip. Data obtained using CFD tool (Johansson et al., 2008).

Jeong et al. (2008) investigated the extent to which ammonia concentration distribution was uniform at the entrance of the SCR catalyst as a function of urea dosing location in the exhaust and the injection angle. The study was conducted using CFD model based on a heavy-duty diesel exhaust with a mobile SCR system. The performance of SCR catalyst was examined by measuring the amount of NOx conversion and NH_3 slip. The results showed that the injector position had a bigger impact on the NH_3 concentration uniformity and the SCR performance than the injection angle. The uniformity of NH_3 concentration improved as a function of increased distance between the SCR catalyst and injector location (Jeong et al., 2008).

The impact of mass flow rate and pulsation frequency on flow distribution across the catalyst monolith was demonstrated by Liu et al. (2003). It was found that for flow at high Reynold number the velocity profile was mainly focussed in the middle of the catalyst (Liu et al., 2003).

2.3 Rationale for this thesis; novelty of the current studies

This chapter has provided a summary of the SCR technology including its description, application and development. This is especially important as the NOx regulations are imposing more and more requirements on the car manufacturers. In order to facilitate the development of the SCR technologies and their application, computational modelling has become one of the main areas of focus. A number of studies were conducted with the aim of understanding the SCR behaviour. As diesel engines became more efficient, exhaust gas temperatures were reduced, which subsequently created more

challenging conditions for the SCR catalyst operation. Thus, copper zoelite became the number one choice for the LDD vehicles application. However, the review has also identified a number of limitations in the currently available data.

- To date, most kinetics studies have been undertaken using laboratory scale gas reactors with NH_3 gas as reductant and were based on HDD engines. As previously described, a gas reactor is a simplification of real engine conditions. The current study addresses this gap and examines the SCR performance using real engine exhaust conditions on a LDD engine with ammonia and urea injections.
- Previous studies have assumed that all urea is hydrolysed to NH_3 and most SCR models are based on this assumption. However, it is important to ascertain whether this assumption is correct. This thesis assesses the validity of this assumption by comparing NH_3 and urea in injection.
- A number of studies have been conducted to understand the SCR behaviour in a wide range of temperatures. However, models were limited in predictions particularly at low temperatures. Therefore, it is important to study Cu zeolite SCR behaviour at low temperatures and high NO_2:NOx ratio. This thesis will focus on low temperatures only in order to understand the SCR behaviour under these conditions.
- The literature has shown that there is a limited number of studies undertaken under transient conditions, which aimed to provide a detailed understanding of the SCR behaviour under these conditions. There is a need to examine the underlying mechanisms of the SCR reactions under such transient conditions.
- Most of SCR kinetics have been developed using 1D reactor data which does not capture the complexity of real engine exhaust flow interaction with the SCR behaviour. This thesis will investigate the effect of 3D diffuser geometry on SCR NOx and NH_3 conversion.
- There is limited evidence on the SCR performance as a function of catalyst length. There is also a need to focus on high space velocities to understand reactions occurring in the front section of the SCR catalyst.

2.4 Objectives of the project

The gaps in knowledge identified by the literature survey will be addressed in this study by the following objectives:

- To examine the SCR performance on a Light Duty Diesel (LDD) engine under steady state and transient conditions using real engine exhaust designed as a 1D system with NH_3 injection and various NO_2:NOx ratios.

- To study and compare the SCR performance with urea injections and ammonia under steady and transient engine testing conditions.
- To improve SCR performance through the development, and subsequent optimisation of an SCR model.
- To investigate the effect of 3D diffuser geometry on SCR NOx and NH_3 conversion.

Chapter 3: Experimental methodology

3.0 Overview

Details of engine test cell, the engine and the exhaust system configuration are described in this chapter. Moreover, ammonia gas dosing control and urea injection system are covered. The steady state and transient testing procedures and operation are also explained along with the application of gas emissions analysers, and their calibration.

3.1 Engine and test cell

The engine used for this study was a modern light duty 2.2 litre Ford Puma (5FM) diesel engine with common rail fuel injection technology. Full specification of the engine is detailed in table 3.1. Figure 3.1a shows the engine mounted to the test bed. The engine was turbocharged using a variable geometry turbo-compressor and charged air temperature was controlled by an intercooler. The amount of air going through the air box was monitored using a mass flow meter sensor (OEM engine MAF). In order to control engine NOx emission, the engine was equipped with exhaust gas recirculation known as the EGR system. To improve a resolution of measured NOx by gas analysers, the EGR control unit was deactivated resulting in an increased engine out NOx concentration. The ECU shown in figure 3.1a (view B) was responsible for engine operation and management. Charged air was cooled down with water intercooler keeping a constant temperature of supplied air to the engine, which was crucial to achieve test-to-test repeatability.

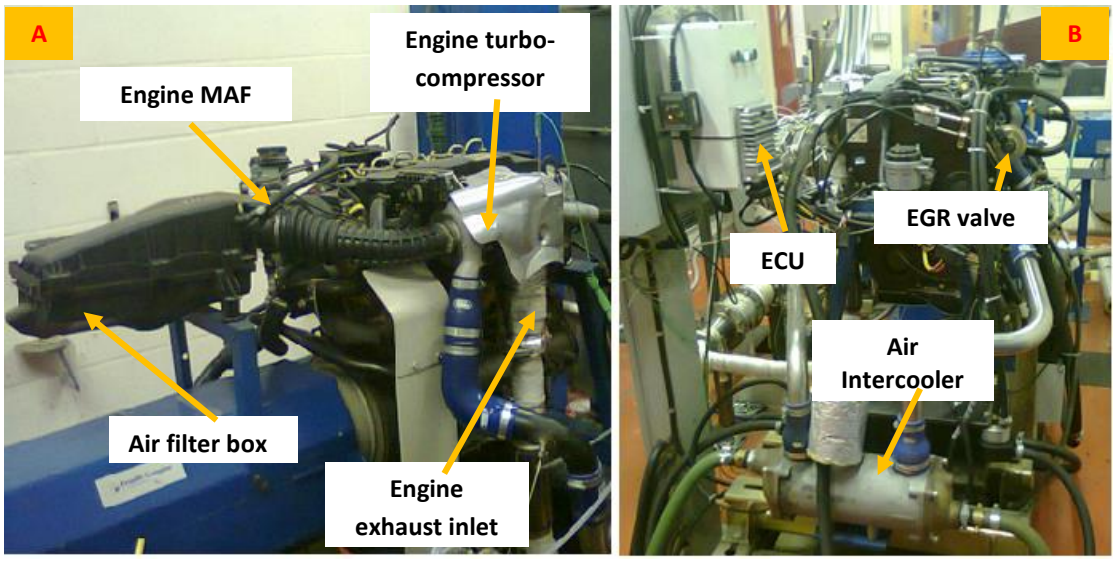

Figure 3.1a Ford Puma 2.2 litres 5FM diesel engine mounted into engine dynamometer. View A: Location of air filter box, Mass Flow Meter (MAF), exhaust inlet. View B: Control Unit (ECU), Exhaust Gas Recirculation (EGR) and Intercooler.

Table 3.1 Ford Puma 5FM engine specification.

Items	Description
Engine capacity	2198 cc
Compression ratio	18.2:1
Number of cylinders	4 inline
Rated maximum power	96.9 kW at 3800 rpm
Rated torque	330 Nm at 1800 rpm
Fuel injection type	Common rail direct injection
Aspiration	Turbo charged

The engine dynamometer used for engine testing was a Froude Hofmann Alternating Current (AC) AC150 motor. The dynamometer was using AC motor responsible for braking the engine. The engine load was controlled via a calibrated throttle control unit. The engine speed and load was controlled by Froude Texcel V12 operating system in a dedicated control room. Temperature and pressure sensors were connected through the transducer box, as shown in Figure 3.1b. The engine mass flow rate data was logged via GREDI, which was connected to the engine ECU.

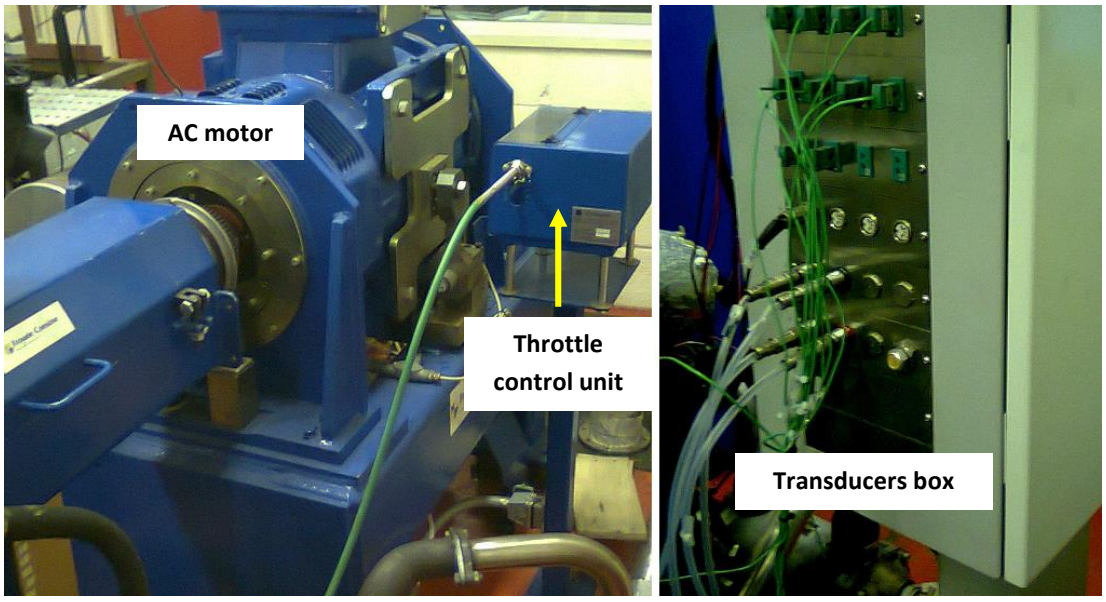

Figure 3.1b Froude Hofmann AC 150 dynamometer and transducers box.

3.2 SCR Exhaust System Setup

For the purpose of this study, the engine OEM exhaust system was replaced with a custom made SCR system, which was designed and constructed at Coventry University. Johnson Matthey supplied the catalysts, while some of the canning work was done by Faurecia. Figure 3.2a is a schematic diagram of engine test cell with SCR exhaust experimental setup.

The exhaust system contained five major sections:

- DPF and DOC assembly was the first section of the exhaust system. The DPF catalyst was responsible for controlling the filtration of soot produced by the engine operation. The DOC was used to remove HC and CO, and to control the amount of oxidised NO to NO_2. In order to make sure that NO_2 produced by the DOC did not react with the soot on the DPF (passive soot regeneration), the DOC was located downstream of the DPF. The DOCs were generally standard DOCs. Pd only DOC functioned as "zero" DOC; it removed HC and CO but did not oxidise NO to NO_2
- An expansion box was designed to provide a uniform mixing of dosed ammonia with exhaust gas.
- The oblique pipe was used with a mixer body downstream during experiments with urea injection.
- The long expansion diffuser was used to ensure uniform gas distribution upstream of the SCR catalyst used for 1D study. The 1D diffuser was interchangeable with a sudden 180^o expansion cone, which was used for the 3D study. This provided a maldistributed flow profile, which was used in modelling study.
- A SCR catalyst was located between two instrumentations cans which allowed for emission sampling, temperature and oxygen level monitoring.

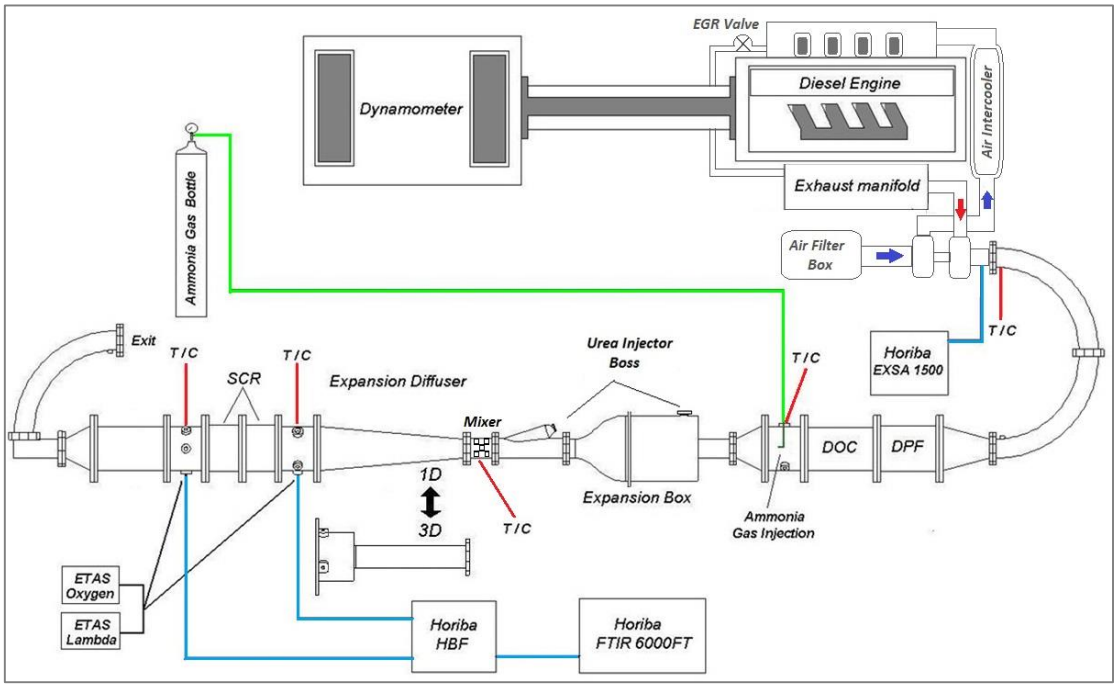

Figure 3.2a: Schematic diagram of the experimental test exhaust connected to the 2.2 litre Diesel engine, showing the expansion box and the angled side branch pipe downstream of the converging nozzle, which were the alternative points for the introduction of urea spray.

3.3 Ammonia Gas Injection

The reductant for the SCR catalyst was supplied in the form of 5 % ammonia gas balance N_2. Removing the complex hydrolysis process of urea from the SCR reactions, allowed the tests to provide more understandable data describing the SCR performance for CFD modelling.

Ammonia gas was supplied from the pressurised bottle at 150 bar. The pressure was reduced to 1.5 bar before it was delivered to gas flow meter shown in figure 3.3a and then was supplied to the gas injection nozzle through the pipeline. The injection nozzle schematic shows the nozzle pointing in flow direction, see figure 3.3b. The amount of dosed ammonia was controlled by the needle valve. The flow meter was only used as a reading guide. The desire amount of dosed ammonia gas was set up by measuring NH_3 concentration in the exhaust gas by FTIR.

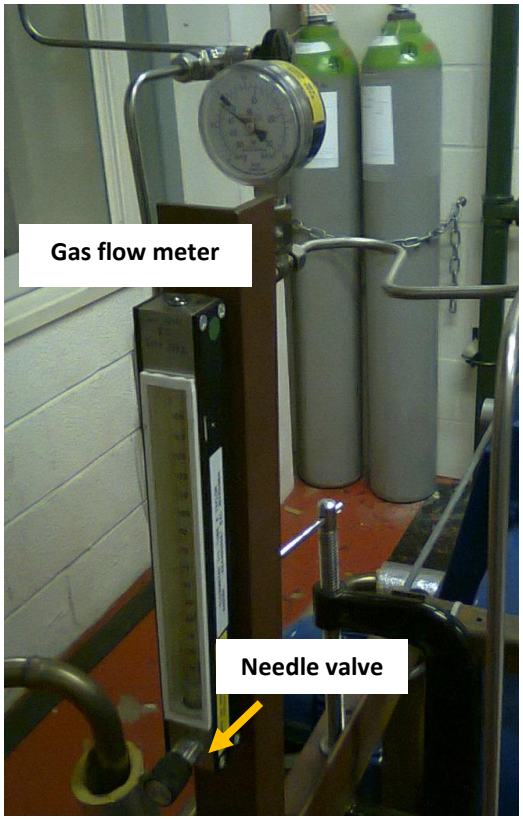

Figure 3.3a Gas flow meter with needle valve used to control dosed NH_3 gas.

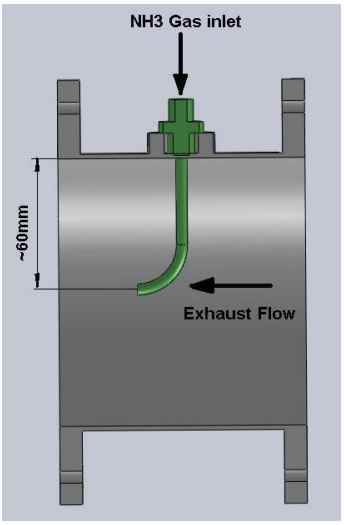

Figure 3.3b Gas injection nozzle.

3.4 Urea in water solution (Adblue) injection system setup

For the urea injection experiment, a custom-build rig was used. The urea was injected using prototype urea injector that was operating under 4.5 bar pressure while nozzle frequency was controlled at 4 Hz. The injector control unit was responsible for the setup of the pulse length. Therefore, a desirable amount of urea could be injected. Figure 3.4a shows the layout of urea injection system in the test cell.

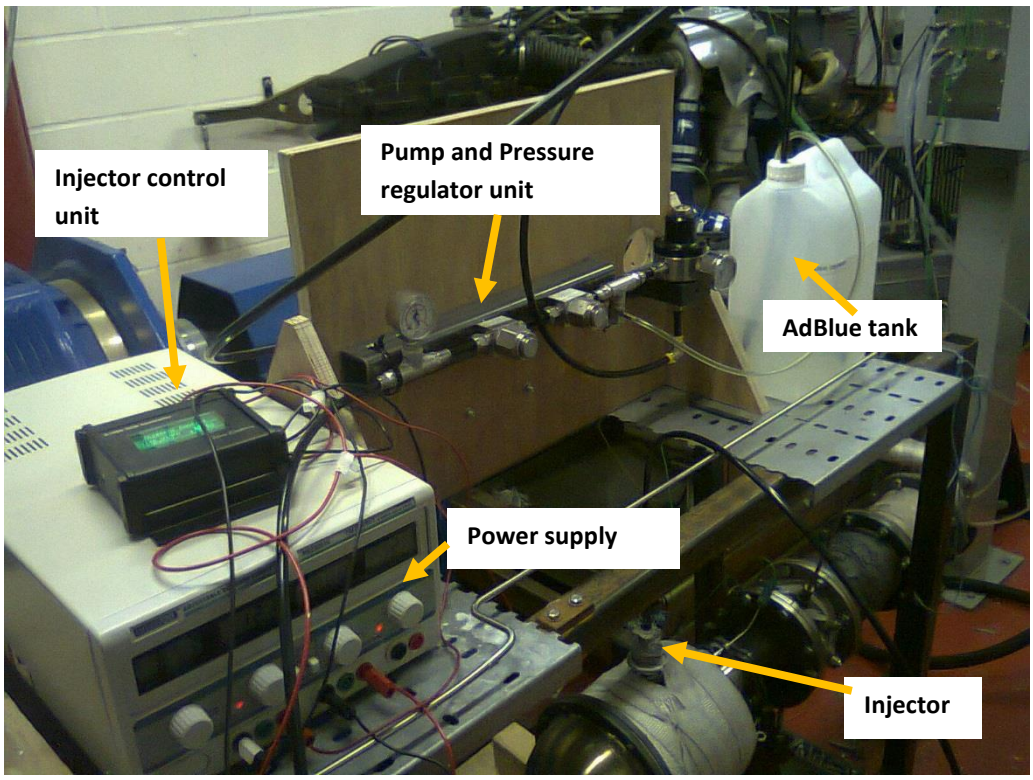

Figure 3.4a Urea injection system layout.

Before testing, the urea injection system was calibrated, by measuring the weight of injected water into a sealed bag at specified injector pulse length. By knowing the weight of the empty bag and bag with water collected in a fixed amount of time, water flow rate could be calculated. Figure 3.4b shows the calibration curves of urea injector after three repeated tests. Correction was made for the different densities of water and aqueous urea solution when using calibration curve.

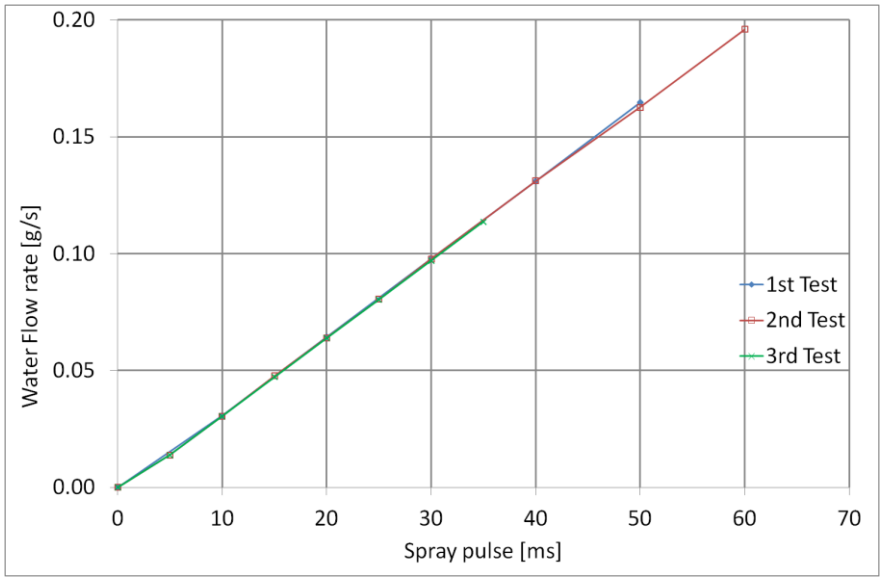

Figure 3.4b Calibration curves of urea injector.

3.5 Engine emissions gas analysers

The composition of the exhaust emissions were measured using gas analysers. These were Horiba EXSA 1500 analyser, Horiba 6000FT FTIR Analyser and Cambustion CLD500 Fast NOx Analyser.

3.5.1 Horiba EXSA 1500 analyser

A Horiba EXSA 1500 analyser was used for monitoring engine out emissions during each experiment. It was used mainly as a reference analyser to provide data for NOx, CO, HC and O_2 that were produced from each test. The collected emission data was very important for tracing potential engine operation problems, thus preventing problems with reliability of the experiments. Figure 3.5a shows specification of Horiba EXSA 1500 analyser used in the experiments used in this thesis. A more detailed description is provided in Appendix 1.

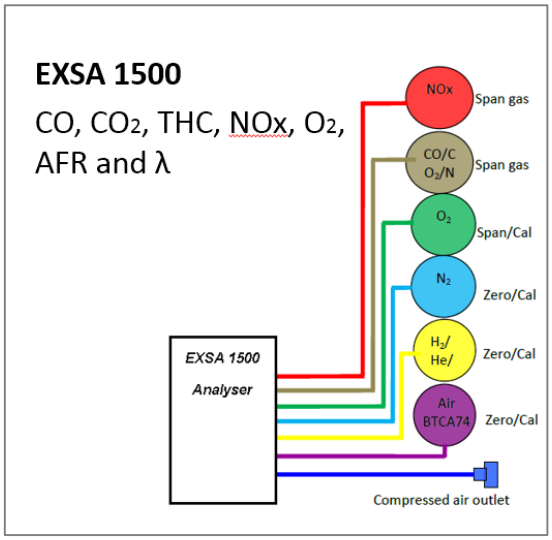

Figure 3.5a Horiba EXSA 1500 analyser sample gas piping layout.

3.5.2 Horiba 6000FT FTIR Analyser

A Horiba 6000FT FTIR analyser was used for measuring the gas composition upstream and downstream of the SCR. The analyser was able to measure NOx, NO, NO_2, NH_3 and N_2O simultaneously with a high resolution. The sampling emission line and external HBF unit was heated to 113 °C. HBF unit had two sampling lines, which were connected before and after the SCR catalyst; this facilitated a switch between two sampling points. Table 3.5.2 shows the full specification of the FTIR analyser used in the experiments in this thesis. There is further information in Appendix 1.

Table 3.5.2 Performance of Horiba 6000FT FTIR analyser (Horiba, 2015)

3.5.3 Cambustion CLD500 Fast NOx Analyser

Cambustion CLD500 Fast NOx Analyser was designed to measure NOx , NO, NO_2 at very high sample rates. The analyser was mainly used during short transient testing to sample emissions with high resolution. The specification of the Cambustion CLD500 Fast NOx Analyser is presented in table 3.5.3. Further information in relation to the piping layout for the calibration gases are described in Appendix 1.

Table 3.5.3 Specification of Cambustion CLD500 Fast NOx Analyser (Cambustion, 2014).

3.6 Test procedures plus engine testing conditions

3.6.1 Cleaning the DPF

To remove any soot and particulate matter, the DPF was located upstream of the DOC, as presented in figure 3.2a. In order to achieve repeatability of engine conditions, cleaning the DPF was introduced before each experiment; this involved removing the DPF filter from the exhaust system to clean the soot. Conventionally, the soot on the DPF is removed using an engine regeneration mode; however, multiple regeneration cycles might have a negative effect on the engine life.

3.6.2 Emission gas analysers; set up and calibration procedure

Before the experiment, a number of steps was required in order to set up each emission analyser. The main steps required across all types of analysers included the filter check, warm-up, purge, calibration and gas span check. Filters were changed on a weekly basis; however filters were also examined before each test and replaced if necessary. Two metallic filters used in EXSA 1500 and

HBF unit required cleaning every month in an ultrasonic bath. The warm-up phase required analyser detector and sample gas heated lines to achieve an operating temperature. Then, each analyser was purged for 60 s with nitrogen and performed zero calibration followed by a gas calibration. To achieve high accuracy in NOx and NH_3 measurement, the FTIR analyser was additionally span checked with certified NOx, NO_2 and NH_3 gas bottles. The sampling gas lines weere cleaned and dried on a monthly basis to prevent any contamination.

3.6.3 Engine warm up procedure

After the engine was started, it operated at 1500 rpm and 4 bar BMEP load until water coolant temperature reached 50 °C. Then, engine load was increased to either 6 or 8.5 bar depending on type of experiment. The experiment commenced after NOx concentration and SCR inlet temperature have reached required steady state.

3.6.4 Engine steady state testing

During steady state engine testing, engine was operating at a constant speed of 1500 rpm and the engine load was set to either 6 or 8.5 bar BMEP. The 6 bar BMEP load was used to test the low temperature (~210 °C) SCR performance and 8.5 bar BMEP load was used to test the high temperature (~260 °C) SCR performance. The conditions for both tests are described in table 3.6.4. Since engine EGR was disabled, the produced engine NOx was significant for both conditions.

Table 3.6.4 Conditions for steady state engine testing.

Test name	Engine load – BMEP [bar]	Engine Speed [rpm]	Engine mass flow rate [kg/h]	Engine out NOx level [ppm]	Inlet SCR temperature [°C]
Low temperature test	6	1500	~110	580 - 620	~ 210
High temperature test	8.5	1500	~118	780 - 810	~ 260

Figure 3.6.4a describes experiment procedure using low temperature test; the same principle was applied to a high temperature test. At the beginning of experiment, the FTIR analyser was measuring emissions upstream of the SCR. The ammonia gas dosing was set up to achieve NH_3:NOx (α) of 0.5, 1 and 1.25 based on measured ammonia (blue line) and NOx concentrations (red line). Then, ammonia gas was turned off and after 5 minutes, the FTIR analyser was switched to measure emissions post the SCR. Using the same ammonia gas dosing set points, the ammonia was dosed starting from α=1.25. The dosing continued for the time period to allow NOx and NH_3 slip to reach stable conditions; then, the same procedure was repeated for α=1 and α=0.5 dosing. After ammonia gas dosing was completed, the FTIR was measure until NOx concentration returned to an initial value

and then FTIR was switched to measure emissions upstream of the SCR catalyst. During this period, the ammonia gas dosing was repeated to check values of dosed ammonia during the experiment.

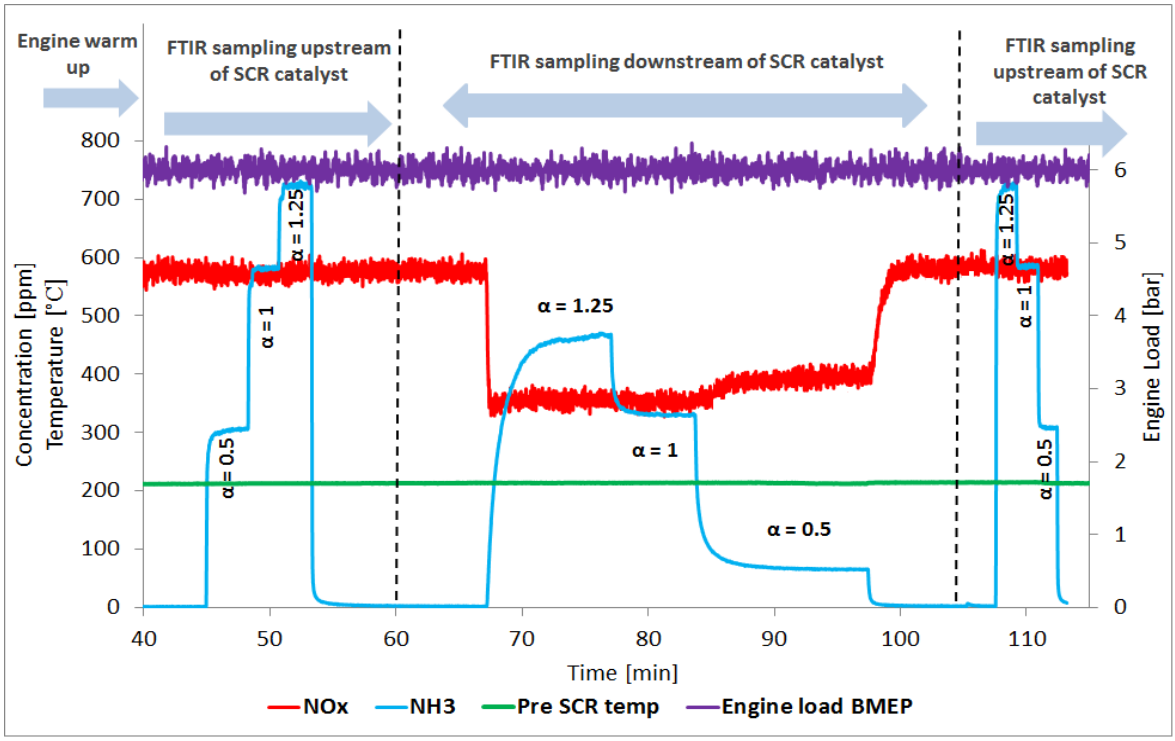

Figure 3.6.4a Example of steady state test procedure with NH_3 gas injection.

3.6.5 Engine transient testing

Two types of transient engine experiments were designed to examine the SCR catalyst under changing conditions; these were short and long transient tests. During the short transient test, the engine speed was kept at 1500 rpm and the initial load was 6 bar BMEP. Then, engine load was ramped linearly to 9 bar BMEP in the time of 5 s and then held at the same engine load for another 5 s; Following that, the engine load was ramped down linearly to initial 6 bar BMEP also in 5 s. This procedure was also used for 10 s and 20 s ramp transient experiments. To measure rapidly changing NOx emissions, the Cambustion CLD500 fast response NOx analyser was used during each short transient experiment. Figure 3.6.5a visualises the engine load ramp during short transient experiment for 5, 10 and 20 s. During the long transient test, the engine was operating at 1500 rpm and the engine load was initially set at 6 bar BMEP. Then, the engine was ramped up to 10 bar BMEP in 20 s and held at the same load until the SCR temperature reached steady condition during a stabilization period. Next, the engine load was ramped down to 6 bar BMEP and held at the same load until exhaust temperature returned to the initial condition. Both engine load ramps were linear as demonstrated in figure 3.6.5b. During the long transient ramp, the FTIR analyser was used to measure NO, NO_2, NH_3 and N_2O upstream and downstream of the SCR. The short transient engine experiment

was conducted with ammonia gas dosing, while the long transient engine test was conducted using ammonia gas and urea injection.

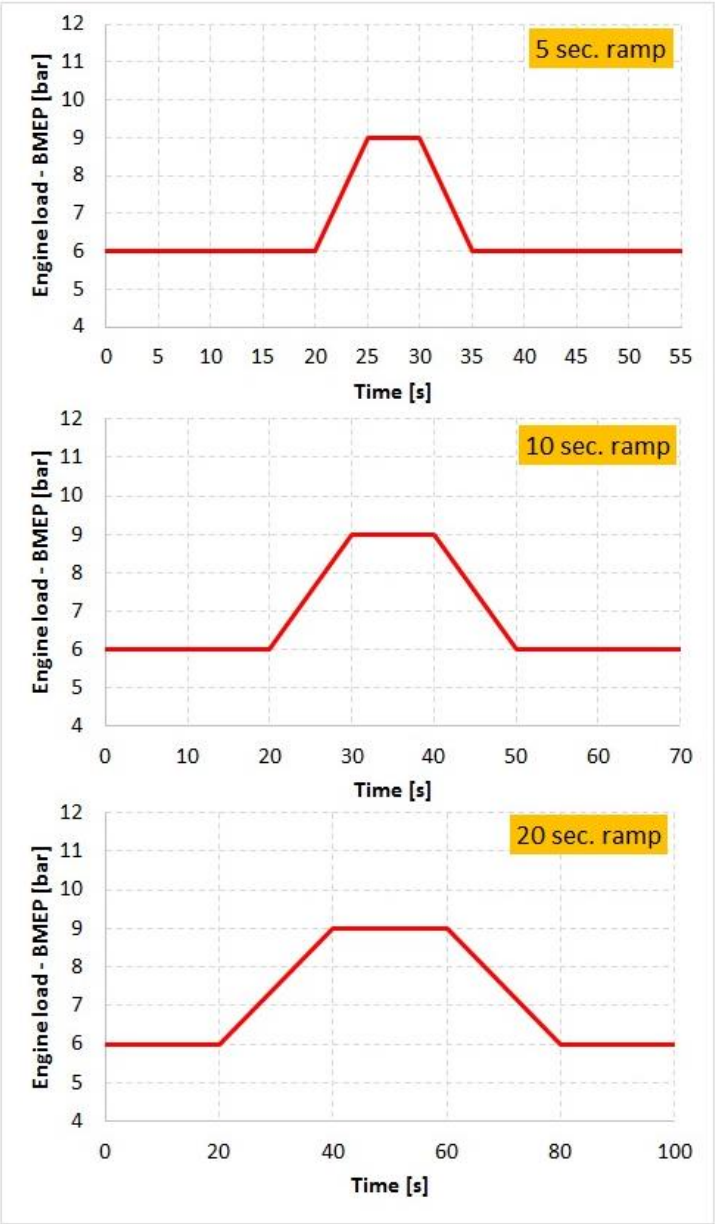

Figure 3.6.5a Engine load change during short transient experiment for 5, 10 and 20 s engine ramp.

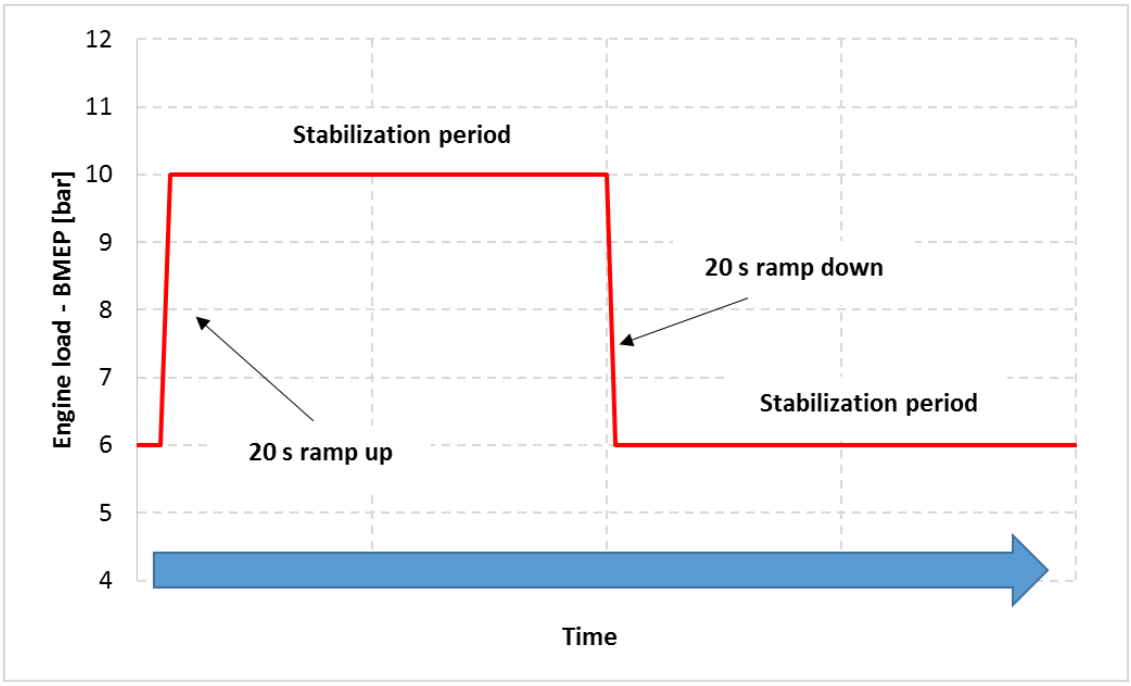

Figure 3.6.5b Engine load change during long transient experiment.

Chapter 4: Experimental results and discussion

4. Overview of experimental configuration

The experimental results from steady state and transient engine conditions tests are presented in this chapter. Ammonia reductant was supplied in the form of 5% NH_3 gas or it was injected as urea water solution (AdBlue). During a steady state engine experiment, the SCR was operating either at 210 ^oC or 260 ^oC. The supplied NO_2:NOx ratio was controlled by the DOC type and size. Additionally, the SCR performance was assessed under long and short transient engine conditions. During long transient test, the engine load was ramped from 6 bar BMEP at 1500 rpm to 10 bar in 20 s and held until steady state conditions were achieved; then, engine was ramped down to 6 bar BMEP in 20 s and held again until steady state conditions were achieved. During short transient tests, the engine load was ramped up in either 5, 10 or 20s; then, it was held constant only for the prescribed time period and then ramped down in the prescribed time. The FTIR analyser measured the NOx (NO and NO_2), NH_3 and N_2O before and after the SCR catalyst during steady state and transient testing. The fast response CLD analyser was used for NOx measurement during the short transient experiments. Table 4.0 provides a summary of the conducted experiments.

Table 4.0 Summary of experiments

Type of experiment	Form of ammonia supplied	Gas analyser	SCR brick size		DOC	
			Volume [litres]	Length [mm]	Type	Volume [litres]
Steady state (high and low temperature)	5% NH_3 gas dosing	FTIR	0.3, 0.5, 0.8	30, 45, 75	Pd only	1
					Standard	0.5, 2
Long transient	5% NH_3 gas dosing	FTIR	0.5	45	Pd only	1
					Standard	0.5
Short transient	5% NH_3 gas dosing	CLD 500	1 (0.5 + 0.5)	90 (45+45)	Standard	0.5, 1
Steady state - 3d Diffuser	5% NH_3 gas dosing	FTIR	0.5	45	Pd only	1
Steady state (high and low temperature)	AdBlue injection	FTIR	0.8	75	Pd only	1
Long transient	AdBlue injection	FTIR	0.8	75	Pd only	1

4.1 Experiment with 5% ammonia gas dosing

4.1.1 Steady state SCR performance for NO_2:NOx=0

This section demonstrates the effect of the SCR catalyst size and temperature on the steady-state NO and NH_3 conversion, when the only component of NOx was NO. The engine was operating at 1500 rpm and 6 bar BMEP to provide an exhaust gas temperature of about 210 °C on the SCR catalyst inlet. Engine load was increased to 8.5 bar BEMP for a higher temperature test. During these conditions, the SCR inlet gas temperature was about 265 °C. A Pd only DOC was used downstream of the DPF, ensuring that no NO_2 was present in the exhaust gas. In order to measure the effect of the SCR catalyst brick length on the NO conversion, three lengths of SCR catalyst were used; 30, 45 and 75 mm long (0.3, 0.5 and 0.8 litre). The ammonia gas dosing was set up for three α conditions, these were deficient ammonia $\alpha \sim 0.5$, stoichiometric ammonia $\alpha \sim 1.0$ and excess ammonia $\alpha \sim 1.25$.

Figure 4.1.1 represents NO and NH_3 conversion profiles for deficient, stoichiometric, and excess ammonia at a low SCR temperature. The blue line is the NO conversion at a low temperature and the red line at a high temperature. In the condition of low temperature and deficient ammonia, 14 % of NO was converted over 30 mm long SCR catalyst, and for α=1 and 1.25 NO conversion increased to 17%. The increase in the temperature from 210 °C to 265 °C improved NO conversion from 17 to 31% at α~1 and 1.25, and from 14 to 24 % at $\alpha \sim 0.5$. No improvement in NO conversion was observed after 30 mm long catalyst was changed to 45 mm. That was true for low and high temperature and all ammonia dosing setups. Also, the NH_3 conversion profile showed no improvement over 45 mm catalyst, therefore no ammonia oxidation occurred. It might be that most of the NO was converted in the front section of the catalyst (first 30 mm) and adding 15 mm of SCR had only a very small impact on the conversion that in this case was not measurable. After the SCR catalyst was changed to 75 mm long, the NO conversion increased for both low and higher temperature experiments by 14 %, when ammonia was deficient. At $\alpha \sim 1$ and 1.25, NO conversion improved from 17 to 33 % during low temperature experiment, and from 30 to 53 % during high temperature experiment. Similarly to NO, the NH_3 conversion also improved as more ammonia was used for the reaction. At $\alpha \sim 1$, NO and NH_3 conversion was equal for low and high temperature experiments. This means that 1 mol of NH_3 was used to react with 1 mol of NO as no NO_2 was available for a reaction. This is in line with the principles of standard SCR reactions, as demonstrated by equation 1.4.3a.

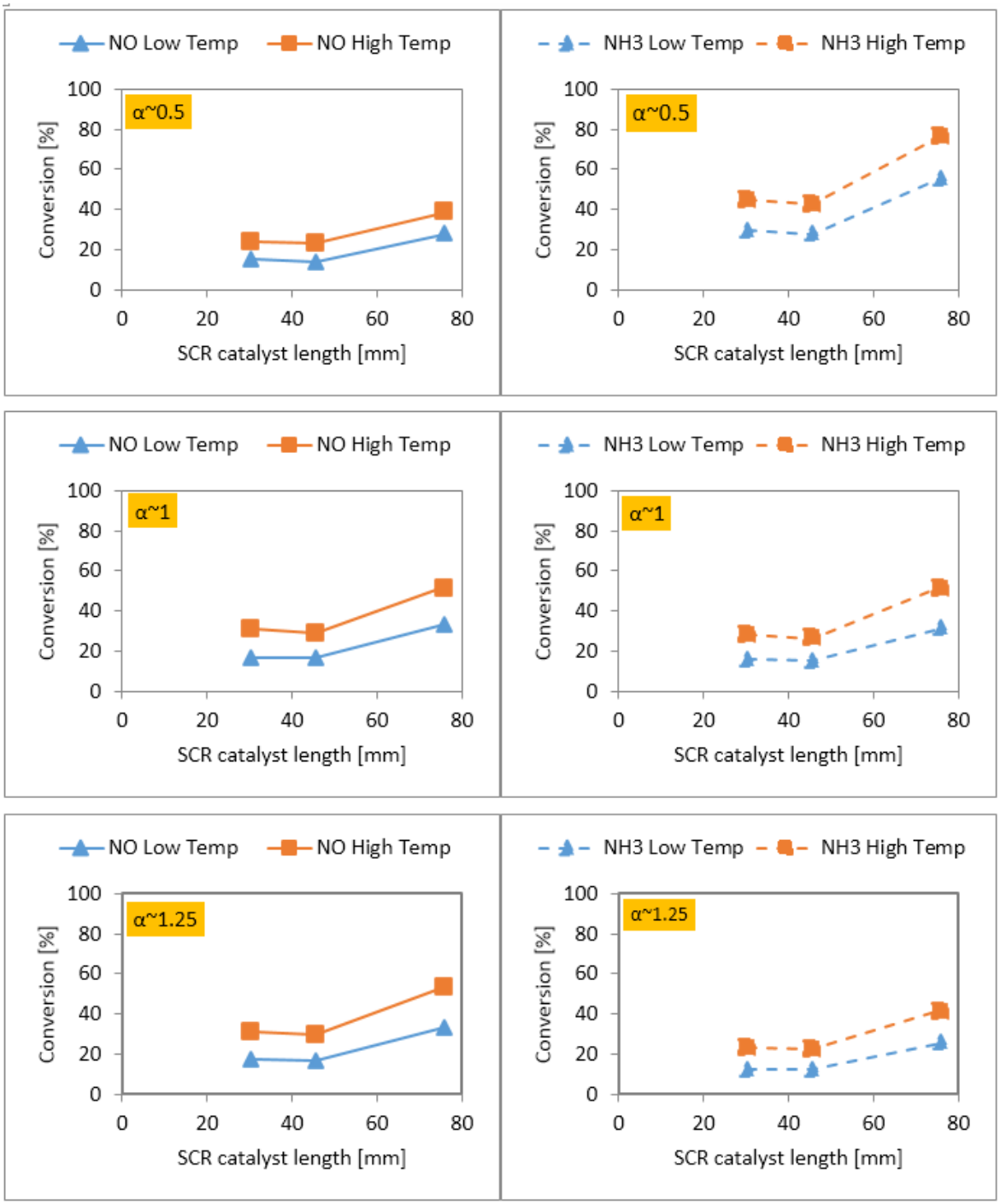

Figure 4.1.1 NO and NH_3 conversion profiles for deficient, stoichiometric, and excess ammonia. For low (T=210°C) and high (T=265°C) SCR temperature and zero NO_2:NOx ratio.

4.1.2 The effect of NO_2:NOx ratio on NOx conversion during a low temperature test

In addition to the set of experiments with NO_2:NOx ratio of 0, the SCR performance was also measured in the presence of NO_2. Proportion of available NO_2 in NOx upstream of the SCR catalyst was controlled by the volume and type of DOC used. Moderate NO_2:NOx ratio of 0.28 and high ratio of 0.66 were achieved. The engine was operating at 1500 rpm and 6 bar BMEP with the SCR catalyst inlet gas temperature close to 210°C. Similar to section 4.1.1, three lengths of the SCR catalyst were used; 30, 45 and 75 mm long (corresponding to 0.3, 0.5 and 0.8 litre). The ammonia gas dosing was set up to achieve deficient $\alpha \sim 0.5$, stoichiometric $\alpha \sim 1.0$ and excess $\alpha \sim 1.25$ ammonia.

Results of the NOx conversion against inlet NO_2:NOx ratio for three catalyst lengths are plotted in figure 4.1.2a and 4.1.2b. During the deficient ammonia test, NOx conversion improved approximately 16 % for each catalyst, after the supplied NO_2:NOx ratio was increased from 0 to 0.28. No further improvement was observed when NO_2 ratio was increased from 0.28 to 0.66. This is because, for 0.5l (red line) and 0.8l (green line) SCR catalysts, NH_3 reached nearly 100% conversion, as illustrated in figure 4.1.2a NH_3 conversion profiles. As a result, an insufficient amount of ammonia was available for reactions. When ammonia was dosed stoichiometric (α~1) more NOx was converted. For 0.8l SCR, the NOx conversion improved from 44 % to 55 %, when NO_2:NOx ratio was 0.28. However, more ammonia available for conversion showed a benefit at high NO_2:NOx ratio, and the conversion improved even more for 0.8 l SCR reaching 72 %. Similarly, 0.3 l and 0.5 l SCR showed an increase in conversion from 34 to 46 % and 39 to 59 % respectively. Increasing ammonia supplied to $\alpha \sim 1.25$ did not improve SCR performance neither for NO_2:NOx 0 nor 0.28 NO_2 ratio because sufficient ammonia was available at $\alpha \sim 1.0$ experiment apart from 0.8 l SCR that converted all supplied ammonia at high NO_2 ratio. Therefore, in case of experiment at excess ammonia this catalyst showed 5% increase in conversion.

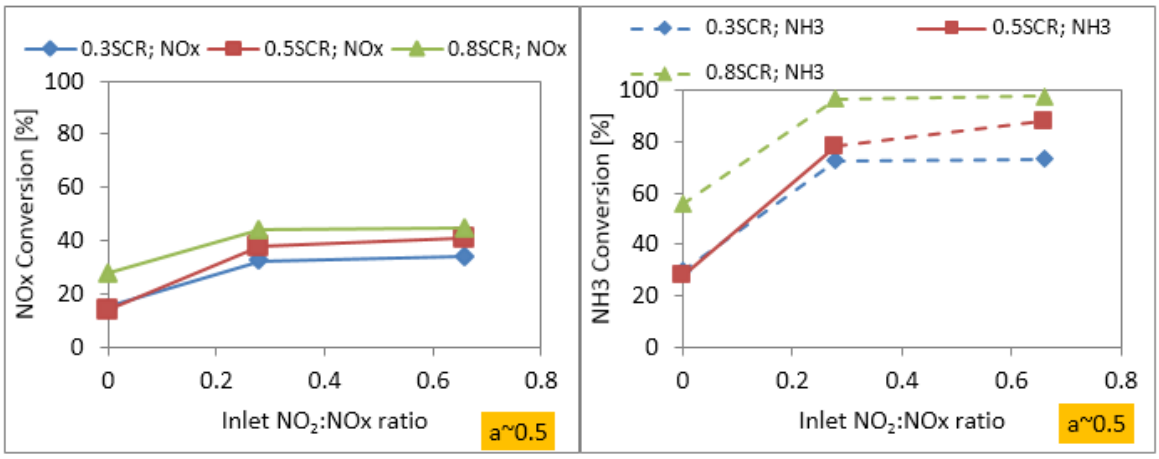

Figure 4.1.2a NO_2:NOx ratio effect on NOx and NH_3 conversion profiles for deficient ammonia at low SCR temperature (T=210 °C).

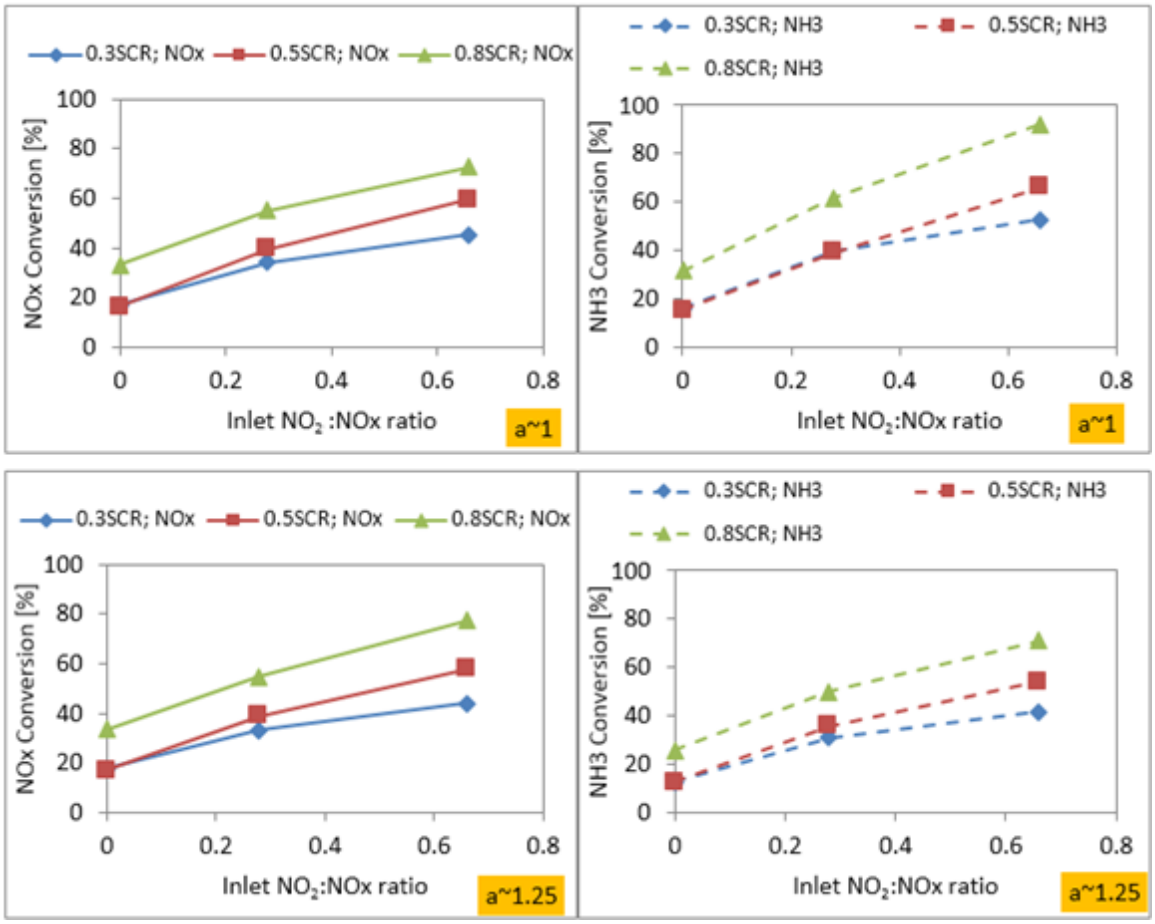

Figure 4.1.2b NO_2:NOx ratio effect on NOx and NH_3 conversion profiles for stoichiometric, and excess ammonia at low SCR temperature (T=210°C).

4.1.3 The effect of NO_2:NOx ratio on NO and NO_2 selectivity

Similarly to the section 4.1.2 showing impact of the supplied NO_2:NOx ratio on the SCR NOx conversion, this section focuses on the SCR selectivity of NO and NO_2. The consumed values were measured over three SCR catalyst lengths (30, 45 and 75 mm) during a steady state experiment at a low SCR temperature. The supplied NO_2:NOx ratio was either 0, 0.28 or 0.66. The consumed NO_2 and NO against the supplied NO_2:NOx ratio is shown in figure 4.1.3. The solid lines represents NO and the dotted lines represents NO_2.

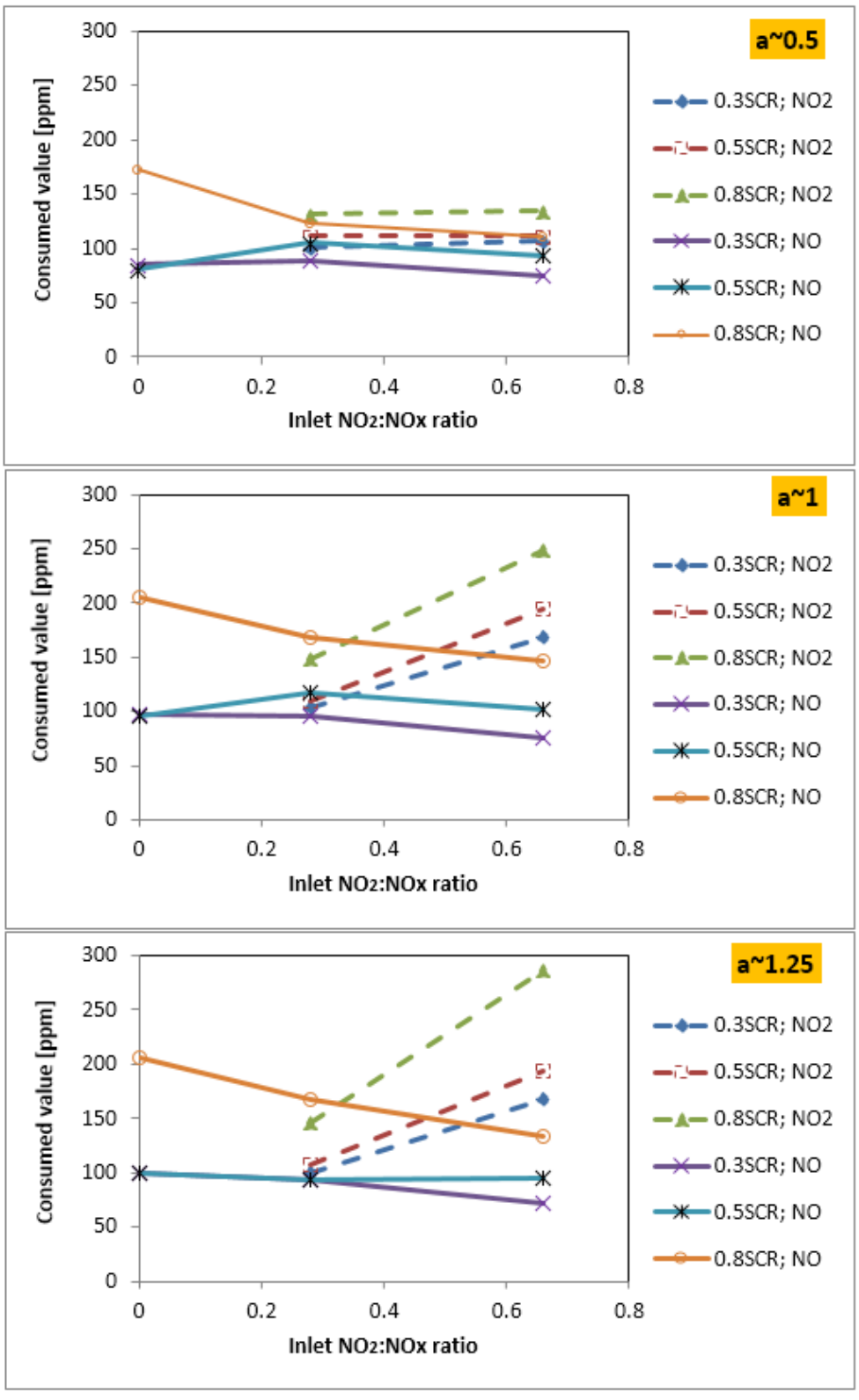

Figure 4.1.3 NO_2:NOx ratio effect on NO and NO_2 consumed profiles for deficient, stoichiometric, and excess ammonia at low SCR temperature (T=210 ^oC).

When deficient ammonia (α~0.5) was supplied the same amount of NO and NO_2 was consumed on the SCR catalyst independently of inlet NO_2:NOx ratio. This was also true for α 0.5 and 1.25 experiment, but only when the inlet NO_2:NOx ratio was 0.28. This suggests that conversion on the SCR catalyst was dominated by the fast SCR reaction when NO_2 was present.

Additionally, it was observed that the amount of consumed NO was similar for each NO_2:NOx ratio, especially for 0.3 and 0.5 SCR. Substantial increase in NO_2 consumption was observed when the supplied NO_2:NOx was increased from 0.28 to 0.66 for α ~ 1 and α ~ 1.25, as a result of more NO_2 being available for reaction with ammonia.

4.1.4. Ammonia slip

The ammonia pollution is not part of emission standards for passenger cars (DieselNet, 2013). However, odour produced from ammonia slip at a tailpipe of passenger car is a real concern for manufactures. In this section, ammonia slip from the SCR catalyst during steady state engine testing was investigated. The experiment was conducted at low SCR temperature of 210°C. Ammonia was supplied in the form of NH_3 gas at three NH_3:NOx ratios; α ~ 0.5, α ~ 1.0 and α ~ 1.25. During the experiment, the FTIR analyser was used for ammonia slip measurement.

Figure 4.1.4a represents ammonia slips measurement at the exit of 0.3, 0.5 and 0.8 litre SCR against ammonia supplied. Linear relationship of ammonia slip to ammonia supplied is observed apart from 0.8 l SCR tested at high NO_2:NOx ratio. In this case much lower ammonia slip is observed at α ~ 1 compared to the 0.5 litre SCR, then at α ~ 1.25 ammonia slip rises to expected level.

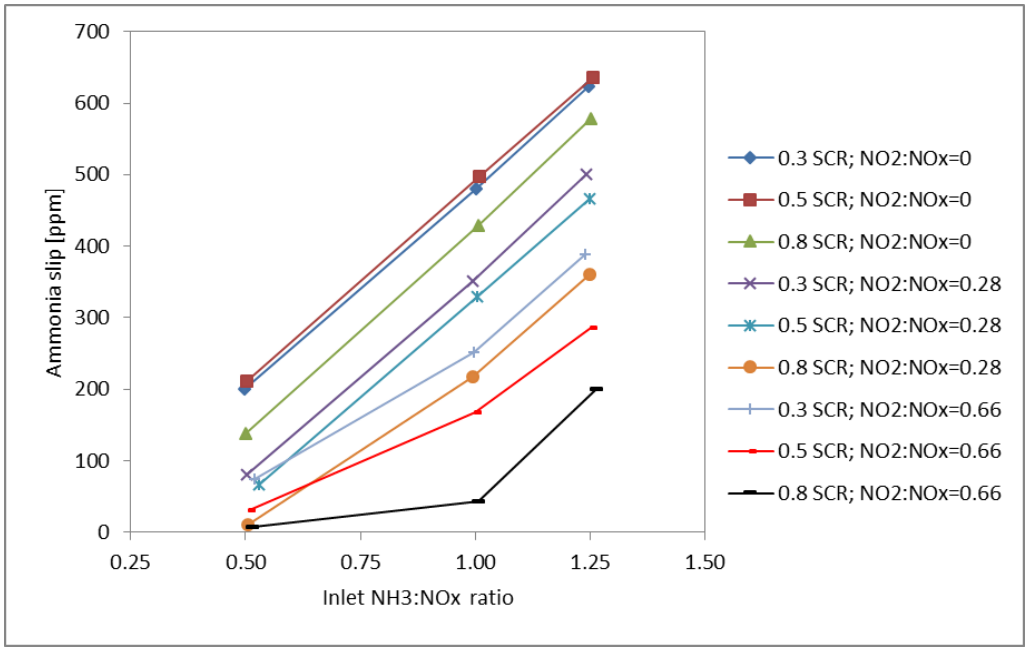

Figure 4.1.4 a. Ammonia slip against inlet NH_3:NOx ratio (α) for range of SCR catalyst length and NO_2:NOx ratio. Low temperature case 210°C.

Relationship between ammonia slip and NOx conversion is presented in Figures 4.1.4b. Each three points on each curve represent a different supplied NH_3:NOx ratio, where the first point (starting from the left) relates to NH_3:NOx=0.5, second point relates to NH_3:NOx=1 and the third point relates to NH_3:NOx=1.25. In case of experiment at NO_2:NOx=0 and for each volume of catalyst, there is a very small improvement in a NOx conversion when the supply of ammonia is increased from NH_3:NOx ratio of 0.5 to 1.25. Therefore, in these conditions, by reducing supplied ammonia to NH_3:NOx ratio of 0.5, it was possible to substantially reduce the ammonia slip without an impact on NOx conversion. Similarly, there was a very small improvement in NOx conversion at NO_2:NOx=0.28 for the SCR volume of 0.3 and 0.5 l; subsequently, the same rule can be applied. When NO_2:NOx ratio was increased to 0.66, it was also observed that a substantial improvement of NOx conversion could be achieved by increasing the supplied ammonia from NH_3:NOx ratio of 0.5 to 1. This was the case especially for 0.5 and 0.8 l SCR with less impact on the ammonia slip. These results highlight the importance of calibrating ammonia dosing strategies in order to gain an optimum NOx performance while reducing the potential ammonia slip from the SCR system.

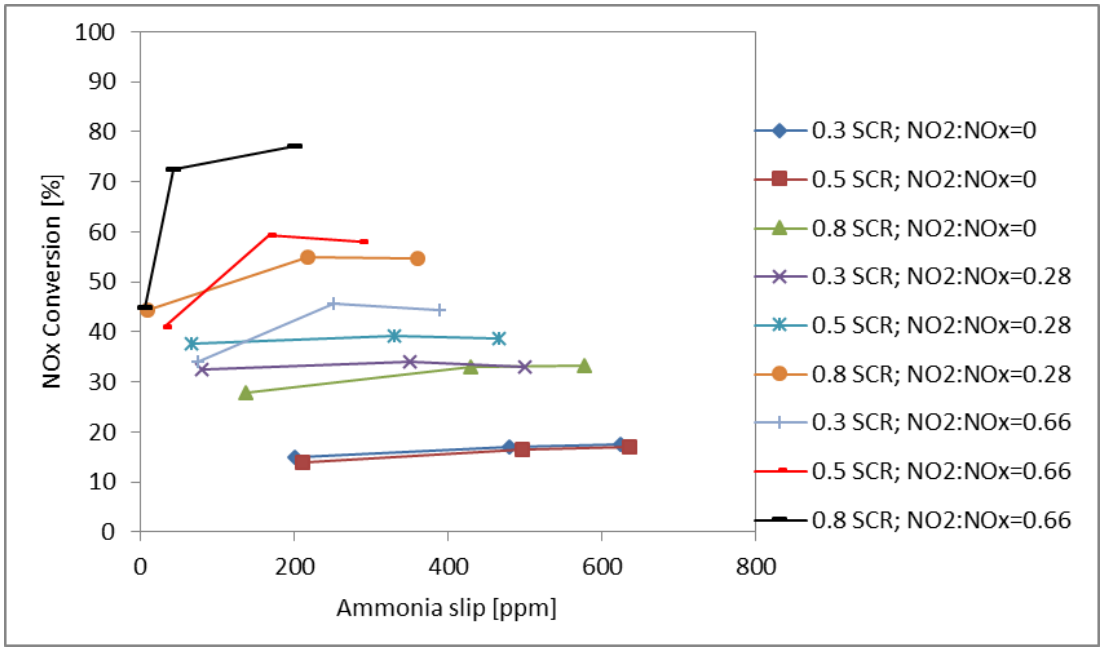

Figure 4.1.4b. Relationship between ammonia slip and NOx conversion for range of SCR catalyst length and NO_2:NOx ratio. Low temperature case 210°C.

4.1.5 N_2O formation

Nitrous oxide (N_2O), is known as a powerful greenhouse gas (GHG) around 300 time more damaging for the same level of emission than CO_2 [EPA 2014]. Nitrous oxide more likely to be formed over the SCR catalyst in presence of NO_2. Equation 4.1.5 describes the reaction of N_2O formation.

$$4NO_2 + 4NH_3 + O_2 \rightarrow 4N_2O + 6H_2O \qquad \text{eq. 4.1.5}$$

In order to measure the sensitivity of the Cu- Zeolite SCR on N_2O formation, a set of steady state low temperature (210°C) experiments were carried out. During these experiments, N_2O concentration was measured before and after the catalyst with the FTIR analyser. Ammonia was supplied at three NH_3:NOx ratios; $\alpha \sim 0.5$, $\alpha \sim 1.0$ and $\alpha \sim 1.25$.

The impact of NO_2:NOx ratio on low temperature N_2O formation is presented in figure 4.1.5a. During test with a deficient supplied ammonia, the formation of N_2O was limited, and maximum 22 ppm was reached at NO_2:NOx ratio of 0.28. After the supplied ammonia for NOx reaction was increased, then the measured concentration of N_2O also increased, especially at high NO_2:NOx ratio, the increase was significant. The volume of the catalysts had a small impact on the N_2O formation, as a very little increase in N_2O was observed with the increasing SCR volume. The only exception was when the ammonia was supplied at NH_3:NOx=1.25 during NO_2:NOx ratio of 0.66 condition, with the used SCR volume of 0.8l.

Luo et al. (2010) observed that N_2O formation over Fe zeolite was only occurring at the NO_2:NOx ratio equal or above 0.5. Temperature also played an important role, with N_2O showing highest measured concentration at 250 ^oC (Luo et al, 2010). But the measurements reported here are showing N_2O formation at NO_2:NOx ratio as low as 0.28. This suggests that Cu-zeolite SCR is likely to produce more N_2O at low operating temperatures.

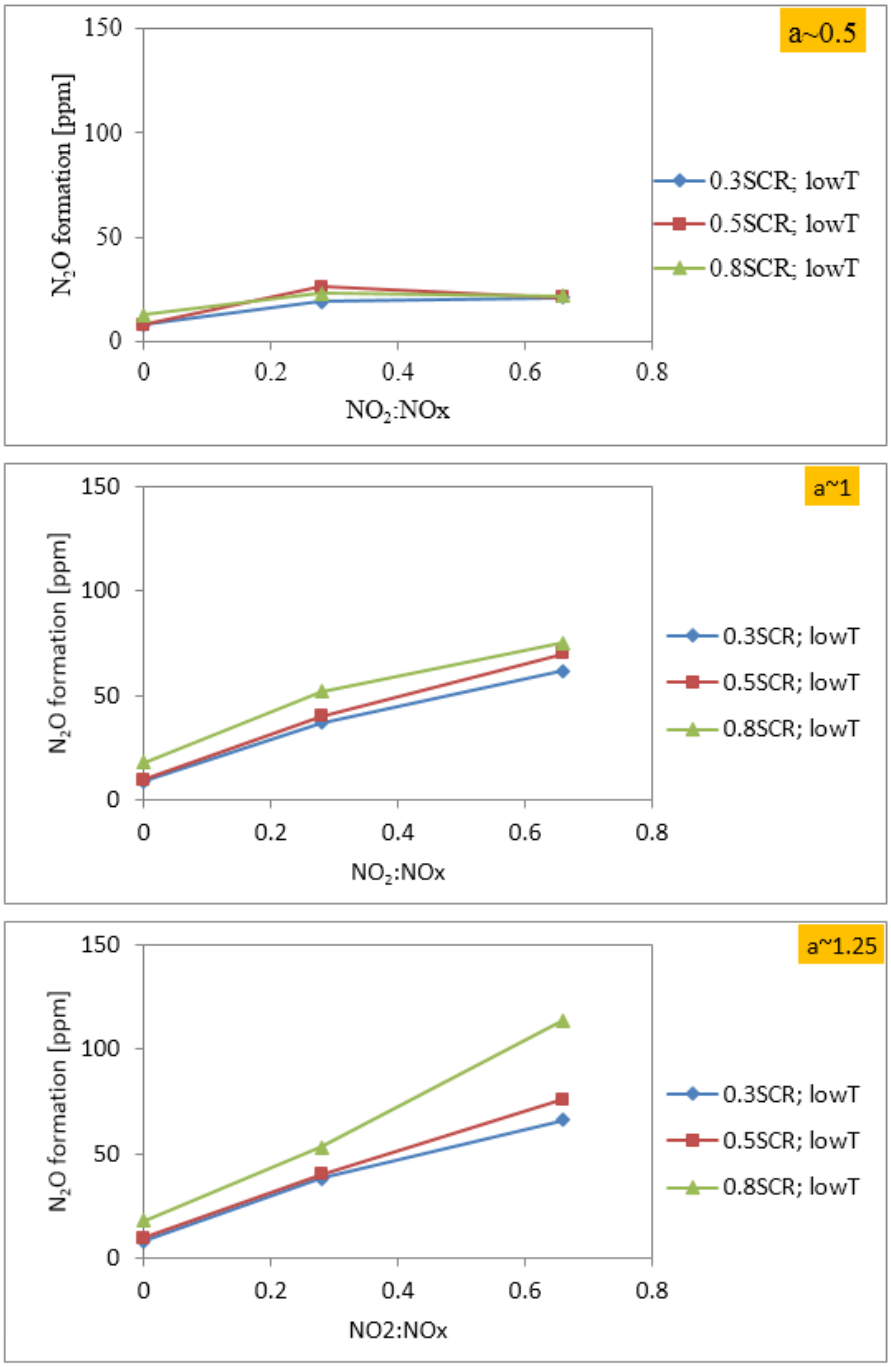

Figure 4.1.5a Impact of NO_2:NOx ratio on low temperature N_2O formation .

4.1.6 SCR measurement with 180° expansion diffuser

The first set of experiments was conducted using 1D diffuser to ensure that the exhaust flow through the catalyst was uniformly distributed across the SCR catalyst. The set of experiments described in this section aimed to investigate the effect of 3D diffuser geometry on SCR NOx and NH_3 conversion. In this case, a 180 ° sudden expansion was used as a 3D diffuser.

Engine conditions of 1500 rpm and 8.5 bar BMEP were used for this set of tests. After the engine reached steady state conditions, the diffuser inlet temperature was 262 °C. To control the absence of NO_2 species in exhaust gas, the Pd only DOC was located after the DPF filter. The 5 % ammonia gas was used as NOx reductant for the 45 mm SCR brick (0.5l). NO and NH_3 concentration profiles together with gas temperature profile were measured 20 mm upstream of the SCR brick in the expansion can and also 30 mm downstream of the SCR brick. Figure 4.1.6a shows the upstream NO and NH_3 concentration profiles measured across the expansion can when ammonia was dosed as deficient ammonia (α~0.5), stoichiometric ammonia (α~1.0) and excess ammonia (α~1.25), where zero on the position axis indicates a centre of a measured distance. The uniform concentration of NO and NH_3 across the diffuser shows that the exhaust and dosed ammonia gas are well mixed, regardless of a high turbulence flow in the expansion diffuser. This confirms a homogenised mixture of ammonia reductant in the exhaust upstream of the SCR brick as a result of the diffusion process in the expander.

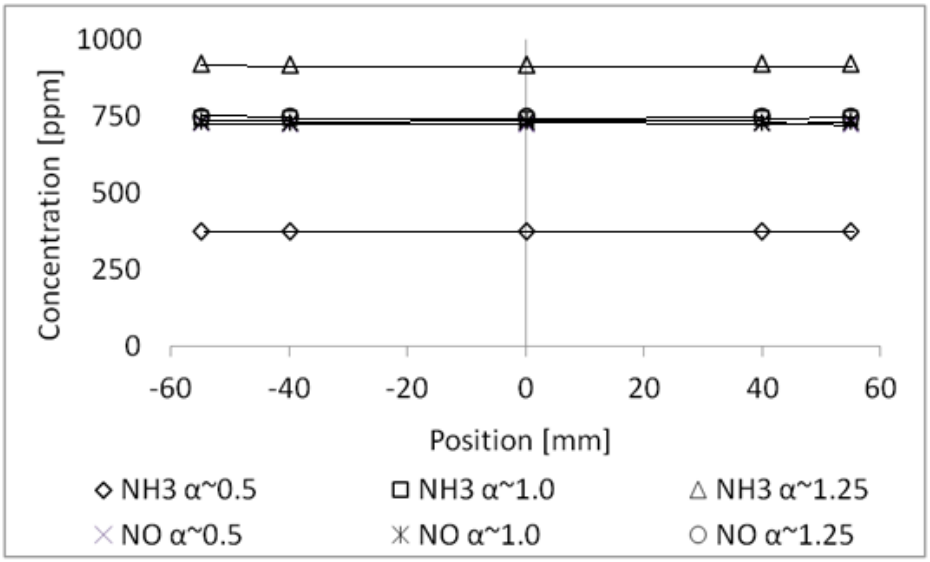

Figure 4.1.6a 3D 180 ° expansion diffuser measurement. NO and NH_3 concentration profiles 20 mm upstream of 45 mm SCR brick in the expansion can; α~0.5 - deficient ammonia, α~1.0 - stoichiometric ammonia, α~1.25 - excess ammonia.

Figure 4.1.6b shows normalised velocity of measured flow profile at the exit of 45 mm long catalyst with an upstream 3D 180 ° sudden expansion diffuser (Benjamin et al. 2012). The experiment was conducted by C.A. Roberts using a hot wire anemometry flow rig. Zero on abscissa corresponds to the centre of the diffuser. Profile of the velocity distribution at the back of the catalyst indicates that most of the flow is concentrated in the middle and close to the catalyst edge. This means that the flow was separated at the exit of the diffuser and some of the flow was forced radially to the diffuser wall immediately upstream of the catalyst face, hitting the diffuser wall and creating a positive static pressure. This resulted in a secondary velocity peak close to the edge of the catalyst (50-60mm).

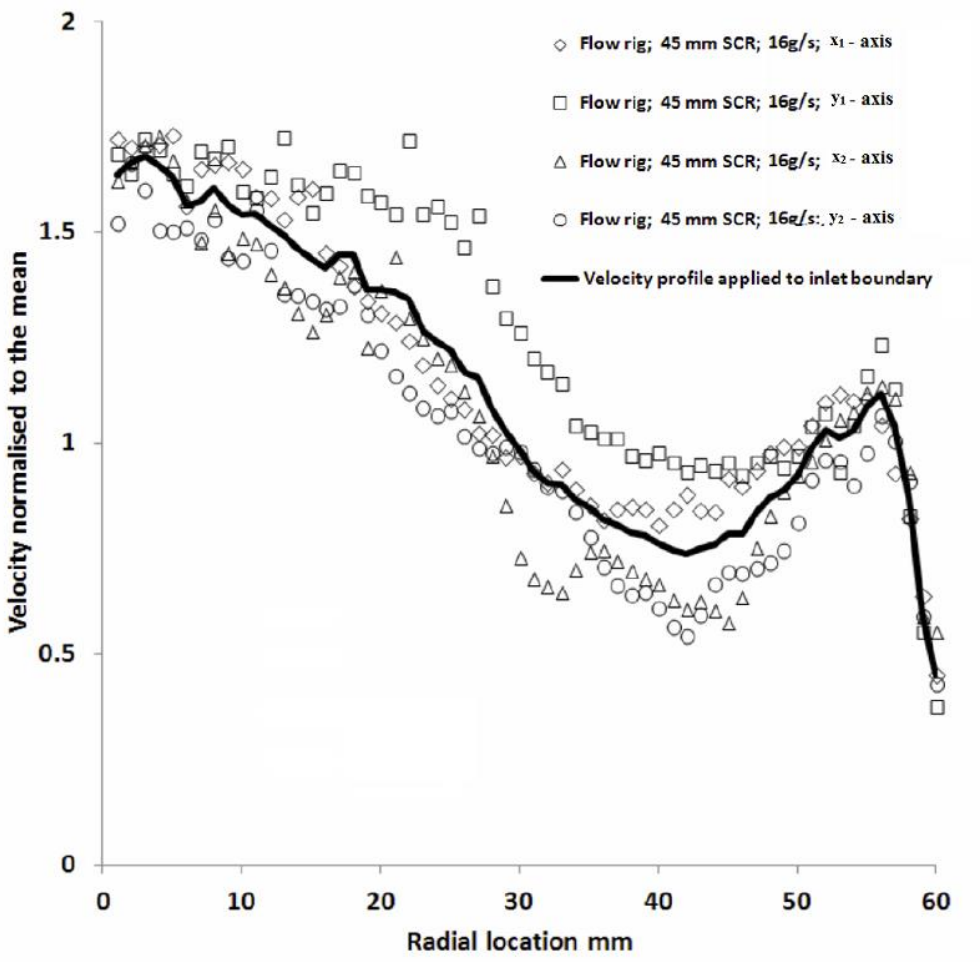

Figure 4.1.6b Normalised velocity measured 30mm downstream of catalyst using hot wire anemometry (HWA) at mass flow of 16 g/s. Horizontal and vertical traverses are indicated by x_1 (-60 to 0mm), x_2 (0 to 60mm) and y_1 (-60 to 0mm), y_2 (0 to 60mm) (Benjamin et al. 2012).

Figure 4.1.6c shows the temperature distribution of the exhaust gas 20 mm upstream of the SCR brick and 30 mm downstream of the SCR brick. Temperature was measured with a single 1.5mm thermocouple mounted on side of expansion can of the diffuser and slid in and out to a required position. In the expansion can of the diffuser, the flow in the middle had a higher temperature than the flow field 30 mm from the centre. The reason for this is likely to be the exhaust gas temperature

loss through the can wall. Downstream of the SCR brick, the temperature distribution across the can was more uniform, especially 40 mm from the centre. This is a result of the heat transfer between the exhaust gas and the SCR brick and the conductivity of the SCR brick itself. Part of the flow located closer to the can wall has lower temperature due to lower gas temperature and heat loss through the brick to the can. It was also observed that the temperature between 50-58 mm was around 15 °C lower than on the opposite site. This is the effect of the additional heat loss from the thermocouple mounting port.

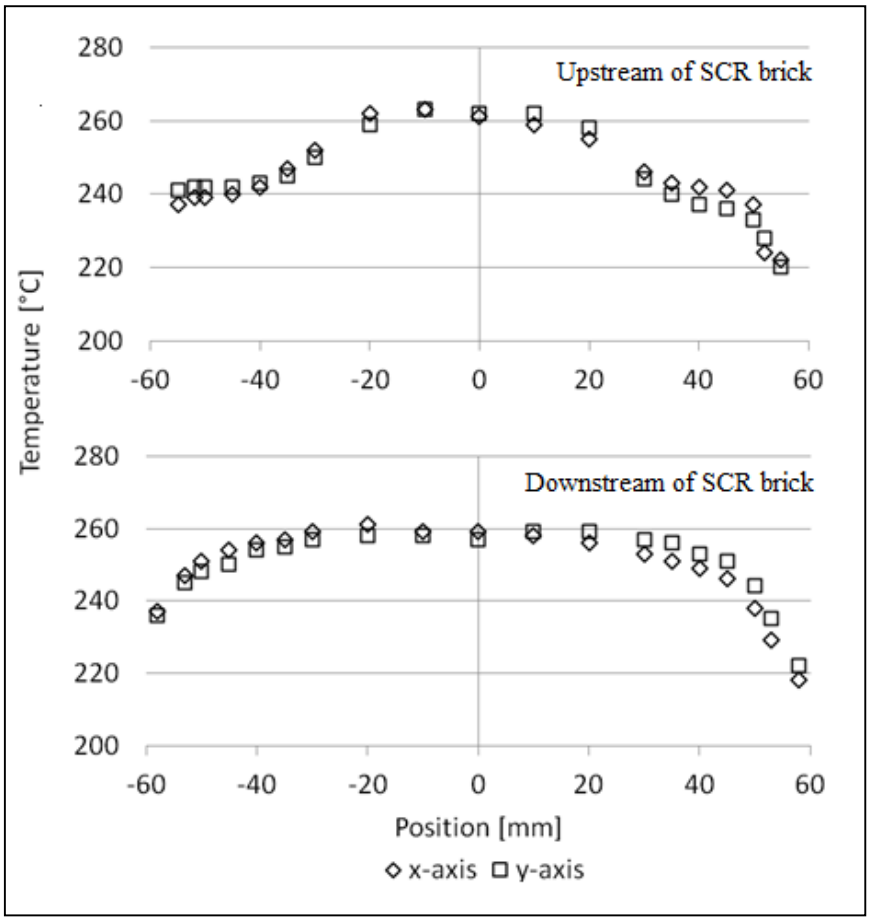

Figure 4.1.6c Temperature profiles 20 mm upstream (top plot) and 30 mm downstream (bottom plot) of 45 mm SCR brick. X-axis and y-axis represent horizontal and vertical traverse.

Concentration profiles of NO and NH_3 measured 30 mm downstream of the SCR brick for deficient ammonia (α~0.5), stoichiometric ammonia (α~1.0) and excess ammonia (α~1.25) case are shown in figure 4.1.6d and figure 4.1.6e respectively. All three cases produced the slip of NO and NH_3 with a significant variation of concentration across the SCR brick. The highest slip occurred in the middle and at the edge of the brick. The smallest slip was observed at around 45 mm from the centre. On average, the difference between highest and lowest concentration of NO and NH_3 was 90 ppm for the deficient ammonia case and 120 ppm for the stoichiometric and excess ammonia case. The concentration profile shapes in figures 4.1.6d and 4.1.6e result from the combined influences of

velocity (figure 4.1.6b) and temperature (figure 4.1.6c). This is discussed further below with reference to the conversion profiles.

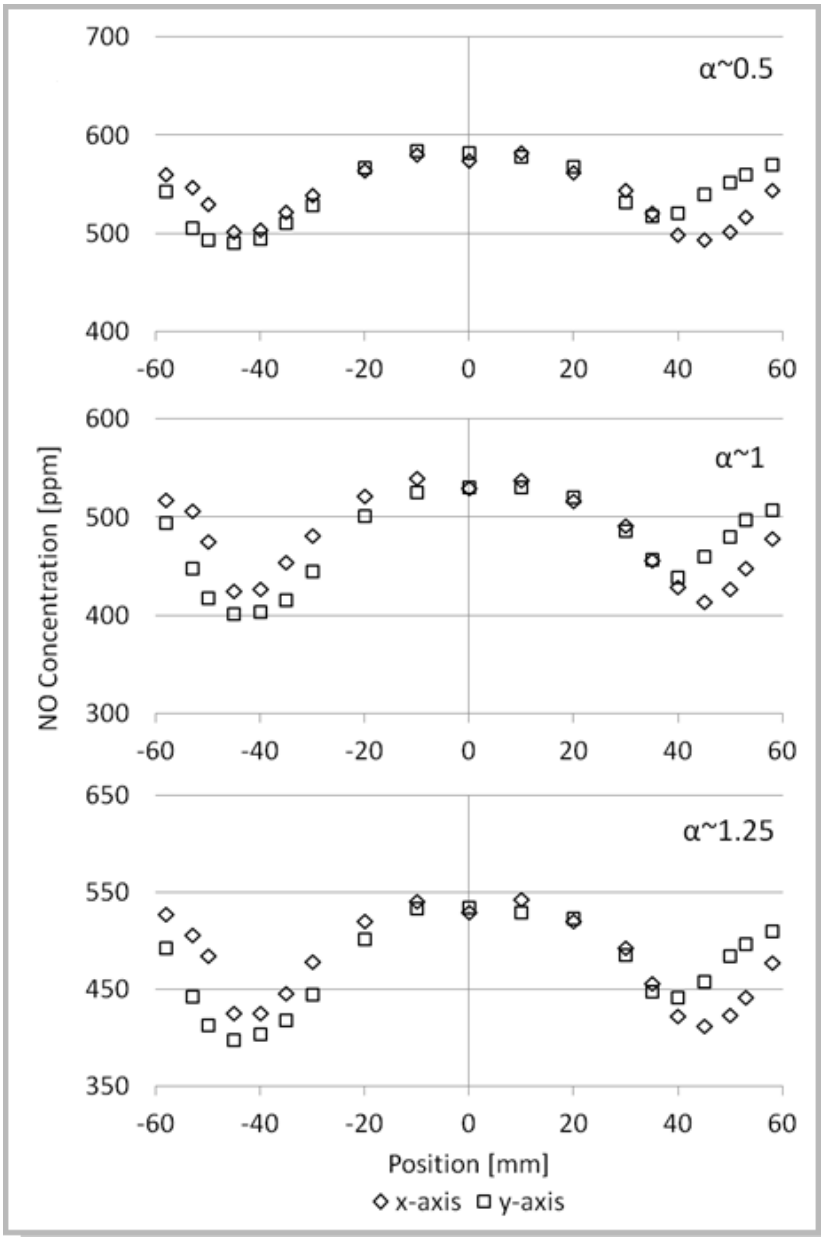

Figure 4.1.6d NO concentration profile 30 mm downstream of the 45 mm SCR brick for deficient ammonia (α~0.5), stoichiometric ammonia (α~1.0) and excess ammonia (α~1.25). X-axis and y-axis represent horizontal and vertical traverse.

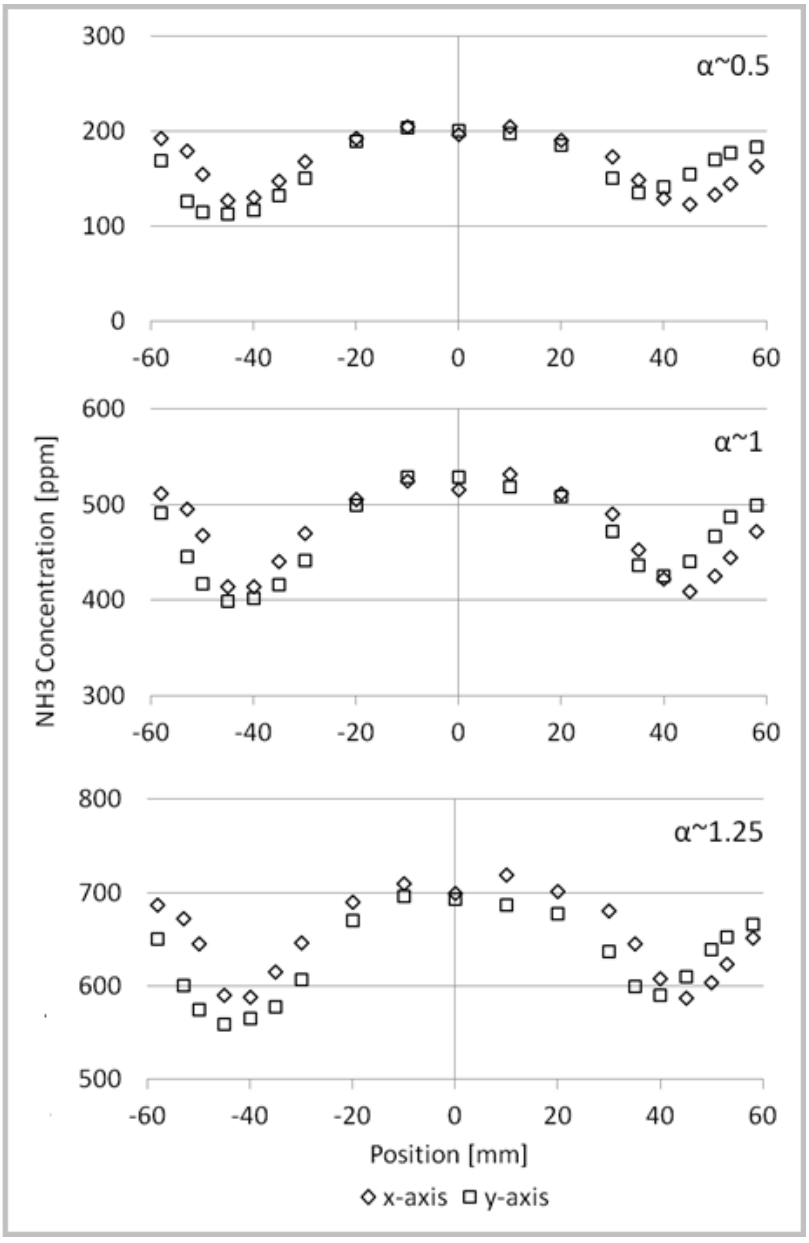

Figure 4.1.6e NH_3 concentration profiles 30 mm downstream of 45 mm SCR brick for deficient ammonia (α~0.5), stoichiometric ammonia (α~1.0) and excess ammonia (α~1.25). X-axis and y-axis represent horizontal and vertical traverse.

Figure 4.1.6f shows the NO conversion efficiency for the 45 mm SCR brick for deficient ammonia (α~0.5), stoichiometric ammonia (α~1.0) and excess ammonia (α~1.25). Lowest NO conversion was observed in the centre and at the edge of the SCR brick. Limited NO conversion at the edge of the SCR brick could be explained by an interaction of low temperature (see figure 4.1.6c) and a relatively higher exhaust gas velocity (see figure 4.1.6b). As demonstrated in figure 4.1.6b, the most of flow of the exhaust gas was concentrated in the middle of the SCR brick (x range of -20 to 20mm), resulting in a highest gas velocity. Therefore, this substantially reduced the residual time available for NO and NH_3 reaction on the catalyst, which in turn lowered NO conversion. The highest NO

conversion was observed at 35-45 mm from the centre, hence a lowest NH_3 and NO slip (see figure 4.1.6d and 4.1.6e). In this location, measured flow velocity was significantly reduced compared to the centre of the brick, while exhaust gas temperature was high enough to support a good SCR operation (presented in figure 4.1.6b and 4.1.6c). Overall, results suggest that the NO conversion was dependent more on gas velocity than gas temperature, which means that residual time available for NO with NH_3 reaction played an important role in the SCR performance. The results presented in this section were used for the development of the kinetics model (Benjamin et al., 2012b)

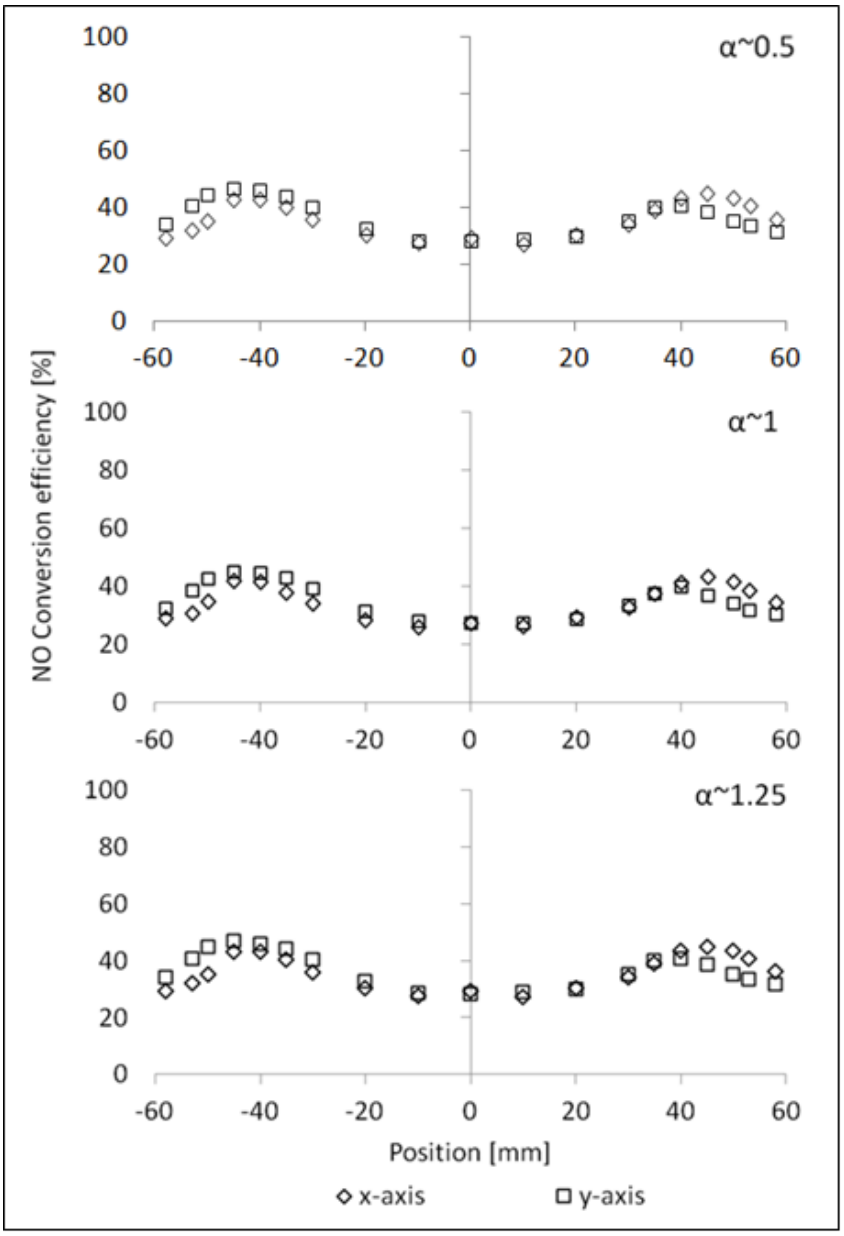

Figure 4.1.6f NO conversion profiles of 45 mm SCR brick for deficient ammonia (α~0.5), stoichiometric ammonia (α~1.0) and excess ammonia (α~1.25). X-axis and y-axis represent horizontal and vertical traverse.

4.1.7 Summary of steady state SCR studies with ammonia gas dosing

The key findings from the steady state SCR studies with ammonia gas dosing were:

- When NO_2:NOx=0, no improvement in NO conversion was observed after the SCR catalyst length was increased from 30 to 45 mm. This finding suggests that most of the NOx conversion occurred in the first 30 mm of the SCR brick.
- The effect of supplied NO_2:NOx ratio (0, 0.28 and 0.66) on NOx conversion for three lengths (30, 45 and 75mm) of the SCR catalyst was examined. It was shown that when ammonia was supplied as stoichiometric, NOx conversion improvement was observed for all lengths of the SCR catalyst.
- During the ammonia slip measurement, it was found that increasing ammonia dosing had less impact on ammonia slip when longer SCR bricks were tested, especially under high NO_2:NOx ratio.
- Increase in NO_2:NOx ratio showed a bigger impact on N_2O formation than the catalyst volume particularly for stoichiometric and excess ammonia dosing.
- The results from the 3D study with a 180 degree sudden expansion diffuser demonstrated that the lowest NO conversion was measured in the centre and near the edge of the SCR brick as a result of a significantly higher gas velocity in these sections of the SCR catalyst.

4.1.8 Overview of transient engine tests

As highlighted in chapter 2, there is a need to measure the SCR performance under changing exhaust gas conditions. Therefore, the transient engine testing program was conducted. The test program was based on two types of engine transients: short transient engine test and long transient engine test.

The aim of the short transient test was to measure the impact of fast changing NOx level on the SCR reactions. For short transient tests, the SCR brick was made up of two 45 mm bricks, which gives 91 mm length of the SCR (equivalent to 1 litre volume). The standard DOC was either 0.5 or 1, depending on a required NO_2:NOx. The Cambustion fast response NOx analyser was used to measure NO and NO_2.

The aim of the long transient test was to measure the impact of changing NOx level and temperature on the SCR reactions. The long transient was tested with the 45 mm SCR brick (0.5l volume), while the inlet NO_2:NOx ratio was controlled by either standard 0.5 DOC or Pd only DOC. In both cases, a 6 bar BMEP load at 1500 rpm was used for the warm-up and the initial steady state condition. Exhaust emission pre- and post- SCR catalyst were measured with Horiba FTIR-6000FT.

4.1.8.1 Transient engine tests: Short transient

After the initial steady state, the engine was ramped up from 6 to 9 bar BMEP at 1500rpm in time period of 5 seconds. The engine load was then held for another 5 seconds and then engine load was ramped down to the initial 6 bar BMEP in the same time period of 5 seconds. The same test was repeated with 10 seconds and 20 seconds sequence. Both engine ramps were linear. Results are plotted with 20 seconds of logged steady state data before the beginning of each ramp. Figure 4.1.8.1a shows the temperatures upstream of the SCR during each engine transient test with standard 0.5 and 1 DOC. The temperature rise that occurred during the engine transient was relatively small; for the longest 20 seconds ramp the temperature increased by 10 °C. The input NO_2:NOx ratios varied during the experiments as shown in figure 4.1.8.1b. This is because the NO level increased as the engine load rose to 9 bar BMEP, which resulted in a NO_2:NOx ratio drop. Then, as the engine load was reduced to 6 bar BMEP, the NO level was reduced to the initial value; however, the residual heat of the exhaust temperature improved the DOC NO oxidation efficiency and as a result, increased the NO_2:NOx ratio. Visible spikes on the graph are likely to be caused by temporary dropout of the analyser NO_2 converter. For all cases, ammonia was dosed in proportions deficient to NOx level in order to prevent the ammonia slip and potential cross-talk with the analyser CLD detector. In order to set up a required NH_3:NOx of 0.5 during the initialisation of steady state period, ammonia concentration was measured with FTIR analyser before the SCR catalyst. The ammonia gas flow was kept constant throughout the test. The calculated input ammonia values are shown in Figure 4.1.8.1c. The noticeable drop in a supplied NH_3 concentration was associated with an increased exhaust mass flow rate, which was a result of an increased engine load from 6 to 9 bar BMEP.

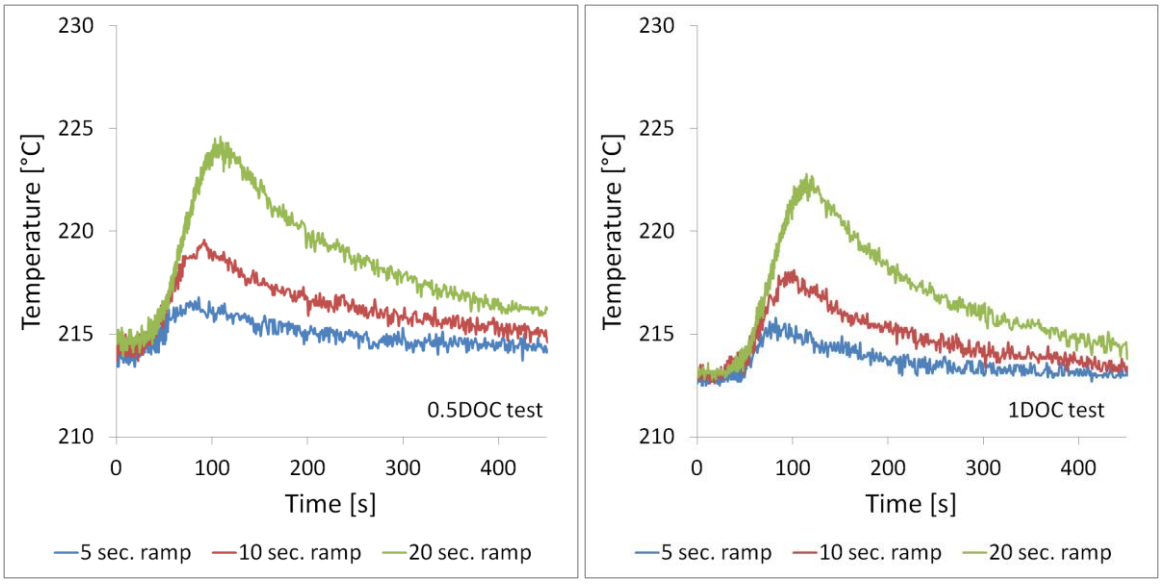

Figure 4.1.8.1a SCR inlet temperatures during the engine transient tests with standard 0.5 (left graph) and 1 (right graph) DOC.

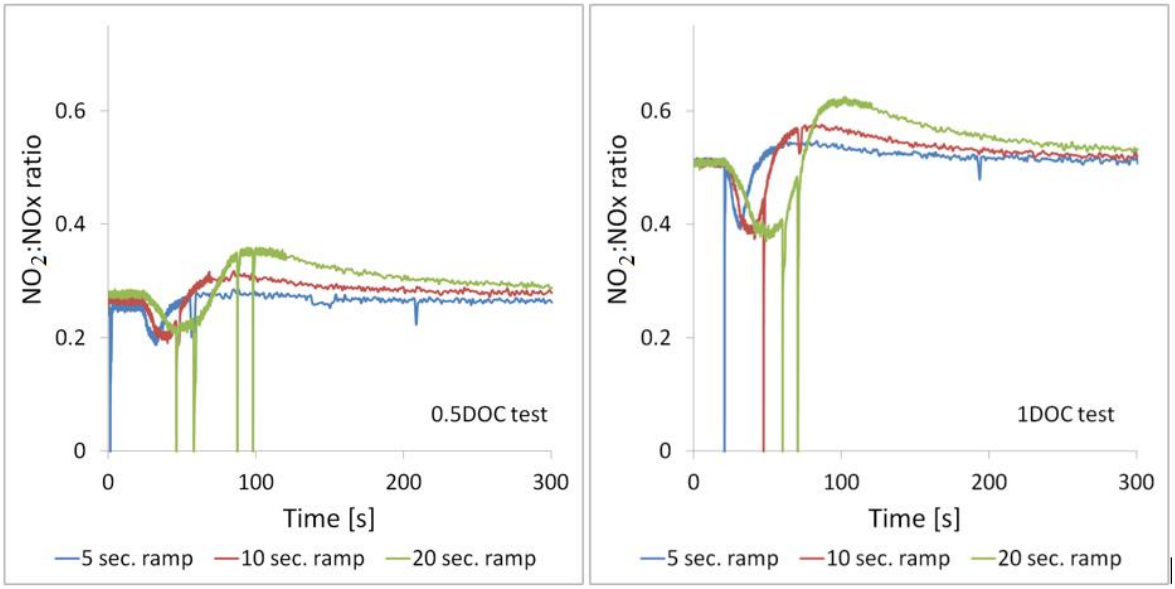

Figure 4.1.8.1b Inlet NO_2:NOx ratios during the engine transient tests with standard 0.5 (left graph) and 1 DOC (right graph).

Figure 4.1.8.1d shows traces of NO and NO_2 data measured upstream and downstream of the SCR for standard 0.5 (left hand side) and 1 (right hand side) DOC for each transient case. With the standard 0.5 DOC, the initial inlet level of NO (black line) was 420 ppm during each transient case. NO peaked at 580 ppm during the 5s engine ramp and close to 600 ppm during 10s and 20s ramp. The inlet initial level of NO_2 (blue line) for the standard 0.5 DOC case was around 150 ppm, which is about half of NO_2 supplied by the standard 1 DOC. The shape of the inlet NO_2 was dependent on the NO concentration and exhaust gas temperature, which influenced DOC response, as described earlier in relation to figure 4.1.8.1b. A high rise in the NO concentration during the engine ramp reduced slightly the NO_2 concentration. The reduction was more noticeable for the standard 1 DOC than for the 0.5 DOC case. Additionally, a rise in NO_2 was observed just after the transient event; the magnitude was bigger for 20 s ramp, especially for standard 1 DOC case. During the test with the standard 0.5 DOC, the entire NO_2 was converted with ammonia by the SCR, shown by zero concentration measured downstream of the catalyst. This was not the case for the standard 1 DOC because the NO_2 level was higher upstream. When NO_2 and NO both present, the NOx is expected to be consumed by the fast reaction.

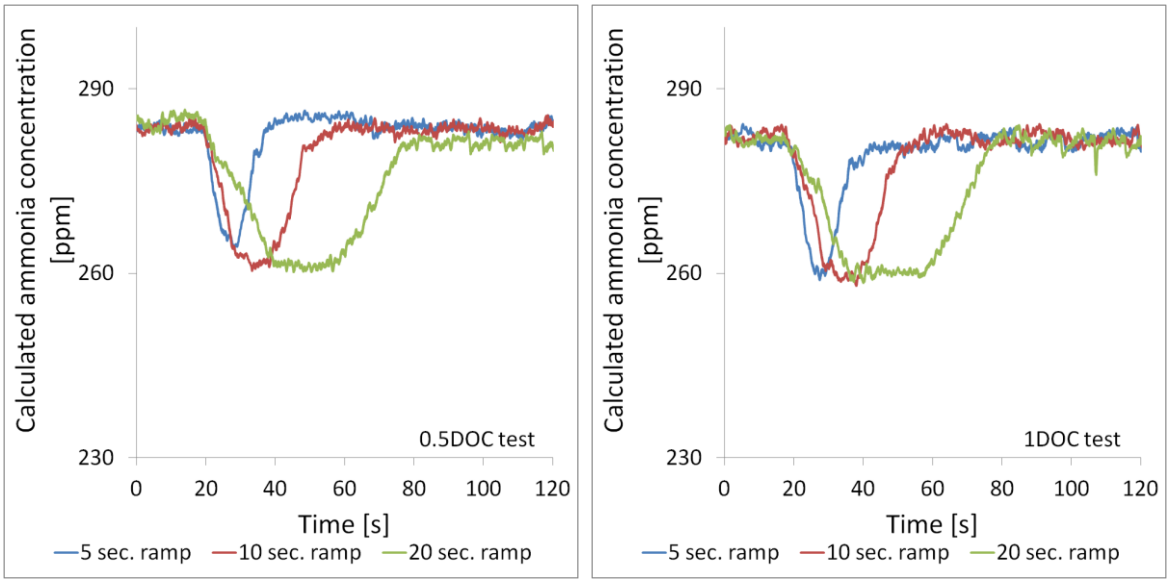

Figure 4.1.8.1c Calculated input ammonia during the engine transient tests with standard 0.5 DOC (left graph) and 1 DOC (right graph).

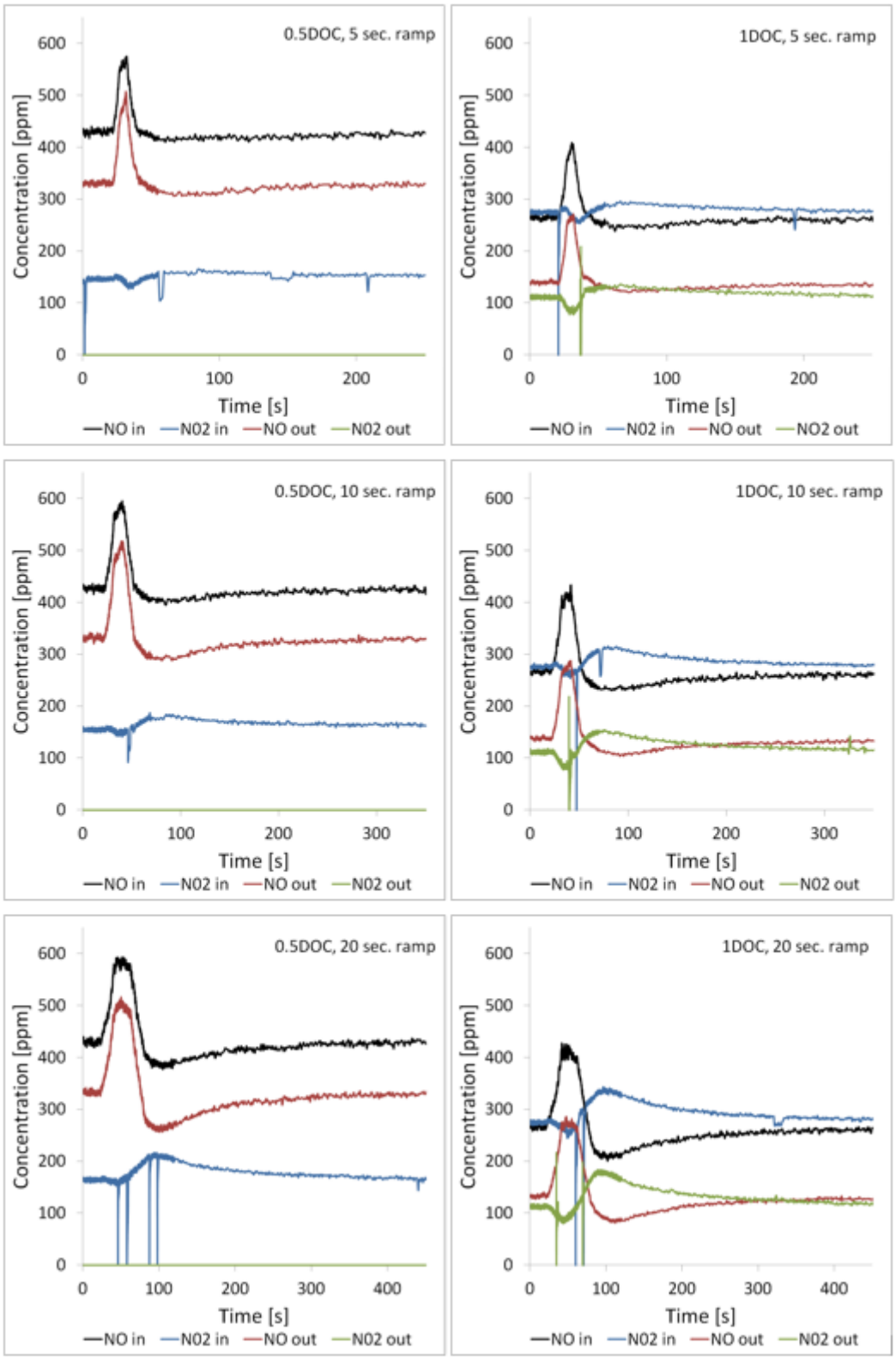

Figure 4.1.8d NO and NO_2 concentration during the engine transient tests with standard 0.5 DOC (left graphs) and 1 DOC (right graphs).

Figure 4.1.8.1e shows a relationship between NOx conversion, supplied NO_2:NOx ratio and the consumed NO_2:NOx ratio for the standard 0.5 DOC and 1 DOC cases. The presented data is plotted for only up to 20 s after transient ramp. The supplied NO_2:NOx ratio for the standard 0.5 DOC cases was initially 0.25 and then dropped to 0.2 during each transient experiment. Only for 20s transient case, the supplied NO_2:NOx ratio rose to 0.3 after the ramp. In case of standard 1DOC, the supplied NO_2:NOx ratio was 0.5, and dropped to 0.4 during the ramp. After the ramp, NO_2:NOx ratio increased to the same value during 5s ramp, to nearly 0.6 during 10s ramp and to over 0.6 for 20s ramp. Regardless of the different inlet NO_2:NOx profiles between standard 0.5 and 1 DOC cases, the consumed NO_2:NOx ratio for each transient case was about 0.6 and remained constant throughout the experiment. This suggests that for the range of inlet NO_2:NOx from 0.2 to 0.6, NO_2 and NO are consumed at similar rate. The initial NOx conversion was around 40% and 50% for standard 0.5 and 1 DOC respectively. During the ramp, the NOx conversion dropped to around 30% for each transient case with the standard 0.5 DOC. Less than 10% drop in NOx conversion was observed for each transient case with standard 1 DOC. The drop in NOx conversion during ramp could be mainly caused by deficient ammonia, however a drop in the supplied NO_2:NOx ratio could also have an impact on the NOx conversion. After the ramp, the NOx conversion either returned to an initial value or showed an improvement; for example NOx conversion increased from 40% to nearly 60% during the 20s ramp with the standard 0.5 DOC. The increase in NOx conversion after the ramp was caused by the increased supplied NO_2:NOx ratio and exhaust temperature. Additionally, it could also be observed that the NOx conversion was slightly less sensitive to change in NO_2:NOx ratio across the transient ramp during cases with standard 1 DOC due to an overall higher NO_2:NOx ratio. In terms of the SCR applications, car manufacturers are likely to operate the SCR at NO_2:NOx ratio closer to 0.5, in order to achieve more stable NOx conversion over the transient cycle.

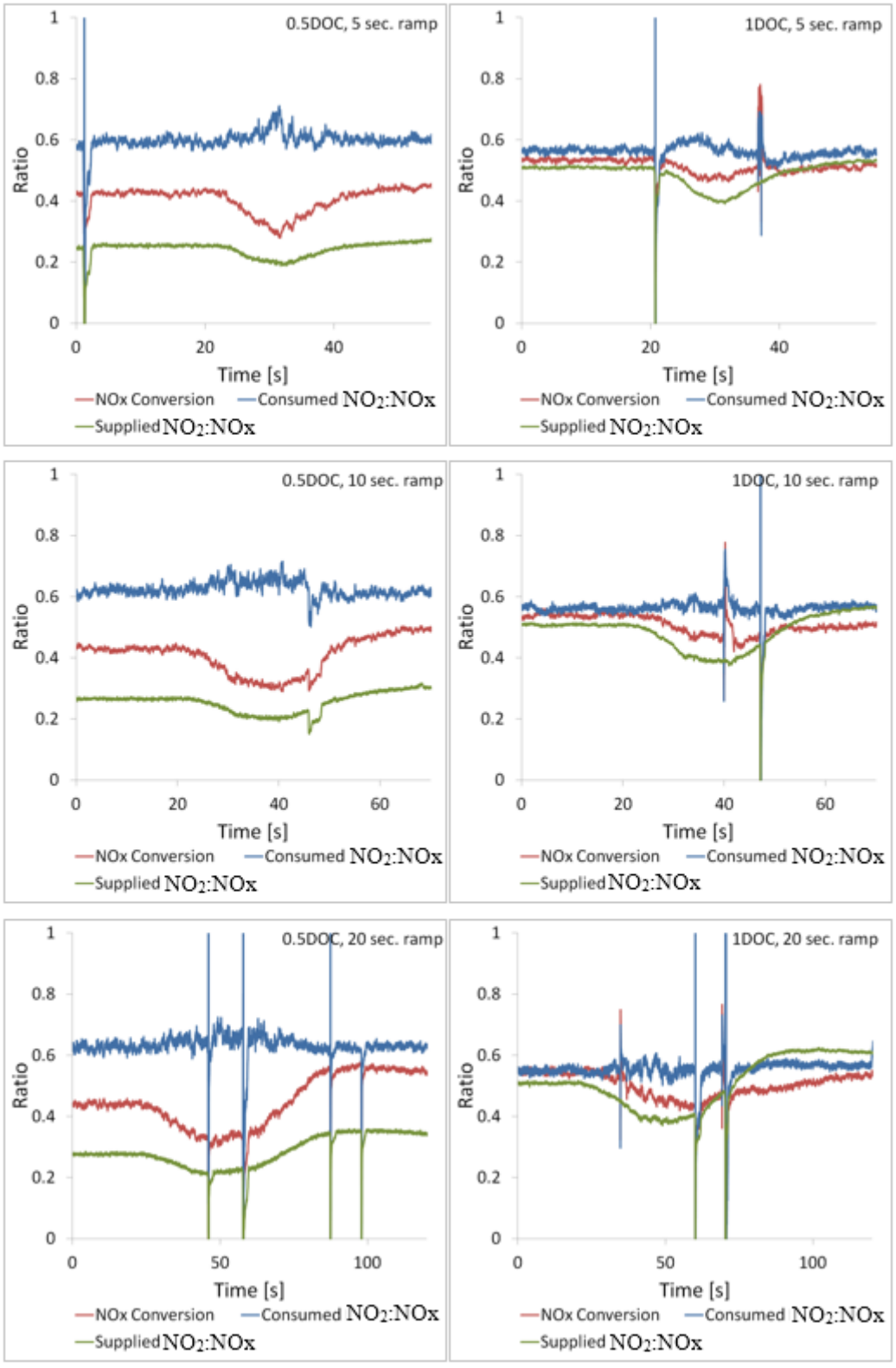

Figure 4.1.8.1e Comparison of consumed NO_2:NOx ratio to supplied NO_2:NOx ratio during the engine transient tests with standard 0.5 DOC (left graph) and 1 DOC (right graph).

4.1.8.2 Transient engine tests: Long transient

After 6 bar BMEP at 1500 rpm warm-up stage and 50 s of initial steady state, the engine was ramped up to 10 bar BMEP in time period of 20 seconds and held until exhaust temperature reached steady condition. Then, the engine was ramped down to 6 bar BMEP and held until exhaust temperature returned to the initial condition. Both engine ramps were linear. The FTIR analyser was used for these experiments to measure NO, NO_2, NH_3 and N_2O. During the test, ammonia gas was supplied for the stoichiometric NH_3:NOx ratio. Figure 4.1.8.2a shows the trace of the SCR inlet temperature during the transient test with Pd only DOC and standard 0.5 DOC. In comparison with the short transient experiment, the engine was held at a higher load for longer. As a result, the exhaust temperature at the inlet to SCR catalyst was also significantly higher and reached above 280 °C.

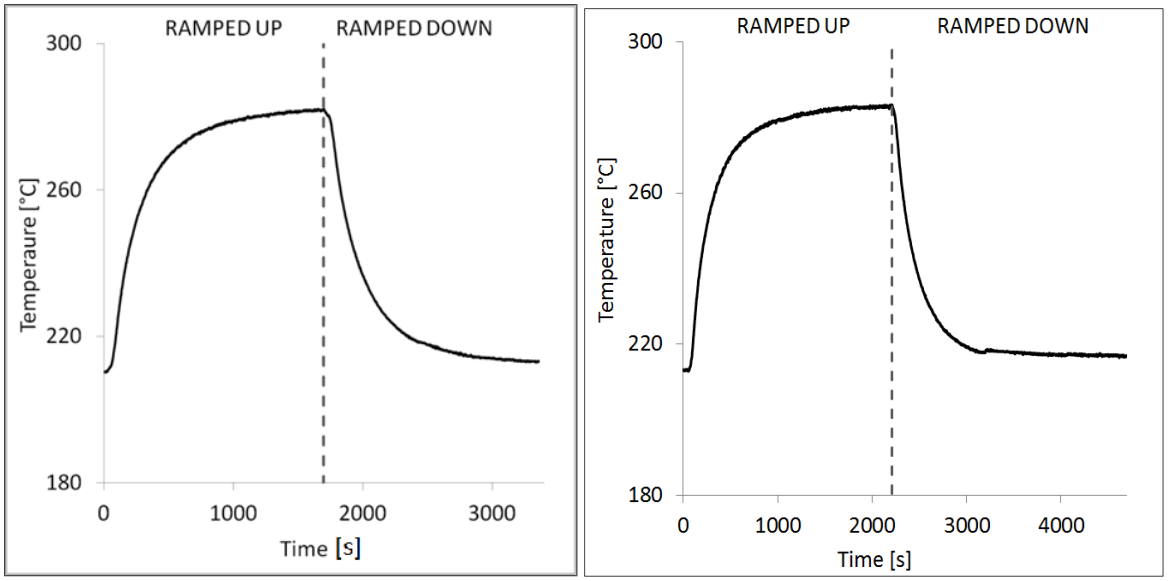

Figure 4.1.8.2a Temperature trace at 45 mm SCR inlet during the long engine transient test with Pd DOC (left graph) and standard 0.5 DOC (right graph).

Throughout the long transient test with Pd only DOC, the inlet NO_2 concentration was zero and concentration traces of NO and NH_3 before and after the SCR are shown in Figure 4.1.8.2b. During the initial steady state, the ammonia gas flow was set up to achieve stoichiometric NH_3:NO ratio and its flow rate was maintained constant throughout the test. After first 20 s engine ramp, the inlet NO level rose from 580 ppm to 850 ppm and inlet NH_3 level dropped from 580 to 530 ppm as a result of the increased exhaust mass flow rate. The engine 10 bar load was maintained for another 1657s to reach a steady state SCR inlet temperature and then ramped down to the initial 6 bar load. Both inlet NO and NH_3 concentration stayed constant during high and low engine load. The downstream SCR measurements are represented by NO and NH_3 outlet concentration. After engine was ramped up,

the measured NO concentration post the SCR catalyst initially increased to nearly 780 ppm; then, NO concentration started to gradually decrease while the gas exhaust temperature started to gradually increase. After the temperature stabilised, the level of NO decreased to 650 ppm. The initial peak in the NO concentration was a result of a sudden increase in the NO concentration upstream of the SCR catalyst. During the same event, the measured NH_3 post the SCR initially decreased from 500 ppm to 450 ppm (after 100 s of the test). This was mainly caused by the reduction in the ammonia concentration upstream of the catalyst discussed above. Then, NH_3 concentration continued to decrease, reaching finally 320 ppm, which was also the result of the increased exhaust temperature leading to the improvement in the efficiency of the SCR catalyst. After the engine load was ramped down from 10 to 6 bar BMEP, the NO concentration upstream of the SCR reduced suddenly from 850 to the initial 580 ppm. Together with reduced engine load, exhaust mass flow rate was also reduced resulting in the increased ammonia concentration, which rose from 530 to 580 ppm. As a result, during these conditions, the supplied NH_3:NO ratio returned to stoichiometric one (after 1657 s), as demonstrated by an overlap between the green and red line in figure 4.1.8.2b. Just after the ramp down, the concentration of NO measured post the SCR reduced suddenly from 650 to 400 ppm. However, as exhaust gas temperature continued to decrease (as shown in figure 4.1.8.2a), NO concentration gradually increased to 480 ppm. The NH_3 concentration measured post the SCR, after the ramp down, gradually increased from 320 to 480 ppm. It was expected that in the absence of the NO_2 only standard SCR reactions (see equation 1.4.3a) took place; therefore, during the stoichiometric NH_3:NO conditions, it was observed that the NOx slip was equal to NH_3 slip.

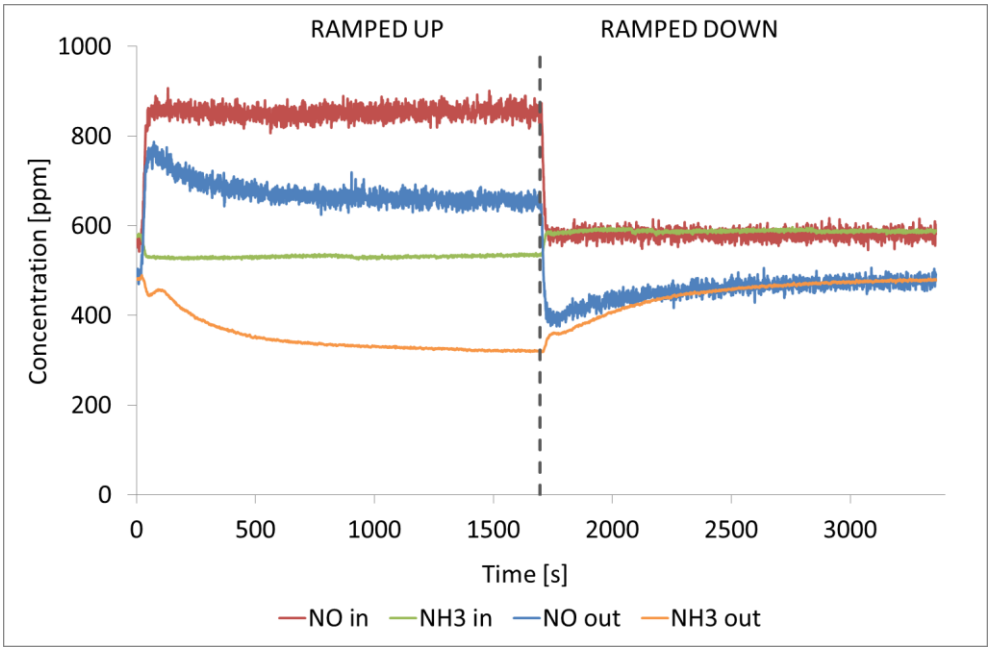

Figure 4.1.8.2b NO and NH_3 concentration during the long engine transient test with Pd only DOC and 45 mm SCR.

Figure 4.1.8.2c shows the NO and NH_3 conversion efficiency profile for the 45 mm SCR brick during the transient experiment with Pd only DOC. The NO conversion improved from 10 % to 20 % as engine was ramped up, while NH_3 conversion increased from 12 % to 40 %. The difference in conversions between NO and NH_3 is a result of deficient ammonia supplied at a higher engine load. After engine was ramped down, the supplied NH_3:NO ratio was close to α=1 and consequently NH_3 conversion was at same level as NO. The small peak in the NO conversion just after the ramp down was caused by a sudden reduction in the supplied NO and residual heat stored in the exhaust from the previous engine load, which temporarily improved the SCR performance.

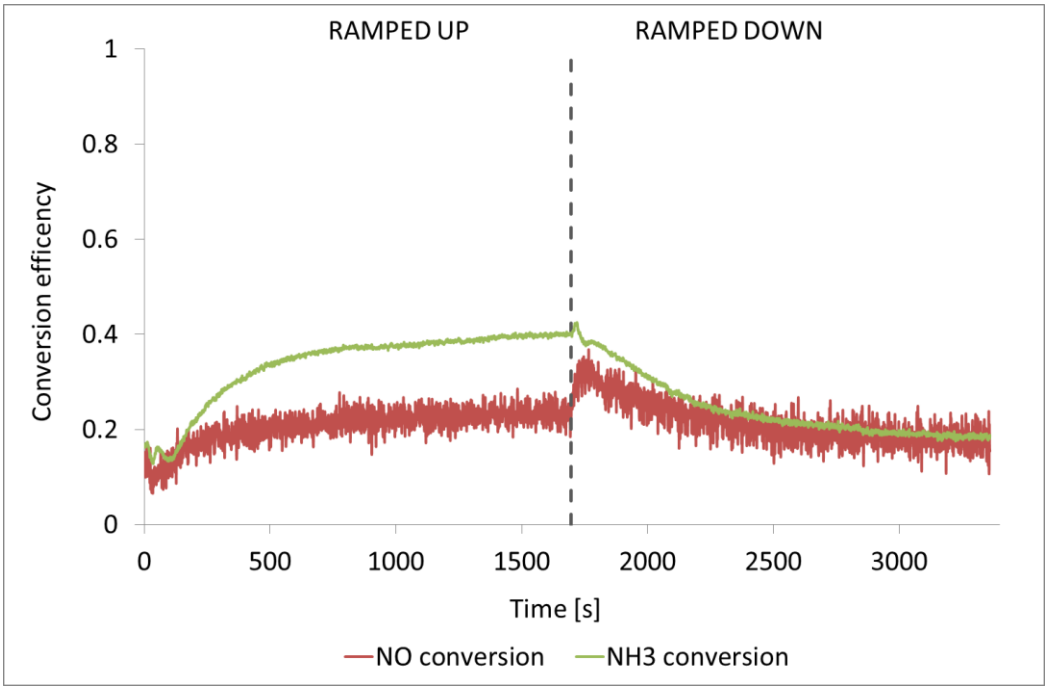

Figure 4.1.8.2c Comparison of NOx and NH_3 conversion profile during the long engine transient test with Pd only DOC and 45 mm SCR.

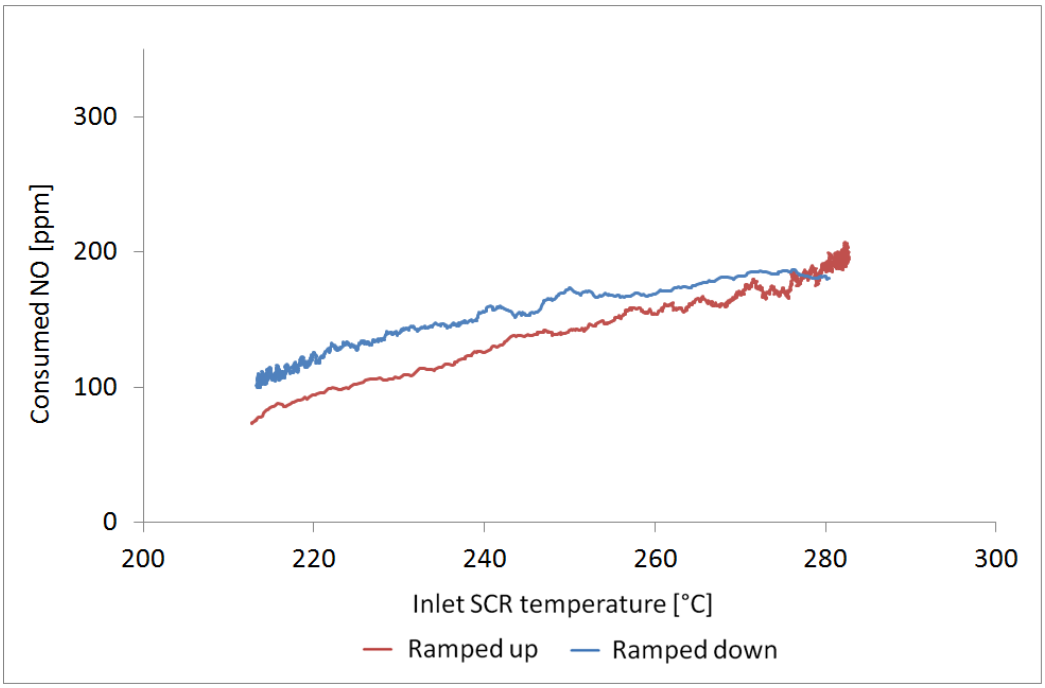

Figure 4.1.8.2d SCR inlet temperature effect on NO consumed during the long engine transient test with Pd only DOC and 45 mm SCR.

The effect of the inlet SCR gas temperature on the amount of the consumed NO for ramp up (red line) and ramp down (blue line) is presented in Figure 4.1.8.2d. During the ramp up transient test, the consumed NO value at 212 °C was 95 ppm and increased to 200 ppm at 282 °C. The blue line, shows a ramp down transient experiment, which is slightly higher than the red line towards the 210 °C SCR inlet temperature. The difference between the red and blue line at lower temperature was caused by a small increase in the exhaust mass flow rate, which affected the SCR performance.

In addition to transient tests involving NO only, as described earlier, the same set of experiments was conducted but with NO and NO_2. Therefore, the Pd only DOC was substituted with standard 0.5 DOC. The species concentration measured upstream and downstream of the SCR during long transient test with standard 0.5 DOC and 45 mm SCR is presented in Figure 4.1.8.2e. Because of the DOC presence in the exhaust, part of NO was oxidised to NO_2 upstream of the SCR. Initially, after engine load was ramped up from 6 to 10 bar BMEP, the inlet NO concentration peaked at 710 ppm and started to drop as the inlet NO_2 concentration started to rise from initial 180 ppm. After the exhaust temperature reached a steady state condition of 280 °C (as shown in figure 4.1.8.2a), NO and NO_2 reached 530 ppm and 300 ppm respectively. Then after 2200s, engine load was ramped down back to 6 bar BMEP and exhaust temperature started to decrease from 280 to 210 °C. As a result, the inlet NO concentration dropped suddenly to 280 ppm and then started to increase, while the inlet NO_2 concentration started to decrease. By the end of the test inlet NO and NO_2 concentrations returned to initial levels of 400 and 180 ppm respectively. Same as for the long

transient test with Pd only DOC, the ammonia gas was supplied to achieve stoichiometric NH_3:NOx ratio during the initial 6 bar BMEP engine condition. Initially, the inlet NH_3 concentration was 580 ppm which dropped to 530 ppm at 10 bar BMEP engine load and then returned to 580 ppm after engine load was ramped down to 6 bar BMEP. It was observed that most of NO_2 was converted on SCR catalyst. Measured NO_2 concentration post SCR shows only 80 ppm slip when engine was ramped up and 20 ppm after engine was ramped down. Also, it can be pointed out that NH_3 slip was much lower compared with the test with Pd only DOC (as shown in figure 4.1.8.2b), this being the result of higher SCR conversion when NO_2 is present.

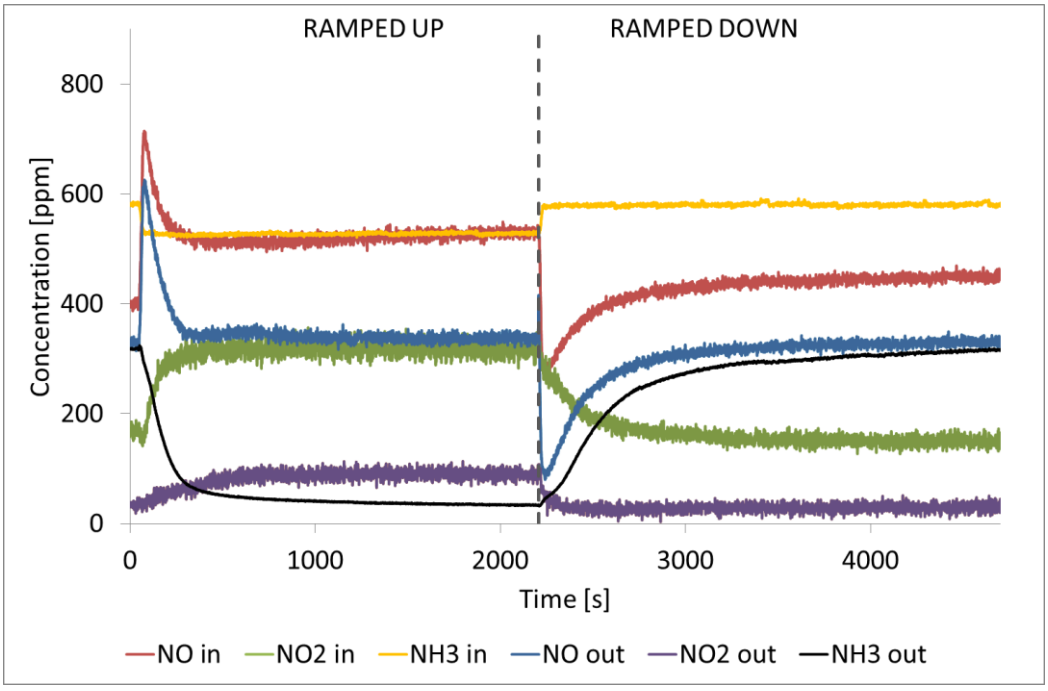

Figure 4.1.8.2e NOx and NH_3 concentration during the long engine transient test with standard 0.5 DOC and 45 mm SCR.

Figure 4.1.8.2f shows a comparison between a consumed NO_2:NOx ratio to supplied NO_2:NOx ratio as well as NOx and NH_3 conversion efficiency. The supplied NO_2:NOx ratio drops from 0.3 to 0.2 at the beginning of the transient test caused by spike of NO concentration, then the ratio rose to 0.4 as a result of higher exhaust temperature which improved DOC NO oxidation . When engine load dropped from 10 to 6 bar BMEP, the supplied NO_2:NOx ratio peaked initially at 0.5 and then dropped gradually to the value of 0.3. Independently from supplied NO_2:NOx ratio the consumed NO_2:NOx ratio was around 0.6 throughout the test and remained constant during the transient test. Similar SCR selectivity behaviour was observed during the short transient experiment (see Figure 4.1.8.1e). In terms of NOx conversion, it is observed that the NOx conversion trace is proportional to the trace of supplied NO_2:NOx ratio; this shows how SCR reaction rate is influenced by supplied NO_2:NOx ratio.

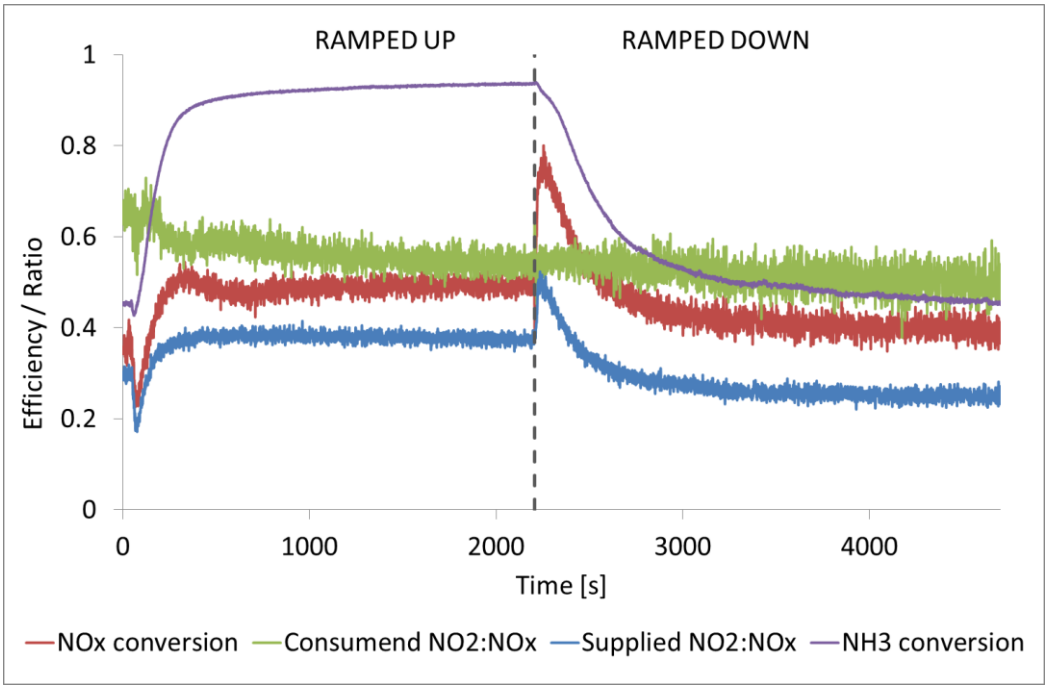

Figure 4.1.8.2f Comparison of consumed NO_2:NOx ratio to supplied NO_2:NOx ratio and NH_3 conversion during the long engine transient test with standard 0.5 DOC and 45 mm SCR.

Figure 4.1.8.2g shows effect of inlet SCR temperature on consumed NOx during long transient test with the standard 0.5 DOC. It is observed that at SCR inlet temperature of 220 °C, 200 ppm of NOx was consumed. After temperature rose to 280 °C, the consumed NOx increased to 440 ppm. In comparison to long transient with Pd only DOC, about twice as much NOx was consumed when standard 0.5 DOC was used. Results from transient testing studies were used for the validation of the SCR kinetics which showed that there was a need to adjust certain model parameters to fit the data (Benjamin et at.,2012a).

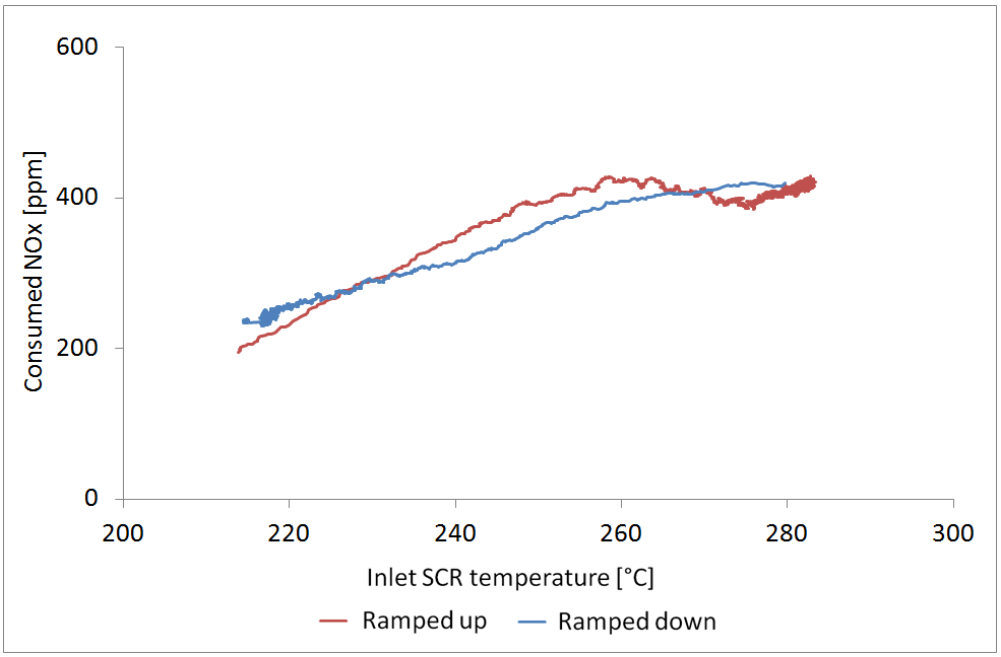

Figure 4.1.8.2g SCR inlet temperature effect on NOx consumed during the long engine transient test with standard 0.5 DOC and 45 mm SCR.

4.1.8.3 Summary of results from transient engine testing

The key findings from the transient engine testing were:

- All NO_2 was converted with ammonia on the SCR during the short transient test with standard 0.5 DOC. When NO_2 level was significantly higher for standard 1 DOC, the NO_2 slip was observed downstream of the SCR because the NOx is expected to be consumed by the fast SCR reaction.
- NOx conversion during the short and long transient tests was mainly influenced by the supplied NO_2:NOx ratio rather than a change in the SCR temperature. It was also found that consumed NO_2:NOx ratio remained constant throughout the transient experiment regardless of changing the supplied NO_2:NOx ratio profile. This was true for short and long transient test.

4.2 Urea dosing

In order to simplify and remove the complex urea hydrolysis phenomena, studies conducted in the earlier section of this thesis used ammonia gas instead of urea injection. This section presents results of the SCR catalyst performance during steady state and transient engine conditions with the urea injection (Benjamin et al., 2014). When urea is injected into a hot exhaust, it hydrolyses and converts into ammonia, which is then used for the NOx reduction on the SCR catalyst. The injected urea was 32.5 % water solution known commercially as AdBlue.

During this set of experiments, urea was injected either through the oblique pipe arrangement with the urea mixer device located downstream or directly to the mixing can, in which case the mixer was replaced with a straight pipe. For this study, a single SCR brick of volume 0.8 litre was fitted and to ensure that the supplied NO_2:NOx ratio was zero, Pd only DOC was used post the DPF. The FTIR gas analyser measured gas composition before and after SCR catalyst.

4.2.1 The effect of the injection position on droplet size

The droplet size measurements were undertaken by C.A. Roberts using the same urea injection system as used during engine testing (Benjamin et al., 2014). When spraying cold distilled water into open air, a droplets size at the peak of the distribution were close to 150 µm, which is much higher than the desirable droplets size for SCR systems application. Additionally, using a replica of the engine exhaust, droplets size distribution was also measured when water was injected into the pipe through the oblique side branch or into the top of the expansion can. For safety reasons, during this experiment, real exhaust gas was substituted with hot air (air temperature of 180 °C).

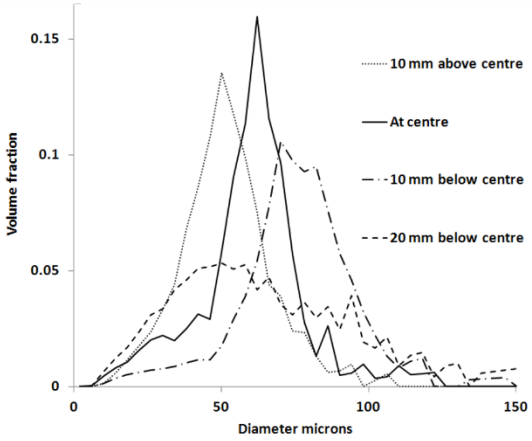

Figure 4.2.1a Droplet size distribution downstream of the urea mixer when water was sprayed into pipe through the oblique side branch. Air flow temperature of 180 ^{o}C.

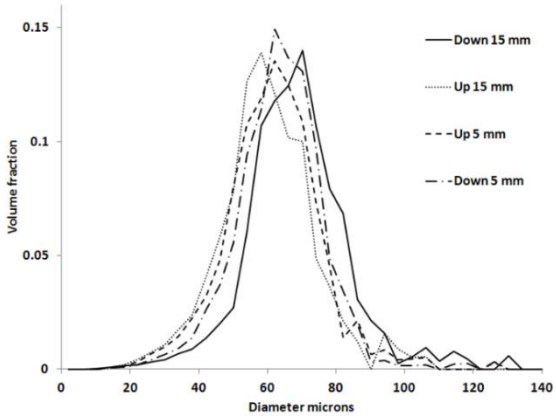

Figure 4.2.1b. Droplet size distribution measurements at the nozzle exit when the spray was sprayed into the top of the expansion can at air flow temperature of 180 ^{o}C.

Figure 4.2.1a shows the droplet size distribution at the exit of the urea mixer. The average droplet size exiting at the centre was reduced to 60 microns. Some droplets measured below and above the centre, showed a variety of size distributions between 50 and 100 microns. Figure 4.2.1b shows droplet size distribution at the exit of the nozzle when water was injected onto the expansion can. Significantly less variation in droplet size was observed when measured off the centre. The droplet size was in the range of 60-70 microns.

It is likely that water droplets bounced off the pipe wall before they got carried by flow downstream into the mixer. Most of the droplets should break down and evaporate after hitting hot angled plates of the mixer. Mixing effect in the can should provide a uniform droplets distribution at the exit of the nozzle. Due to much lower gas velocity in the can, some of the big water droplets could potentially drop into the bottom of the can and then evaporate from the surface.

4.2.2 Steady state engine testing

During steady state testing, the engine was running with a constant speed of 1500 rpm and the SCR catalyst temperature was controlled by the engine load. For low temperature case, engine was running at 6 bar BMEP to achieve catalyst temperature close to 220 ^{o}C. For high temperature case, engine load was increased to 8.5 bar BMEP to achieve SCR temperature close to 260 ^{o}C. For each experiment, the urea injection quantities were calculated for three NH_3:NOx ratios of 1, 0.75 and 0.5, assuming a complete urea hydrolysis to ammonia. . The concentration of NH_3 and NO was measured

using FTIR analyser and the exhaust gas was sampled 25 mm before the front face of the SCR catalyst.

Table 4.2.2 shows inlet conditions for low and high temperature tests, when urea was injected either through the oblique pipe arrangement or directly to the mixing can. It is observed that only low concentration of ammonia was detected upstream of the catalyst, which was much lower from expected concentration for setup urea dosing rates.

Table 4.2.2. Inlet conditions for the urea injection steady-state tests at low and high temperature.

	Urea injection	***Upstream measured NO (ppm)***	***PreSCR Temp (°C)***	***Upstream measured NH_3 (ppm)***		
				α~0.5	**α~0.75**	**α~1**
Low temperature	Can	660	224	22	25	29
	Pipe	630	215	33	56	80
High temperature	Can	834	259	38	46	55
	Pipe	801	260	49	84	125

The potential NH_3 concentration of the injected urea into exhaust, assuming full hydrolysis can be calculated using the equation below:

$$NH_{3_{potential}}\,[ppm] = \left(2 \times \frac{Urea_{injected}\left[\frac{g}{s}\right]}{urea_{mass}\left[\frac{g}{mols}\right]}\right) \div Exhaust\ flow_{total}\left[\frac{mols}{s}\right] \times 10^6 \quad \text{(Eq. 4.2.2)}$$

Figure 4.2.2a shows proportion of the measured NH_3 to the calculated potential NH_3. It can be seen that during each test cases, only small proportion of ammonia was released from urea upstream of SCR catalyst. The amount of ammonia released was only slightly higher when urea was injected into the pipe and marginally increased with increased supplied NH_3:NOx ratios. Also, slightly more ammonia was released at higher temperature making at most 14 % of the potential ammonia available as ammonia gas upstream..

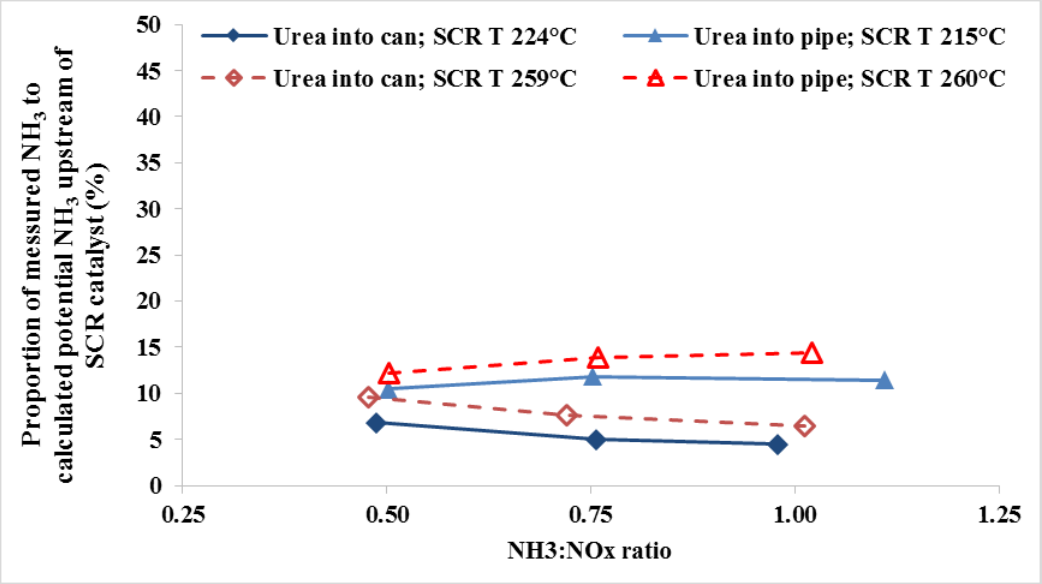

Figure 4.2.2a Proportion of the measured NH_3 to the calculated potential NH_3 25 mm before SCR catalyst.

Figures 4.2.2b and 4.2.2c shows downstream comparison between the urea injection into pipe with mixer system and urea injection into expansion can for a lower temperature case (220 ºC). Blue and green solid lines represents measured concentration of NO and NH_3 respectively downstream of the SCR catalyst. The pink dotted line represents flow rate of the injected urea in mg/s. After 200 s of the experiment the urea was dosed at NH_3:NOx=1 and the measured NO concentration decreased while NO was reacting with ammonia on the SCR catalyst. During the experiment urea was injected through the oblique pipe, NO was reduced by 152 ppm and NH_3 slip reached 350 ppm. Then, the urea injection was reduced to NH_3:NOx=0.75 and the NH_3 slip dropped from 350 to 222 ppm. Finally the NH_3 slip dropped to 128ppm when the NH_3:NOx was reduced to 0.5. It is observed that, the same amount of NO was consumed during both urea injection methods for each NH_3:NOx urea dosing. However, the measured NH_3 slip was much lower when urea was injected into the expansion can reaching only 218 ppm at NH_3:NOx=1, 168 ppm NH_3:NOx=0.75 and 115 at NH_3:NOx=0.5. Additionally, the measured NH_3 slip was more unstable when urea was injected into the pipe-mixer system, particularly at NH_3:NOx=1.

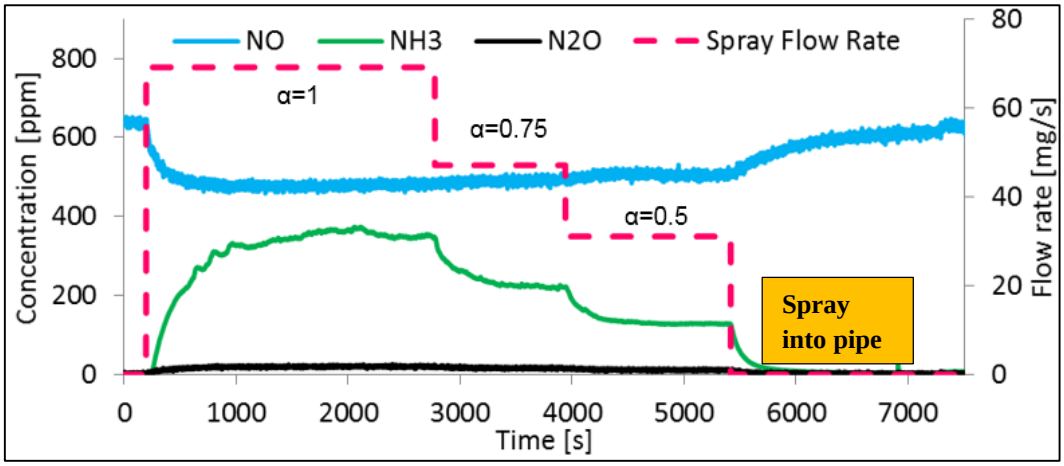

Figure 4.2.2b NO, NH_3 and N_2O concentration measured after the SCR during spray into pipe. Low temperature experiment.

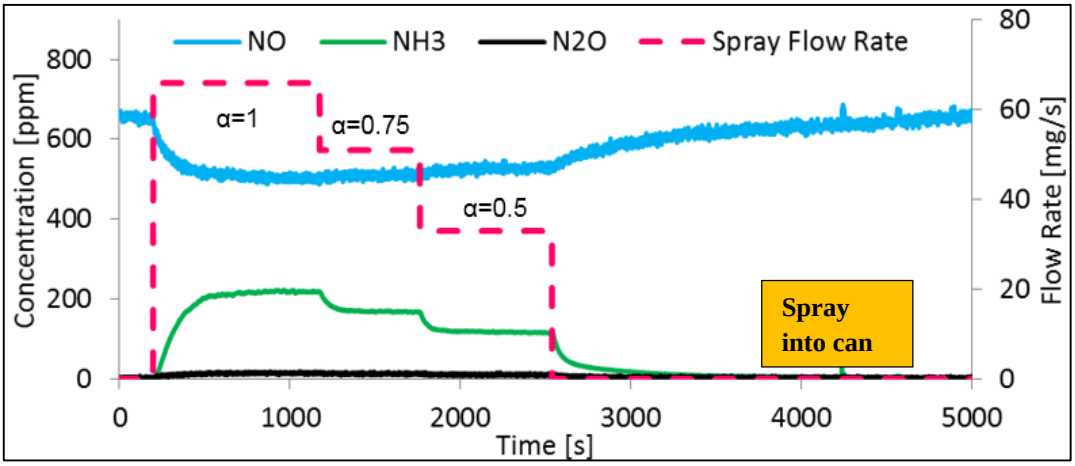

Figure 4.2.2c NO, NH_3 and N_2O concentration measured after the SCR during spray into to the can test. Low temperature experiment

Experiment was repeated for a high temperature case with inlet SCR catalyst temperature increased to 260°C. Just like during low temperature case, urea was injected either through an oblique pipe or into expansion can. In order to achieve the same NH_3:NOx ratio (1, 0.75 and 0.5), urea dosing quantities were increased accordingly to compensate for a higher NO concentration. Figure 4.2.2d and 4.2.2e show NO and NH_3 concentration measured after the SCR catalyst. The urea injection started at the NH_3:NOx=1, 200 seconds into the test. It was observed that NH_3 slip reached higher values when urea was injected into the pipe for the NH_3:NOx=1 and 0.75, which was similar to the low temperature experiment. However, after the dosing was reduced to NH_3:NOx=0.5, the slip was 10 ppm higher when urea was injected into the expansion can. Unlike in low temperature tests, more NO was consumed when urea was injected into the expansion can.

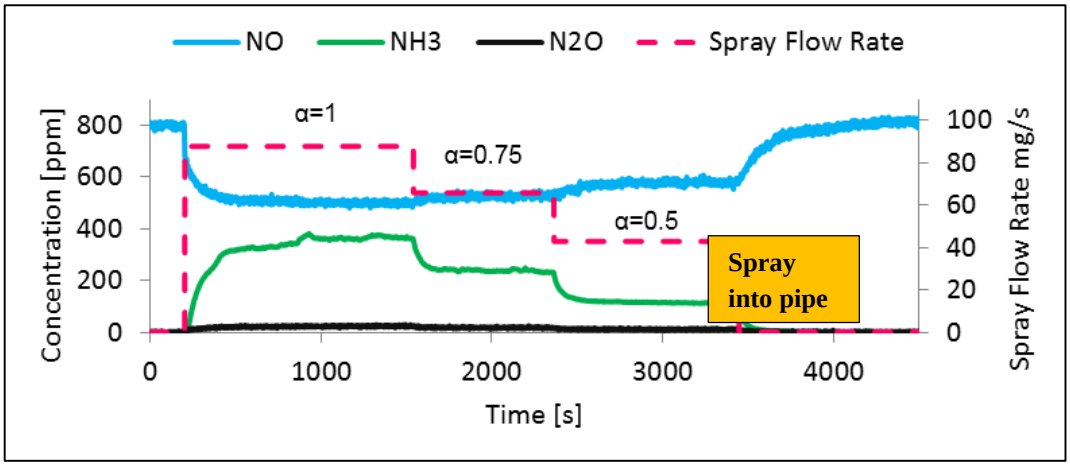

Figure 4.2.2d NO, NH_3 and N_2O concentration measured after the SCR during spray into the pipe. High temperature experiment

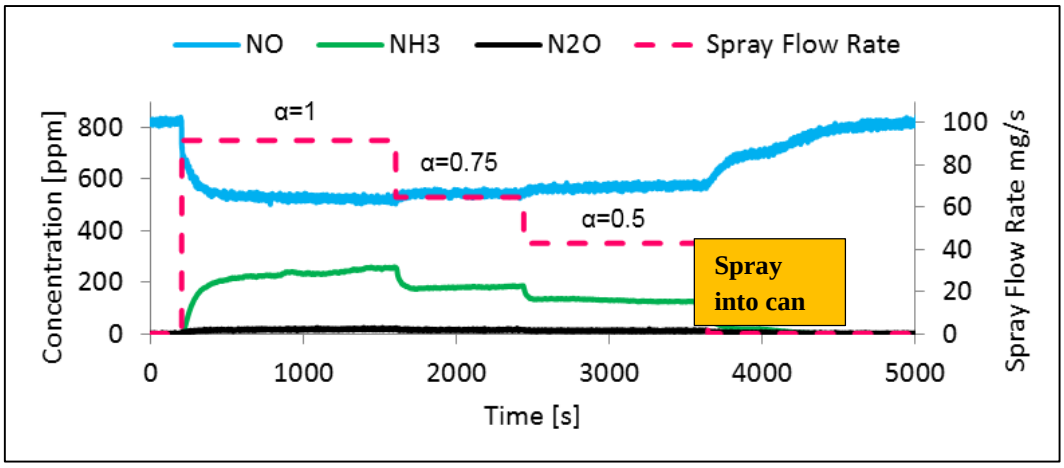

Figure 4.2.2e NO, NH_3 and N_2O concentration measured after the SCR during spray into the can test. High temperature experiment.

After the urea injection is turned off (pink line equals zero), ammonia stored on the catalyst will continue reacting with NO until whole amount of ammonia is used. It was observed that time needed for NO to return to the initial concentration was different between two injection methods, especially during low temperature test. In the case of urea dosing into expansion can, it took 500s longer for stored ammonia to purge, in comparison to the pipe injection case. This could be explained by either higher ammonia storage level for experiment with urea dosing into expansion can or by the ammonia released from the urea stored in the exhaust system upstream of the SCR. As exhaust temperature and NOx conversion was very similar in both cases, there should not have been any difference in the amount of stored ammonia. Also, amount of stored ammonia should not have been affected by the

injection method. In the expansion can, the gas velocity is much lower and some of the bigger urea droplets could drop and splash at the bottom of the can and create deposit as solid urea crystals. Slow decomposition of accumulated solid urea could be the cause of the observed lag in NO response. As some of the injected urea is deposited in the exhaust, less quantity is available for the hydrolysis on the catalyst surface. As a result, the ammonia slip in this case is lower for each NH3:NOx injection setup.

4.2.3 Urea hydrolysis and NO conversion during steady state experiment

When urea is injected into the hot exhaust flow stream, water content will evaporate; then urea will decompose into NH_3 and HCNO (Koebel et al., 2000). In the next step, the HNCO will hydrolyse to NH_3 and CO_2. In the full process, one molecule of urea will release two molecules of NH_3.

Table 4.2.3. Consumed NO and measured NH_3 slip at the end of each urea dosing periods (α~0.5, 0.75 and 1) during steady state tests at low and high temperatures.

	Urea injection	***PreSCR Temp (°C)***	***Converted NO (ppm)***			***NH_3 slip (ppm)***		
			α~0.5	**α~0.75**	**α~1**	**α~0.5**	**α~0.75**	**α~1**
Low temperature	Can	224	132	149	155	116	168	218
	Pipe	215	124	136	148	128	221	352
High temperature	Can	259	258	290	312	126	186	256
	Pipe	260	222	272	300	115	233	365

In the absence of NO_2, only standard SCR reaction takes place, hence 1 mol of NH_3 is required to convert 1 mol of NO, which is an equivalent to 1 ppm of NH_3 used for 1 ppm of NO. As the tests were conducted until the steady state of NH_3 slip was reached, by then the level of ammonia storage would have reached a stable value. Consequently, concentration of the theoretical ammonia released (tNH_3) from the injected urea, can be calculated by adding concentration of converted NO and concentration of NH_3 slip. These values can be found in table 4.2.3. It is clear that the measured level of ammonia before the SCR brick, shown in table 4.2.2, is much lower when compared to the level of the theoretical ammonia released (tNH3). This indicates that only small proportion of ammonia is released in the exhaust before the catalyst and most of the urea decomposition and hydrolysis occurs on the surface of the SCR catalyst. Koebel and Strutz, (2003) showed that at temperatures of around

300°C, less than 20 % of ammonia was released in exhaust from the injected urea. This is in line with the experimental data in the current study.

Further analysis showed that concentration of potential ammonia from injected urea was greater than tNH_3. Percentage of the ammonia deficit can be calculated using below equation:

$$ammonia\ deficit\ [\%] = \frac{NH_{3_{potential}}[ppm] - (\Delta NO[ppm] + NH_3 slip[ppm])}{NH3_{potential}[ppm]} \qquad (Eq.\ 4.2.3)$$

The summary of calculated ammonia deficit for low and high temperature tests is shown in figure 4.2.3a. There is a visible relationship between the ammonia deficit and the urea injection method, showing more of missing ammonia for urea injected into the expansion can, particularly when dosing NH_3:NOx=1. Surprisingly, up to 42 % of potential ammonia is missing during the low temperature experiment. Clearly, the deficit is greater with an increased urea injection quantities and for a lower temperature experiment for both dosing configurations.

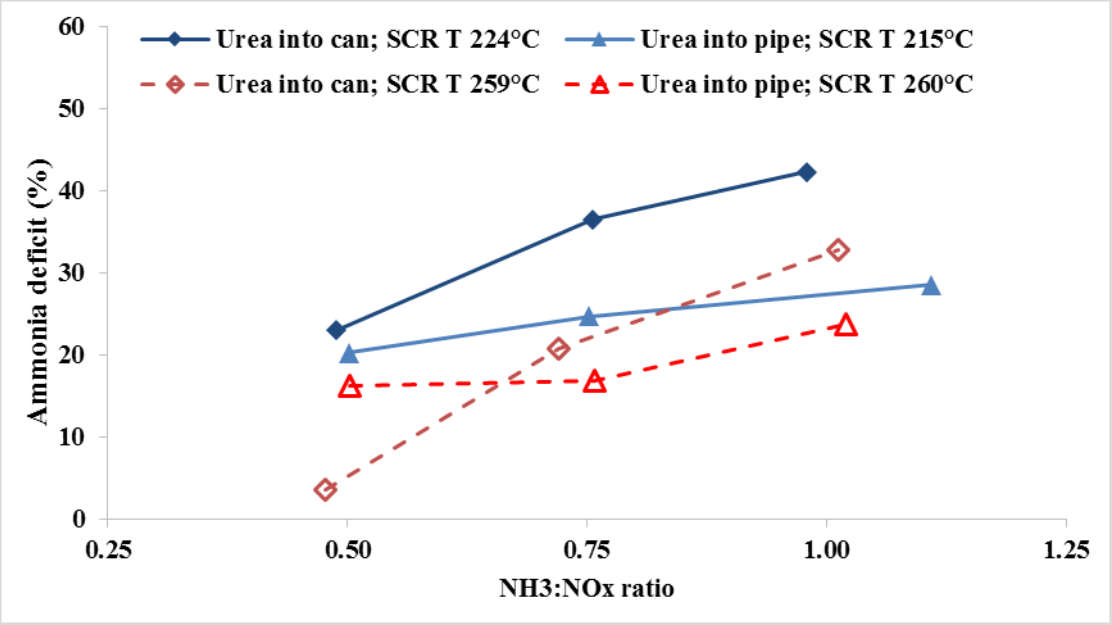

Figure 4.2.3a Calculated ammonia deficit during urea injection at low and high temperature for both dosing configurations.

As established earlier, 85 % or more of injected urea had to be decomposed and hydrolysed to ammonia on the surface of the SCR catalyst. Therefore, there is a great probability that ammonia was still in the form of HCNO or perhaps of undecomposed urea; as a result, it would be undetected by the FTIR analyser. Spray measurement presented in section 4.2.1, showed that some of the droplets were still quite large even after the mixer plate. It is possible that these larger droplets were too big to fully hydrolyse to ammonia even after contact with hot surface of SCR catalyst. Also, ammonia could be converted to other forms like N_2O and potentially absorbed on the catalyst; however, in the absence of NO_2 and at these low temperatures, the amount of N_2O formation would be negligible.

Figure 4.2.3b represents the NO conversion comparison between steady state urea injection experiments and steady state ammonia gas dosing experiments at a similar catalyst temperature. Low temperature experiment showed no difference between the urea pipe injection and the can injection. Only small improvement in conversion was observed when spraying into the can at higher temperature during NH_3:NOx=0.5 dosing; otherwise, both urea injection methods showed similar performance. When the ammonia was supplied in gas form, 8 % more of NO was converted for a given NH_3:NOx ratio. Particularly, ammonia gas dosing showed a better conversion at high temperature; for example, at NH_3:NOx 1 dosing the conversion was 13 % higher than urea injection experiment.

The difference in NO conversion performance between gas dosing and urea injection cannot be easily explained. The SCR catalyst was saturated with ammonia for each urea dosing, as evidenced by the detection of the NH_3 slip. Therefore, there was sufficient amount of ammonia available to react with NO. With urea injection, SCR catalyst needs to constantly hydrolyse urea to ammonia while simultaneously converting this ammonia with NO. Most probably, there is a competition on the SCR between those two reactions; therefore gas injection can provide slightly better conversion.

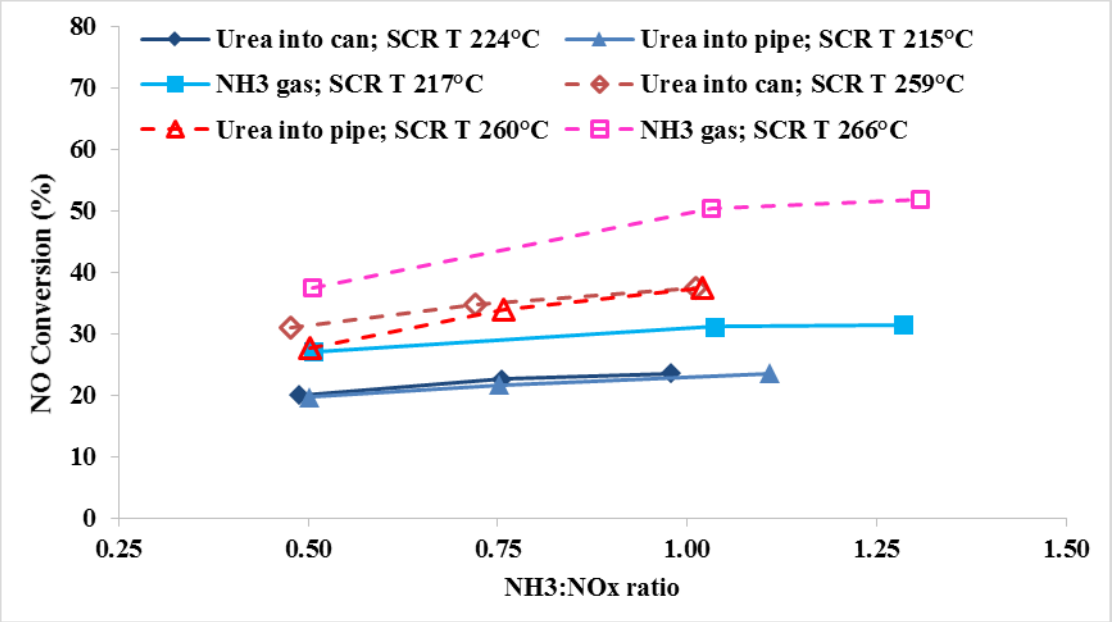

Figure 4.2.3b Steady state NO conversion against NH_3:NOx ratio for 0.8 litre SCR. Comparison of NH_3 gas injection and urea injection at low and high temperature

4.2.4 Urea spray under transient engine conditions test

In addition to steady state measurements, the experiment with urea injection was carried out under transient engine conditions using simple engine load ramp to measure SCR performance. The urea was injected only via the oblique pipe with the mixer located downstream. Similarly to steady state experiment, the SCR catalyst had volume of 0.8 litre and the DOC was palladium only.

Figure 4.2.4a shows the measurement of NO and NH_3 concentration and temperature trace at inlet of the SCR catalyst during the transient test. During first 200 s, engine was operating at 1500 rpm and 6 bar BMEP. The measured NO concentration upstream of SCR was around 660 ppm and the exhaust temperature reached 210 ^oC. The urea injection was set up at the flow rate of 66 mg/s to achieve NH_3:NOx close to 1 and same amount was injected throughout the test. After SCR was saturated with ammonia, and the NO conversion and NH_3 slip reached a stable condition, as seen in figure 4.2.4b, the engine was ramped up to 10 bar BMEP in 20 s. Similarly to transient testing with ammonia gas the engine ramp rate was linear. NO concentration increased rapidly to around 960 ppm and then temperature started to rise, reaching just above 280 ^oC at 2500 s of the test. The engine was held at these conditions until exhaust temperature reached a steady condition. Then the engine was ramped down in 20 s to the initial engine load and also held until a stable exhaust temperature was achieved. It was observed that the increase in the exhaust temperature had an effect on NH_3 concentration measured before the SCR. Initially measured concentration of NH_3 was 80 ppm, when engine load was ramped up 10 bar BMEP the NH_3 concentration increased rapidly to 160 ppm by 640 s then dropped to 100 ppm by the end of 10 bar BMEP engine load stage. After engine load was ramped down to 6 bar BMEP, the NH_3 concentration stayed constant throughout test just above 70ppm. The measured peak of NH_3 concentration could be a result of ammonia which was thermally released from undecomposed urea stored in the exhaust system. Only insignificant concentration of N_2O was detected upstream of the SCR catalyst.

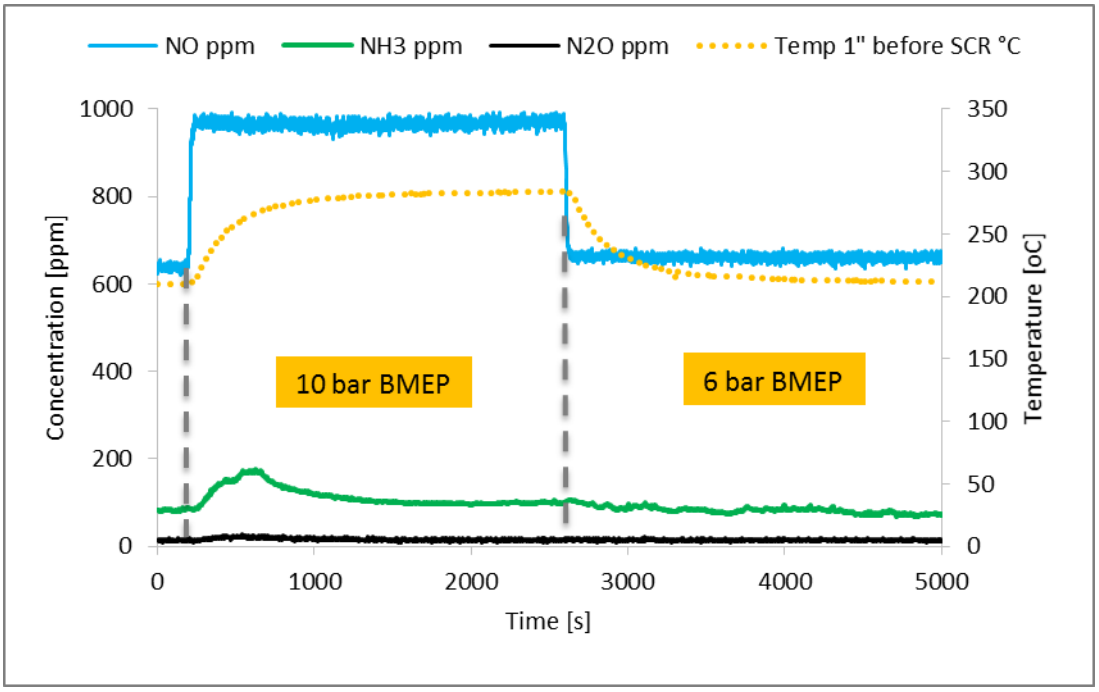

Figure 4.2 4a FTIR measurements and gas temperature profile during the transient experiment measured upstream of the SCR catalyst

Figure 4.2.4b represents the measurement of NO, NH_3 measured after the SCR catalyst. At the beginning of the test, NO was reduced to around 500 ppm and NH_3 slip was nearly 270 ppm. After engine load was ramped to 10 bar engine load in 20 s, the NO concentration peaked at 800 ppm, then gradually dropped to 640 ppm because the performance of the SCR catalyst improved at a higher temperature. Initially, the concentration of NH_3 slip increased to around 360 ppm because slightly more ammonia was present upstream of the SCR catalyst. Also, some of the stored ammonia could have been released from the catalyst when the ammonia storage capacity was reduced at higher exhaust temperature. Then, by the end of the 10 bar load period the NH_3 slip was gradually reduced to 160 ppm, while more ammonia was used for NO reaction. After engine load was ramped down in 20 s to 6 bar BMEP, the measured NO level dropped suddenly to 360 ppm caused by sudden reduction in supplied NO. At the lower engine load, exhaust temperature was gradually reduced to 210 °C; consequently the SCR performance was reduced and the measured NO and NH_3 increased to 500 ppm and 270 respectively. No additional N_2O was detected post SCR during the whole transient experiment.

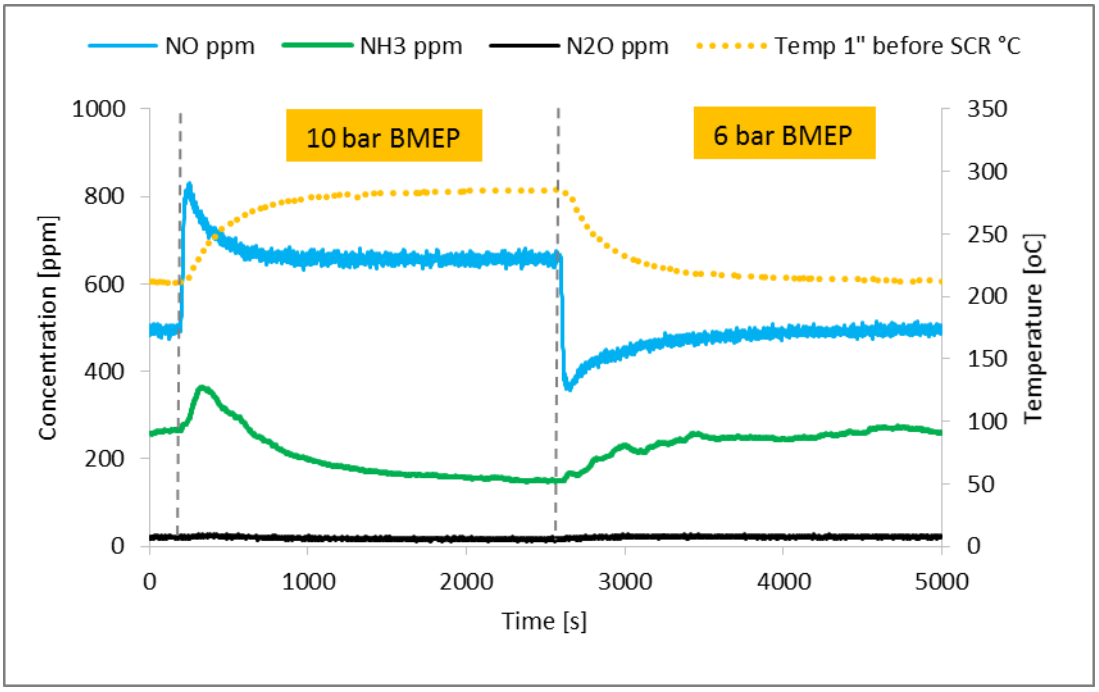

Figure 4.2.4b. FTIR measurements and gas temperature profile during the transient experiment measured downstream of the SCR catalyst.

Further analysis of the transient experiment is presented in figure 4.2.4c and in Benjamin et al., 2014. The blue line represents concentration of the calculated potential ammonia from the injected urea. The urea dosing was set up to achieve NH_3:NOx=1 at 6 bar engine load, therefore calculated potential ammonia (eq. 4.2.1) at the start of experiment (between 0-200 s) was 660 ppm. Then was reduced to 580 ppm, due to increased exhaust mass flow rate after the engine load was ramped up at to 10 bar BMEP. After engine load was reduced back to 6 bar, the potential ammonia increased to the initial value of 660 ppm. The red line represents consumed NO over SCR catalyst. It took around 1000 s for the consumed NO to increase from the initial 150 ppm to 300 ppm after the engine load was ramped from 6 bar to 10 bar. Then after the engine load was ramped down 6 bar, the value of the consumed NO was slowly reduced and reached 150 ppm by the end of experiment. The amount of consumed NO was mainly influenced by the exhaust temperature, however mass flow rate and NH_3:NOx ratio would also have a impact on the SCR conversion efficiency. The changing NH_3:NOx ratio and the SCR NOx conversion is demonstrated in figure 4.2.4d. In the absence of NO_2, only the standard SCR reaction took place hence 1 ppm of consumed NO is equal to 1 ppm of consumed NH_3.

Similarly to the steady state experiments, concentration of theoretical ammonia released from injected urea tNH_3 can be calculated adding concentration of consumed NO and ammonia slip; green line represents [ΔNO+NH_3 slip]. Hence, the difference between the potential NH_3 and tNH_3 represents the undetected ammonia by FTIR analyser downstream of the SCR catalyst (NH_3 deficit in ppm), possibly still in the form of HCNO or urea. This calculated ammonia deficit is shown in figure 4.2.4c; yellow

line. However, the above statement is only accurate when ammonia storage rate is zero, consequently the measured concentration of NH_3 slip has to reach the steady state. At the steady state, before upward engine load ramp (0-220 s) about 250 ppm was calculated as missing, which is nearly 40% of potential NH_3. Then, at the start of the high load stage ammonia deficit reduced rapidly to 0 ppm when the consumed NO and NH_3 slip quickly increased. At the same time, slightly more ammonia was measured upstream of the SCR and possibly some ammonia was thermally released from the catalyst. By the end of the high load stage, the ammonia deficit increased to around 100 ppm. This is 17% of the potential NH_3 released from the injected urea. Additionally, the NH_3 concentration measured upstream of the SCR (figure 4.2.4a) is much lower than the calculated consumed NO (ΔNO) (red line in figure 4.2.4c). This suggests that urea decomposition and HNCO hydrolysis occurs on SCR catalyst to allow the reactions with ammonia to occur, which is similar to the findings during steady state testing.

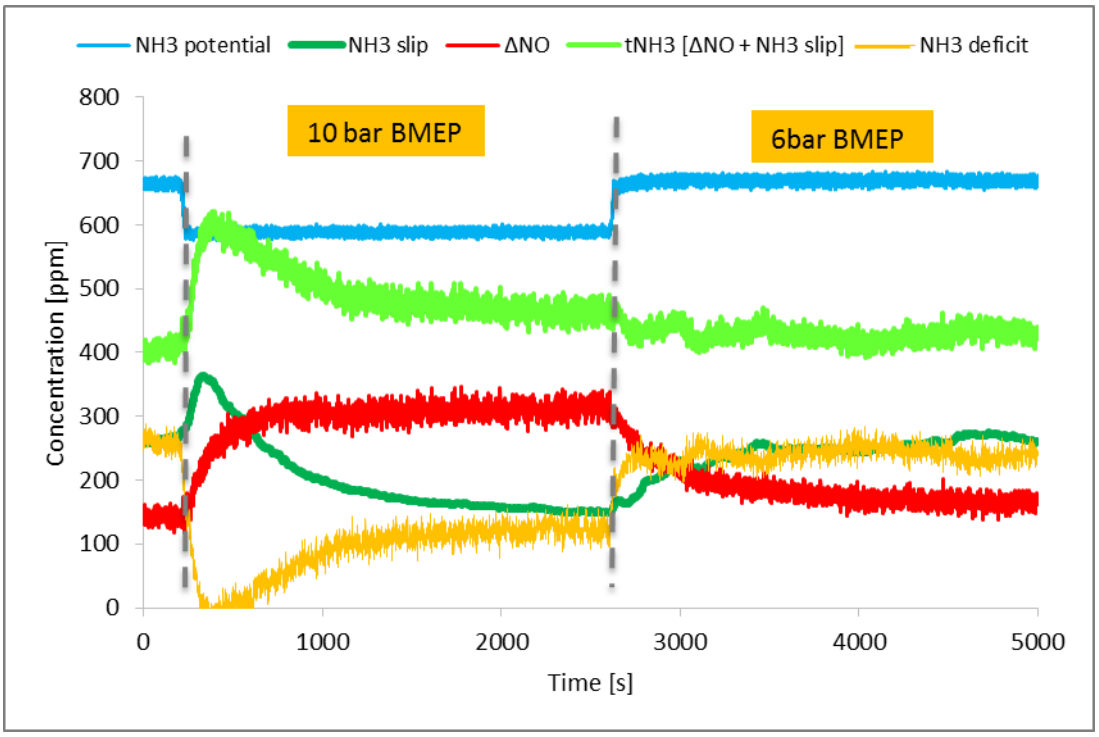

Figure 4.2.4c. Analysis of data from transient test showing deficit of ammonia that possibly passed through the SCR catalyst as undetected substance.

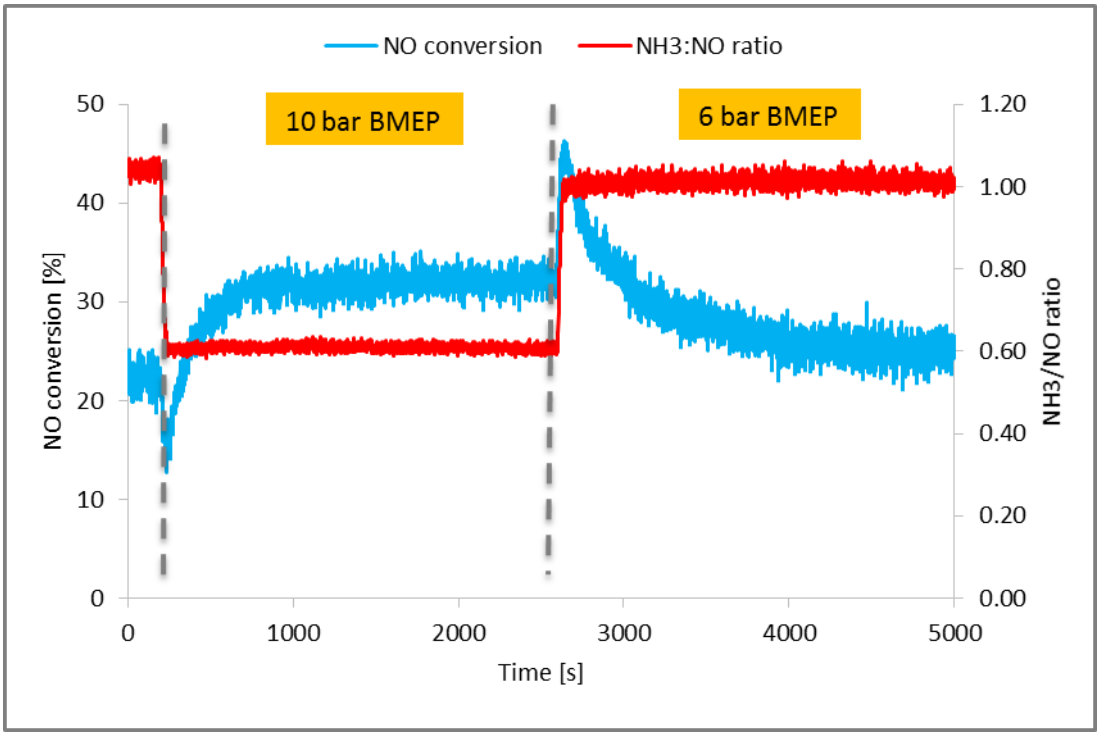

Figure 4.2.4d NO conversion and changing NH_3:NOx during transient experiment

4.2.5 Summary of results from the SCR studies with urea injection

The key findings from the SCR studies with urea injection were:

- During the high temperature study, maximum of 15% of injected urea was hydrolysed to ammonia upstream of the SCR catalyst when urea was dosed into the pipe at stoichiometric NH_3:NOx ratio. During the same conditions, only 7% of urea was hydrolysed to ammonia when urea was dosed into the can.
- When urea was injected into the pipe, it was observed that nearly twice as much of NH_3 was slipped in comparison to the urea injected into the expansion can at a stoichiometric NH_3:NOx ratio. This was the case for high and low temperature conditions.
- There was no difference in the NO conversion between two methods of urea injection.
- Results from steady state and transient studies with urea injection showed that a large proportion of urea decomposition and hydrolysis occurred on the SCR catalyst.

Chapter 5: Conclusions

5.0 Overview of the work undertaken

This chapter describes the summary of the results and their implications along with recommendations for future work.

The focus of this project was to gather data and measure the SCR catalyst performance under real engine exhaust conditions with the aim of improvements through the development and subsequent optimisation of an SCR model. Previous work indicated a promising future for the zeolite catalysts for low and high temperature in light duty diesel vehicles. However, these studies had a number of limitations. Firstly, most of the studies conducted in this area used laboratory scale gas reactors using NH_3 as a reductant. This has a limitation of being a simplification of real engine conditions. Studies which did use real engines, mainly focused on HDD applications. Secondly, most of the SCR model kinetics were based on the assumption that all urea is hydrolysed to NH_3. Thirdly, previous studies focused on examining the SCR behaviour in a wide range of temperatures, and only limited number examined it for low temperatures. Fourthly, there was also a paucity of studies examining the mechanisms of the SCR reactions under transient engine conditions. Fifthly, there was also lack of studies investigating the effect of the 3D geometry on the SCR behaviour. Finally, so far there have been fewer published studies on the SCR performance as a function of the catalyst lenght. This study aimed to address these gaps in order to further the understanding and knowledge of using Cu-Zeolite catalysts.

5.1 Strengths of the project

5.1.1 Testing programme

The testing programme was designed to gain a better understanding of the SCR performance and to fill the identified gaps in the knowledge.

- In order to understand how the SCR works, the test programme was developed to measure and compare the results between gas and urea injections. Ammonia gas injection is a simplification of the real life conditions, however it can provide a detailed understanding of how the SCR performance catalysts work, as we can control a number of factors.
- Three ammonia dosing levels were investigated, including deficient, stoichiometric and excess levels, which enabled measurement of the limitations of the catalysts performance.
- A number of different SCR brick lengths were used, which allowed a measurement and comparison at a different space velocity. This in turn led to a better understanding of the reactions in the front section of the catalyst.

- The measuring of the SCR performance under various NO_2:NOx ratios and different exhaust temperature allowed comparison of the SCR performance under varied engines conditions (low vs. high load) thus resembling real engine conditions

5.1.2 Novelty of the results

5.1.2.1 Testing under steady state conditions

Testing programme under steady state conditions was a starting point for gaining an understanding of the basic principles of the SCR catalyst behaviour. In order to simplify and remove the complex urea hydrolysis phenomena, ammonia gas was initially used instead of urea dosing. Additionally, only small volume SCR catalyst bricks were used to better understand the SCR reactions. Also, the effect of the ammonia concentration was studied by testing at deficient, stoichiometric and excess ammonia.

The data showed that conditions such as temperature and NO_2:NOx ratio had the biggest impact on the SCR performance. In the absence of NO_2, no improvement in NO conversion was found when the length of the catalysts was increased from 30 mm to 45 mm. This was shown to be true for both low and high temperature and each dosing set up. This may suggest that most of the NO was converted in the front section of the catalyst (first 30 mm) and adding 15 mm of SCR had only a very small effect on the conversion that in this case was not measurable. The effect of the SCR catalyst lengths on the NOx conversion was less noticeable under deficient ammonia dosing, regardless of the NO_2:NOx ratio, because all of the available ammonia was converted at the front of the catalyst.

There are important implications of these results; overall, it is important to understand the behaviour of the SCR catalyst under low temperature as future applications will require operating at even lower temperatures to ones currently used. These results can be also used as a basis for tuning the SCR model in LDD and HDD applications. Finally, they also highlight the significance of calibrating ammonia dosing strategies and finding the most advantageous NO_2:NOx in order to gain an optimum NOx performance while reducing a potential ammonia slip from the SCR system.

5.1.2.2 Testing under transient engine conditions

Data obtained from ammonia gas injection built a strong base for our understanding of the SCR catalysts behaviour under transient engine conditions. One of the key findings during the transient tests with standard 0.5 and 1 DOC was that regardless of the supplied NO_2:NOx ratio, the consumed NO_2:NOx ratio was 0.6 and constant throughout these tests. This could be explained by the rate of NO_2 consumption which had to be higher for NO_2:NOx ratio close to 0.5 than for NO_2:NOx ratio close to 0.2. It was also found that during short transient test with standard 1 DOC (overall high inlet NO_2:NOx ratio), the NOx conversion was slightly less sensitive to the variation of supplied NO_2:NOx ratio across the transient ramp.

This step allowed progression to the next stage; data obtained during the transient tests was used in the further development of the SCR kinetics, in order to better predict the SCR behaviour under changing engine conditions.

Findings from the Pd only DOC studies during the transient tests were used to tune the model adsorption multiplier in order to predict the SCR behaviour during the ramp up and ramp down conditions. It was found that changing the adsorption multiplier had a greater effect when there was a more substantial change in the temperature; for example during the ramp up and ramp down of long transient test (Benjamin et al., 2012a). It was also found that in the presence of both NO and NO_2, the model under predicted the amount of the consumed NO_2. Therefore, the rate of slow reaction (see equation 1.4.3c) used in the model had to be increased by factor of 20 in order to predict the correct conversion of NO_2.

5.1.2.3 Urea dosing experiments

Urea dosing experiments were conducted to ascertain whether the assumption that all urea is hydrolysed to NH_3 is correct. During urea injection experiments, urea was injected either through an oblique pipe arrangement with a mixer device placed downstream or directly into a mixing can. The results from the experiments suggest that the assumption was not valid; during the low temperature experiment up to 42 % of potential ammonia was missing from the injected urea.

Results from steady state and transient studies with urea injection showed that a large proportion of urea decomposition and hydrolysis occurred on the SCR catalyst; maximum of 15% of injected urea was hydrolysed to ammonia upstream of the SCR catalyst when urea was dosed into the pipe at stoichiometric NH_3:NOx ratio.

NOx performance between urea injection and ammonia gas dosing experiment was compared; it was found that more NO was converted for a given NH_3:NOx ratio when ammonia was supplied in the form of gas. Particularly, ammonia gas dosing showed a better conversion at high temperature (263 °C); for example, at NH_3:NOx=1 the conversion was 13 % higher than urea injection experiment.

There was no difference in the NO conversion between two methods of urea injection for a given NH_3:NOx ratio. That was true for low and high temperature tests.

5.1.2.4 The effect of 3D diffuser geometry on SCR performance

This study investigated the effect of 3D diffuser geometry using 180 degree sudden expansion diffuser, in order to measure the influence of temperature and velocity profiles on SCR NOx and NH_3 conversion. The results showed that the flow and temperature distribution upstream of the SCR catalyst had an effect on the NOx conversion, and that gas velocity has bigger impact on NOx conversion than gas temperature.

5.2 **Limitations and recommendations for future work**

- The work undertaken as part of this thesis highlighted the complexity of process of urea hydrolysis and decomposition, which occur in the SCR aftertreatment system. In order to gain an in depth understanding of these processes combined with SCR reactions, there is a need for a more extensive study with a dedicated analyser equipment.
- CFD Modelling using further data collected with urea injection will be the next step.

Urea injections:

- The result under urea injection condition shows that the understanding of the urea decomposition and hydrolysis is limited especially at low operating temperatures. Developments in gas analysers available for measurements of ammonia and the by-products of urea may be necessary before such programme of study could be indicated.

- Measuring ammonia proved to be challenging. More studies need to be conducted with urea injection under low temperature conditions. Again, advances in gas analysis techniques would help with this.

References:

Alimin, A., Benjamin, S., & Roberts, C. (2009). Lean NOx trap study on a light-duty diesel engine using fast-response emission analysers. *International Journal of Engine Research, 10*(3), 149-164.

Babu, M., Ravindra, M., Sagar, B., & Sachin, B. (2007). Strategy to Meet Euro IV Emission Norms on Common Rail Sports Utility Vehicle: SAE Technical Paper.

Benjamin, Gall, M., & Roberts, C. A. (2014). Conversion of nitric oxide in an engine exhaust by selective catalytic reduction with a urea spray under steady-state and transient engine-load conditions. *Proceedings of the Institution of Mechanical Engineers, Part D: Journal of Automobile Engineering, 228*(7), 758-770.

Benjamin, S., Gall, M., & Roberts, C. (2012a). Modelling of NOx conversion in a 1D diesel engine exhaust SCR catalyst system under transient conditions using ammonia gas as the reductant: SAE Technical Paper.

Benjamin, S., Gall, M., & Roberts, C. (2012b). Tuning the Standard SCR Reaction Kinetics to Model NO Conversion in a Diesel Engine Exhaust SCR Catalyst System Under Steady State Conditions in 1D and 3D Geometries Using Ammonia Gas as the Reductant: SAE Technical Paper.

Benjamin, S., Gall, M., Sturgess, M., & Roberts, C. (2011). Experiments on a light duty SCR test exhaust system using ammonia gas to provide data for validation of a CFD model. *Internal Combustion Engines: Improving Performance, Fuel Economy and Emissions*, 219.

Birkhold, F., Meingast, U., Wassermann, P., & Deutschmann, O. (2006). Analysis of the injection of urea-water-solution for automotive SCR DeNOx-systems: modeling of two-phase flow and spray/wall-interaction: SAE Technical Paper.

Bosteels, D., & Searles, R. A. (2002). Exhaust emission catalyst technology. *Platinum metals review, 46*(1), 27-36.

Cambustion (2014). Ultra fast-response gas analyzers for transient HC, NOx, CO& CO_2 exhaust, intake and in-cylinder applications. Retrieved from: http://www.cambustion.com/sites/default/files/instruments/CLD500/Cambustion500seriesgasanalyzers.pdf Accessed on 16.02.2015

Castagnola, M., Caserta, J., Chatterjee, S., Chen, H.-Y., Conway, R., Fedeyko, J., . . . Walker, A. (2011). Engine performance of Cu-and Fe-based SCR emission control systems for heavy duty diesel applications: SAE Technical Paper.

Chatterjee, D., Burkhardt, T., Weibel, M., Nova, I., Grossale, A., & Tronconi, E. (2007). Numerical simulation of zeolite-and V-based SCR catalytic converters: SAE Technical Paper.

Costigan, M., Cary, R., & Dobson, S. (2001). Vanadium pentoxide and other inorganic vanadium compounds.

DieselNet. (2013). Emission Standards: Europe. Cars and Light Tracks. Revision: 2013.07. Retrieved 15.08.2014, from https://www.dieselnet.com/standards/eu/ld.php

Emitec. Technology: In tank-solutions. Retrieved 17.08.2014, from http://www.emitec.com/en/technology/scr-dosiersysteme/tankintegriert-gen-iii-iv.html

EPA. (2008). Integrated Science Assessment for Oxides of Nitrogen – Health Criteria (Final Report). EPA/600/R-08/071, 2008. Washington, DC, : U.S. EPA.

European Commission. (2006). Impact Assessment for Euro 6 emission limits for light duty vehicles Brussels.

European Commission. (2013). Euro 5 and Euro 6 - emissions from light duty vehicles. Retrieved 15.08.2014, from http://ec.europa.eu/enterprise/sectors/automotive/environment/euro5/index_en.htm

Faiz, A., Weaver, C. S., & Walsch, M. (1996). *Air Pollution from Motor Vehicles. Standards and Technologies for Controlling Emissions* Washington: The World Bank.

Grossale, A., Nova, I., & Tronconi, E. (2008). Study of a Fe–zeolite-based system as NH< sub> 3</sub>-SCR catalyst for diesel exhaust aftertreatment. *Catalysis Today, 136*(1), 18-27.

Heck, R. M., & Farrauto, R., J (2009). *Catalytic Air Poluution Control. Commercial Technology* (Third ed.). New York: John wiley & Sons.
Heywood, J. B. (1988). *Internal combustion engine fundamentals* (Vol. 930): Mcgraw-hill New York.
Horiba (2015). MEXA-6000FT-E: Specification. Retrieved from: http://www.horiba.com/automotive-test-systems/products/emission-measurement-systems/analytical-systems/standard-emissions/details/mexa-6000ft-e-12797/. Accessed on 15.02.2015
Hotta, Y., Inayoshi, M., Nakakita, K., Fujiwara, K., & Sakata, I. (2005). Achieving lower exhaust emissions and better performance in an HSDI diesel engine with multiple injection: SAE Technical Paper.
Jeong, S.-J., Lee, S.-J., & Kim, W.-S. (2008). Numerical study on the optimum injection of urea-water solution for SCR deNOx system of a heavy-duty diesel engine to improve deNOx performance and reduce NH3 slip. *Environmental Engineering Science, 25*(7), 1017-1036.
Johansson, Å., Wallin, U., Karlsson, M., Isaksson, A., & Bush, P. (2008). Investigation on uniformity indices used for diesel exhaust aftertreatment systems: SAE Technical Paper.
Johnson. (2009). Review of diesel emissions and control. *International Journal of Engine Research, 10*(5), 275-285.
Kamasamudram, K., Currier, N., Szailer, T., & Yezerets, A. (2010). Why Cu-and Fe-zeolite SCR catalysts behave differently at low temperatures: SAE Technical Paper.
Katare, S. R., Patterson, J. E., & Laing, P. M. (2007). Diesel Aftertreatment Modeling: A Systems Approach to NOx Control. *Industrial & Engineering Chemistry Research, 46*(8), 2445-2454. doi: 10.1021/ie0612515
Kodama, Y., & Wong, V. W. (2010). Study of On-Board Ammonia (NH3) Generation for SCR Operation: SAE Technical Paper.
Koebel, M., Elsener, M., & Kleemann, M. (2000). Urea-SCR: a promising technique to reduce NO< sub> x</sub> emissions from automotive diesel engines. *Catalysis today, 59*(3), 335-345.
Konieczny, R., Müller, W., Cherington, B., Presti, M., Jayat, F., Davies, M. J., & Murphy, P. R. (2008). Pre-Turbocharger-Catalyst-Catalytic Performances on an Euro V Type Diesel Engine and Robust Design Development: SAE Technical Paper.
Konstandopoulos, A. G., Kostoglou, M., Skaperdas, E., Papaioannou, E., Zarvalis, D., & Kladopoulou, E. (2000). Fundamental studies of diesel particulate filters: transient loading, regeneration and aging: SAE Technical Paper.
Liu, Z., Benjamin, S. F., & Roberts, C. (2003). Pulsating flow maldistribution within an axisymmetric catalytic converter-flow rig experiment and transient CFD simulation: SAE Technical Paper.
Maus, W., & Brück, R. (2007). *Exhaust Gas Aftertreatment Systems for Commercial Vehicles–Technologies and Strategies for the Future.* Paper presented at the ICPC conference, paper.
Mohan, B., Yang, W., & Kiang Chou, S. (2013). Fuel injection strategies for performance improvement and emissions reduction in compression ignition engines—A review. *Renewable and Sustainable Energy Reviews, 28*, 664-676.
Narayanaswamy, K., & He, Y. (2008). Modeling of copper-zeolite and iron-zeolite selective catalytic reduction (SCR) catalysts at steady state and transient conditions: SAE Technical Paper.
Parks, J. E., Watson, J., Campbell, G., Wagner, G., & Campbell, L. (2000). Sulfur Sorbate Catalysts for Diesel Aftertreatment: Temperature Effects on the Release of Sulfur: SAE Technical Paper.
Russell, A., & Epling, W. S. (2011). Diesel Oxidation Catalysts. *Catalysis Reviews, 53*(4), 337-423. doi: 10.1080/01614940.2011.596429
Sjovall, H., Blint, R. J., & Olsson, L. (2009). Detailed kinetic modeling of NH3 SCR over Cu-ZSM-5. *Applied Catalysis B: Environmental, 92*, 138-153.
Stumpp, G., & Ricco, M. (1996). Common rail-an attractive fuel injection system for passenger car DI diesel engines: SAE Technical Paper.
Sturgess, M. (2012). *Selective Catalytic Reduction for 'Light-Duty'Diesel Engines using Ammonia Gas. PhD thesis.* Coventry University

Sultana, A., Nanba, T., Sasaki, M., Haneda, M., Suzuki, K., & Hamada, H. (2011). Selective catalytic reduction of NO< sub> x</sub> with NH< sub> 3</sub> over different copper exchanged zeolites in the presence of decane. *Catalysis Today, 164*(1), 495-499.

Transport Policy. (2014). China: Light-duty: Emissions. Retrieved 15.08.2014, from http://transportpolicy.net/index.php?title=China:_Light-duty:_Emissions

Wang, Y., Raman, S., & Grizzle, J. W. (1999). *Dynamic modeling of a lean NO x trap for lean burn engine control.* Paper presented at the American Control Conference, 1999. Proceedings of the 1999.

Watling, T. C., Tutuianu, M., Desai, M. R., Dai, J., Markatou, P., & Johansson, A. (2011). Development and validation of a Cu-Zeolite SCR catalyst model: SAE Technical Paper.

Wurzenberger, J. C., & Wanker, R. (2005). Multi-scale SCR modeling, 1D kinetic analysis and 3D system simulation: SAE Technical Paper.

Yi, Y. (2007). Development of a 3D numerical model for predicting spray, urea decomposition and mixing in SCR systems: SAE Technical Paper.

Zhang, X., Romzek, M., Keck, M., & Kurz, F. (2005). Numerical Optimization of Flow Uniformity inside Diesel Particular Filters: SAE Technical Paper.

Zheng, G., Palmer, G., Salanta, G., & Kotrba, A. (2009). Mixer development for urea SCR applications: SAE Technical Paper.

Appendix 1. Gas emission analysers

This item has been removed due to 3rd party copyright. The unabridged version of the thesis can be viewed in the Lanchester Library Coventry University.

Table A.1 Specifications of EXSA 1500 Common gas analyser [Horiba Ltd, EXSA 1500 operating manual Oct 2004]

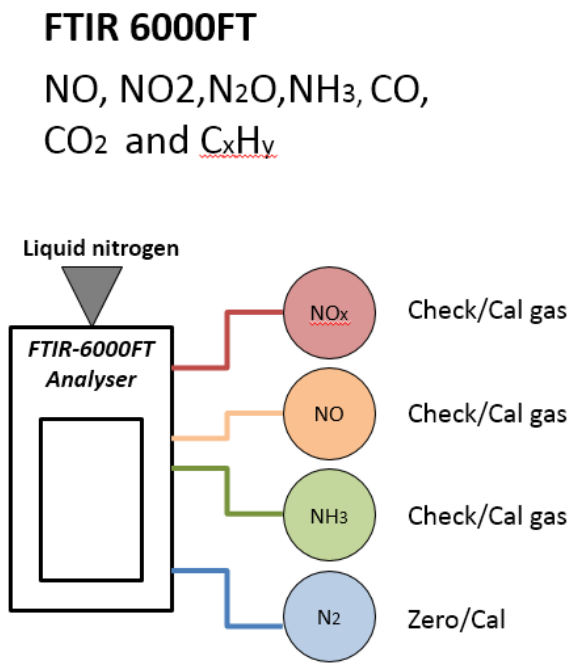

Figure A.1 Horiba 6000 FT FTIR analyser gas piping configuration.

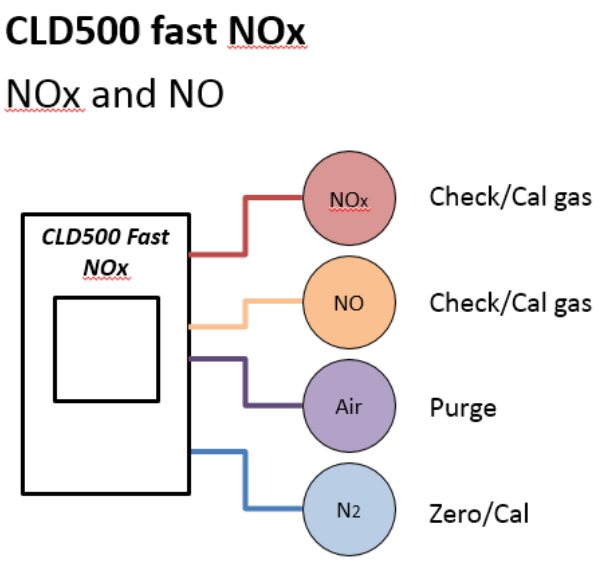

Figure A.2 Cambustion CLD 500 analyser gas piping configuration.

Appendix 2. Urea dosing

AdBlue calculation – ammonia exhaust concentration

AdBlue Flow rate [g/s] = Water Flow rate [g/s] x 1.09

- 32.5% Urea in water solution

Urea Flow Rate [g/s] = AdBlue Flow rate x 32.5%

- $(NH_2)_2CO + H_2O \rightarrow 2\ NH_2 + CO_2$ - Urea hydrolysis

1 mol urea = 2 mol ammonia

Ammonia concentration = Ammonia Flow Rate / (Exhaust Flow Rate + AdBlue Flow Rate)

	Ammonia Concentratio Calculator												
	date	01/03/2012			Bosh spray setup [Hz]		4		Average Air/Fuel ratio				28.5
	Injector frequency [Hz]			4	Molecular mass of exhaust gas [g/mol]			28.72	Average air mass flow rate [kg/h]				116.7
	Pressure regulator [bar]			5.7	Molecular mass of AdBlue (NH2)2CO+2.08H20			46.85	Average air mass flow rate [g/s]				32.41667
	After filter pressure [bar]			4.8	Molecular mass of urea (NH2)2CO [g/mol]			60	Average fuel mass flow rate [g/s]				1.14
	BOSH water static flow [g/h]			2990					Total exhaust molar flow rate [g/s]				33.55
	BOSH AdBlue static flow [g/h]			3120					Total exhaust molar flow rate [mol				1.17
	Spray pulse setup	Spray water flow setup	AdBlue flow rate (water	Urea flow rate (AdBlue	AdBlue molar flow rate	Urea molar flow rate	Ammonia molar flow rate (1mol	Total exhaust molar flow	Ammonia concentration				
	[ms]	[g/s]	[g/s]	[g/s]	[mol/s]	[mol/s]	[mol/s]	[mol/s]	[ppm]				
a~0.5	13	0.039811	0.043	0.0141	0.000926	2.35E-04	4.70E-04	1.1692	402				
a~0.75	19	0.060146	0.066	0.0213	0.001399	3.55E-04	7.10E-04	1.1697	607				
a~1	25	0.081	0.088	0.0287	0.001885	4.78E-04	9.56E-04	1.1702	817				

Figure A.3 Example of ammonia concentration calculation for three urea dosing setup point.

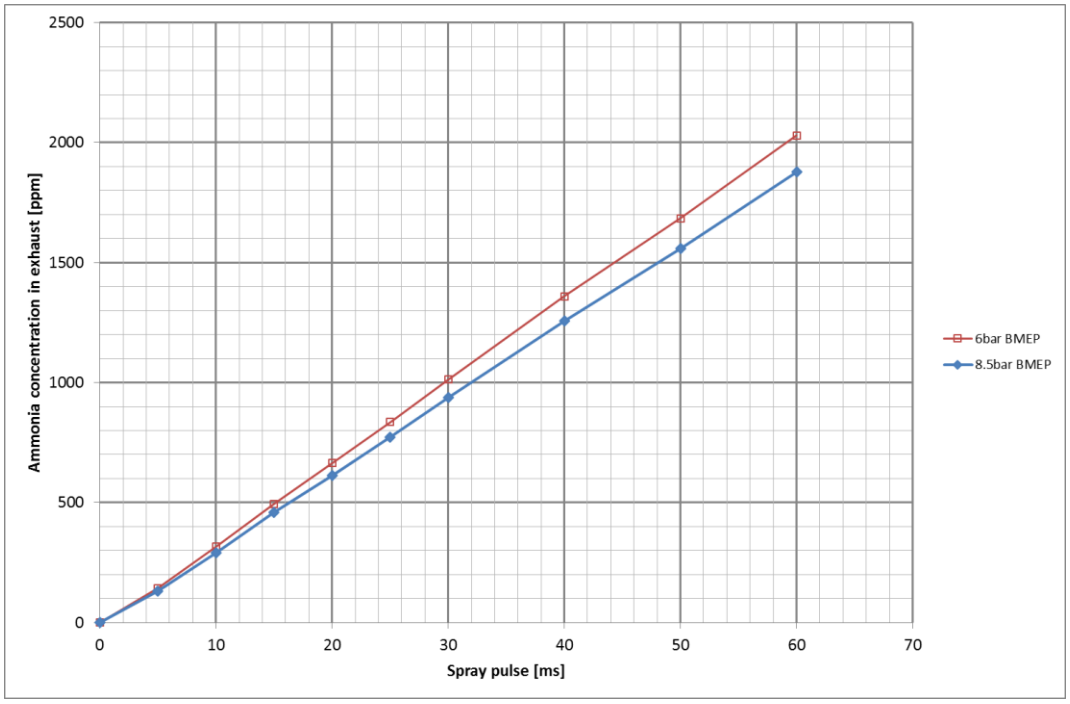

Figure A.4 Ammonia concentration in exhaust at 6 bar BMEP and 8 bar BMEP engine load.

Average AdBlue flow rate = 0.06g/s.

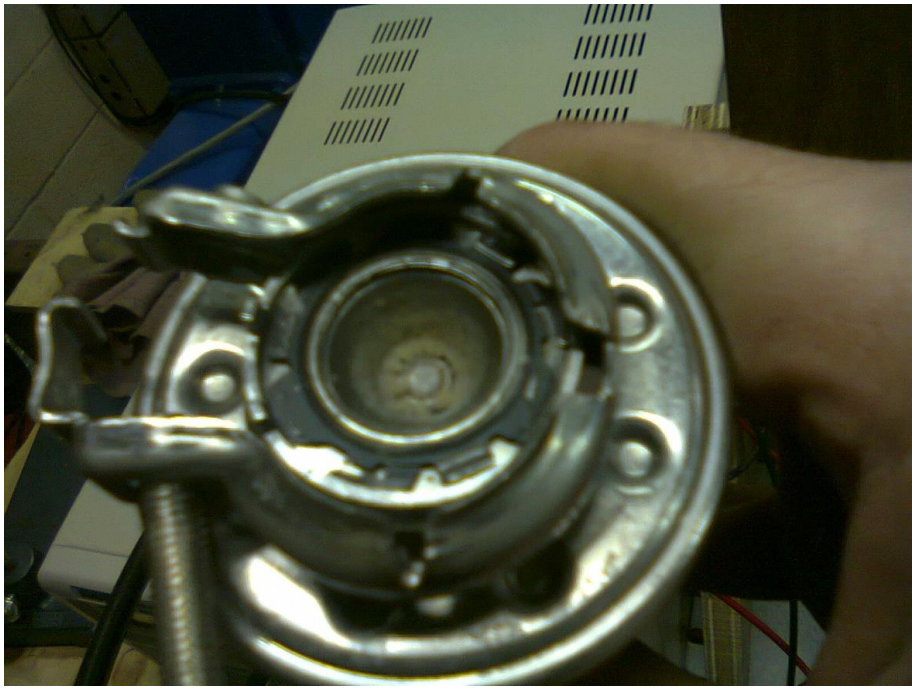

Figure A.5 Deposit on the tip of the injector after ~80 minutes of spraying.

Figure A.6 Deposit on the tip of the injector after ~200 minutes spraying.

Figure A.7. Top view of urea mixer unit.

This item has been removed due to 3rd party copyright. The unabridged version of the thesis can be viewed in the Lanchester Library Coventry University.